



Schweizerische Eidgenossenschaft  
Confédération suisse  
Confederazione Svizzera  
Confederaziun svizra

Federal Department of the Environment, Transport,  
Energy and Communications DETEC

**Swiss Federal Office of Energy SFOE**  
Energy Research and Cleantech

**Final Report**

---

## ATTRACT

### Advanced techniques for the characterisation of photovoltaic modules

---



Source: SUPSI 2024



University of Applied Sciences and Arts  
of Southern Switzerland

# SUPSI

**Date:** 17/09/2024

**Location:** Mendrisio

**Publisher:**

Swiss Federal Office of Energy SFOE  
Energy Research and Cleantech  
CH-3003 Bern  
[www.bfe.admin.ch](http://www.bfe.admin.ch)

**Subsidy recipients:**

SUPSI Scuola Universitaria Professionale della Svizzera Italiana  
SUPSI PVLab  
Via Flora Ruchat Roncati, 15  
CH-6850, Mendrisio  
[www.supsi.ch/isaac](http://www.supsi.ch/isaac)

**Authors:**

Gabi Friesen, SUPSI PVLab, [gabi.friesen@supsi.ch](mailto:gabi.friesen@supsi.ch)  
Flavio Valoti, SUPSI PVLab, [flavio.valoti@supsi.ch](mailto:flavio.valoti@supsi.ch)  
Ebrar Özkalay, SUPSI PVLab, [ebrar.ozkalay@supsi.ch](mailto:ebrar.ozkalay@supsi.ch)  
Giovanni Bellenda, SUPSI PVLab, [giovanni.bellenda@supsi.ch](mailto:giovanni.bellenda@supsi.ch)  
Mauro Caccivio, SUPSI PVLab, [mauro.caccivio@supsi.ch](mailto:mauro.caccivio@supsi.ch)

**SFOE project coordinator:**

Stefan Oberholzer, Swiss Federal Office of Energy, [stefan.oberholzer@bfe.admin.ch](mailto:stefan.oberholzer@bfe.admin.ch)

**SFOE contract number:** SI/502036-01

**The authors bear the entire responsibility for the content of this report and for the conclusions drawn therefrom.**



## Summary

The photovoltaic market has seen a number of technological innovations in recent years, driven by the availability of larger and more efficient c-Si solar cells and the introduction of new module designs, materials and manufacturing processes. The very rapid introduction and combination of multiple technological innovations has introduced new failures in the field, that are not always detected in advance and may affect the long-term reliability of PV systems installed today. The knowledge on technology specific energy yield potential, degradation rate and expected lifetime is crucial for investors to minimise the risks associated with underperformance and new products entering the market. There are several approaches to assess the energy yield of a particular PV module technology, each with its own advantages and disadvantages. One approach is to monitor the modules in the field, while another is based on full characterisation in accordance with the Energy Rating (ER) standard IEC 61853 and subsequent calculation of the energy yield using a full year meteorological data set. While the former is representative of real operating conditions and can detect degradation, the latter provides only a theoretical value, representative of the first year, but with the advantage of being fast, reproducible and applicable to any climate. Depending on the scope of testing one or the other method or a combination of the two is applied. Both rely on high-precision measurements and expertise in technology-specific module testing capabilities.

The ATTRACT project aims to support R&D and industry with scientific field data and insights into the electrical performance and degradation rates of some of the new mainstream module technologies supported by faster and accurate test solutions for high efficiency modules.

In 2022 SUPSI started its 14<sup>th</sup> outdoor measurement campaign (test cycle 14) to assess the performance and reliability of recent photovoltaic (PV) cell technologies. Seven types of commercial crystalline silicon mono-facial PV modules, including PERC, TOPCon, IBC, HJT modules, were selected. Data from the first two years of outdoor testing revealed that the specific energy yield ( $Y_f$  [kWh/W]) of 6 out of 7 tested module types were very close ( $\pm 0.9\%$  spread) when mounted under optimal conditions (open-rack, south-facing, close to optimum tilt) whereas the spread increased up to  $\pm 2.1\%$  when mounted at 10° tilt, due to different angular responses and soiling losses. **With this, the project highlighted the need for testing under application representative conditions, as could be flat roof systems or BIPV facades, to reveal potential advantages or disadvantages of single PV technologies and/or module designs. Under optimal conditions the initial technological differences are close to negligible, considering minor degradation is occurring.**

The limited number of products tested within the project does not allow generalisation about any specific technology but gives insight into single products and manufacturing related quality aspects. **The first 2 years data permitted to: (1) detect an early-stage failure within one of the products, (2) identify potentials for product optimisation and (3) quantify the first year degradation and stabilisation trends.** Following technology specific observations have been made:

- The first-generation p-type **TOPCon** modules tested here, moving now towards n-type TOPCon, have systematically shown the highest energy yields, also due to the lowest degradation rates. An inter-comparison to new generation TOPCon modules is envisaged for the future.
- The tested **IBC** modules revealed some minor degradation and lower winter yield in the low tilted test stand, which could potentially be overcome by improving the angular response. UV induced degradation has been identified as a potential cause for the degradation, but further investigations are needed to prove it.
- **PERC** modules revealed the highest variability within modules of the same type, which is probably related to manufacturing tolerance especially related to the cell cutting and new inter-connection



technologies, particularly evident in shingled modules, and differences in light induced degradation. All observed differences are relatively small, but longer data sets are needed to monitor its evolution over time, crucial for better understanding of long term reliability of new module designs and to separate different degradation mechanisms.

- The **HJT** modules tested here are considered as outlier. Despite their favourable temperature coefficient, positioning the technology potentially within the top-players, the modules have performed poorly due to a significant degradation, exceeding the warranty claims (-5.75%/year power loss in the first year followed by -1.57%/year), mainly caused by the use of a wrong bill of material (BOM) not preventing moisture ingress through the backsheet. The effectiveness of different in place mitigation measures to prevent moisture induced degradation in HJT modules will be investigated in future by comparing different products.

Technology benchmarking and energy rating relies both on accurate and extensive indoor testing. The time and cost, in particular of high precision ER measurements according to IEC 61853 Part 1, are a clear barrier for research and industry. The project aimed to improve the electrical characterization of high efficiency modules affected by capacitive effects, by reducing the time effort needed for measurements at different irradiance and temperature levels without affecting the measurement uncertainty. **A modified dragon-back approach was introduced and validated, demonstrating a reduction in the effective measurement time for a full power matrix to approximately 42 minutes, 10 times less than the best reference method at SUPSI without affecting the measurement uncertainty.** One of the bottlenecks remains the duration of thermal stabilisation, when measuring module performance at different temperatures. The power matrix measurement has been validated within an international laboratory inter-comparison, demonstrating uncertainties close to the STC uncertainty for all measurement points. Some new technological challenges or limitations related to the testing of large size modules were identified.

Last but not least, the development of (Pk/Si) perovskite-silicon tandem solar cells have gained significant traction due to its potential to exceed the conversion efficiency limit of (c-Si) crystalline silicon single junction at a foreseeable affordable cost. Therefore, the project aimed to assess the testing capabilities of the SUPSI PVLab for the upcoming perovskite technology, starting from PK single junction modules. A software was written to test the modules under STC conditions according to a test procedure developed by the ESTI of the Joint Research Centre (JRC), as well as outdoors under variable light conditions and different voltage sweep times. **SUPSI upgraded its test facility for single junction PK module. The next step will be the upgrade for the testing of multi-junction perovskite modules and the optimisation of maximum power point tracking algorithms which would in future allow SUPSI to include PK/Si modules to the outdoor technology benchmarking campaigns.**



## Zusammenfassung

Der Photovoltaikmarkt hat in den letzten Jahren eine Reihe technologischer Innovationen erlebt, die durch die Verfügbarkeit größerer und effizienterer c-Si-Solarzellen und die Einführung neuer Moduldesigns, Materialien und Herstellungsverfahren vorangetrieben wurden. Die sehr schnelle Einführung und Kombination mehrerer technologischer Innovationen hat zu neuen Fehlern in diesem Bereich geführt, die nicht immer im Voraus erkannt werden und die langfristige Zuverlässigkeit der heute installierten PV-Anlagen beeinträchtigen können. Das Wissen über das technologiespezifische Energieertragspotenzial, die Degradationsrate und die erwartete Lebensdauer ist für Investoren von entscheidender Bedeutung, um die Risiken im Zusammenhang mit Leistungsmängeln und neuen Produkten auf dem Markt zu minimieren. Es gibt mehrere Ansätze zur Bewertung des Energieertrags einer bestimmten PV-Modultechnologie, die jeweils ihre eigenen Vor- und Nachteile haben. Ein Ansatz besteht darin, die Module im Feld zu überwachen, während ein anderer auf einer vollständigen Charakterisierung gemäß der Energiebewertungsnorm IEC 61853 und der anschließenden Berechnung des Energieertrags anhand eines meteorologischen Datensatzes für ein ganzes Jahr basiert. Während ersterer für reale Betriebsbedingungen repräsentativ ist und Degradation erkennen kann, liefert letzterer nur einen theoretischen Wert, der für das erste Jahr repräsentativ ist, aber den Vorteil hat, dass er schnell, reproduzierbar und auf jedes Klima anwendbar ist. Je nach Umfang der Prüfung wird die eine oder die andere Methode oder eine Kombination aus beiden angewendet. Beide basieren auf hochpräzisen Messungen und Fachkenntnissen in technologiespezifischen Modulprüfverfahren.

Das ATTRACT-Projekt zielt darauf ab, Forschung und Entwicklung sowie die Industrie mit wissenschaftlichen Felddaten und Erkenntnissen über die elektrische Leistung und Degradationsraten einiger der neuen Mainstream-Modultechnologien zu unterstützen, die durch schnellere und genauere Testlösungen für hocheffiziente Module unterstützt werden.

Im Jahr 2022 startete die SUPSI ihre 14. Freilandmesskampagne (Testzyklus 14) zur Bewertung der Leistung und Zuverlässigkeit aktueller Photovoltaik (PV)-Zelltechnologien. Es wurden sieben Typen von handelsüblichen monofazialen PV-Modulen aus kristallinem Silizium ausgewählt, darunter PERC-, TOPCon-, IBC- und HJT-Module. Die Daten aus den ersten beiden Jahren der Freilandtests zeigten, dass der spezifische Energieertrag ( $Y_f$  [kWh/W]) von 6 der 7 getesteten Modultypen unter optimalen Bedingungen (offenes Gestell, Südausrichtung, nahezu optimale Neigung) sehr ähnlich war (Abweichung  $\pm 0,9\%$ ), während die Abweichung bei einer Neigung von  $10^\circ$  aufgrund unterschiedlicher Winkelreaktionen und Verschmutzungsverluste auf  $\pm 2,1\%$  anstieg. **Damit hat das Projekt die Notwendigkeit von Tests unter anwendungsrelevanten Bedingungen, wie z. B. Flachdachsystemen oder BIPV-Fassaden, hervorgehoben, um potenzielle Vor- oder Nachteile einzelner PV-Technologien und/oder Modulkonstruktionen aufzudecken. Unter optimalen Bedingungen sind die anfänglichen technologischen Unterschiede angesichts der geringen Degradation nahezu vernachlässigbar.**

Die begrenzte Anzahl der im Rahmen des Projekts getesteten Produkte lässt keine Verallgemeinerungen über eine bestimmte Technologie zu, gibt jedoch Aufschluss über einzelne Produkte und herstellungsbezogene Qualitätsaspekte. **Die Daten der ersten zwei Jahre ermöglichen es, (1) einen frühzeitigen Ausfall bei einem der Produkte festzustellen, (2) Potenziale für die Produktoptimierung zu identifizieren und (3) die Degradation und Stabilisierungstrends im ersten Jahr zu quantifizieren.** Folgende technologiespezifische Beobachtungen wurden gemacht:

- Die hier getesteten p-Typ-TOPCon-Module der ersten Generation, die nun durch n-Typ-TOPCon-Module ersetzt werden, haben systematisch die höchsten Energieerträge erzielt, was auch auf die niedrigsten Degradationsraten zurückzuführen ist. Ein Vergleich mit TOPCon-Modulen der neuen Generation ist für die Zukunft geplant.



- Die getesteten IBC-Module zeigten eine geringfügige Degradation und einen geringeren Winterertrag im Teststand mit geringer Neigung, was möglicherweise durch eine Verbesserung der Winkelempfindlichkeit behoben werden könnte. Als mögliche Ursache für die Degradation wurde eine UV-induzierte Degradation identifiziert, die jedoch noch weiter untersucht werden muss.
- PERC-Module wiesen die höchste Variabilität innerhalb von Modulen desselben Typs auf, was wahrscheinlich mit Fertigungstoleranzen zusammenhängt, insbesondere im Zusammenhang mit dem Zellzuschnitt und neuen Verbindungstechnologien, die besonders bei Shingled-Modulen deutlich werden, sowie mit Unterschieden in der lichtinduzierten Degradation. Alle beobachteten Unterschiede sind relativ gering, aber es sind längere Datensätze erforderlich, um die Entwicklung im Laufe der Zeit zu überwachen, was für ein besseres Verständnis der langfristigen Zuverlässigkeit neuer Modulkonstruktionen und zur Unterscheidung verschiedener Degradationsmechanismen von entscheidender Bedeutung ist.
- Die hier getesteten HJT-Module gelten als Ausreißer. Trotz ihres günstigen Temperaturkoeffizienten, der die Technologie potenziell in die Spitzengruppe einreicht, haben die Module aufgrund einer erheblichen Degradation, die über die Garantieansprüche hinausgeht (-5,75 %/Jahr Leistungsverlust im ersten Jahr, gefolgt von -1,57 %/Jahr), eine schlechte Leistung gezeigt, was hauptsächlich auf die Verwendung einer falschen Stückliste (BOM) zurückzuführen ist, die das Eindringen von Feuchtigkeit durch die Rückseitenfolie nicht verhindert. Die Wirksamkeit verschiedener Maßnahmen zur Verhinderung von feuchtigkeitsbedingter Degradation in HJT-Modulen wird in Zukunft durch den Vergleich verschiedener Produkte untersucht werden.

Technologie-Benchmarking und Energiebewertung beruhen sowohl auf genauen als auch auf umfangreichen Tests unter Laborbedingungen. Der Zeit- und Kostenaufwand, insbesondere für hochpräzise ER-Messungen gemäß IEC 61853 Teil 1, stellen ein klares Hindernis für Forschung und Industrie dar. Das Projekt zielte darauf ab, die elektrische Charakterisierung von hocheffizienten Modulen, die von kapazitiven Effekten beeinflusst werden, zu verbessern, indem der Zeitaufwand für Messungen bei unterschiedlichen Bestrahlungsstärken und Temperaturen reduziert wurde, ohne die Messunsicherheit zu beeinträchtigen. **Ein modifizierter Dragon-Back-Ansatz wurde eingeführt und validiert, der eine Reduzierung der effektiven Messzeit für eine Vollleistungsmatrix auf etwa 42 Minuten demonstrierte, was 10-mal weniger ist als die beste Referenzmethode bei SUPSI, ohne die Messunsicherheit zu beeinträchtigen. Einer der Engpässe bleibt die Dauer der thermischen Stabilisierung bei der Messung der Modulleistung bei verschiedenen Temperaturen.** Die Leistungsmatrixmessung wurde im Rahmen eines internationalen Laborvergleichs validiert und zeigte Unsicherheiten, die für alle Messpunkte nahe an der STC-Unsicherheit lagen. Es wurden einige neue technologische Herausforderungen oder Einschränkungen im Zusammenhang mit der Prüfung von großformatigen Modulen identifiziert.

Nicht zuletzt hat die Entwicklung von (P<sub>k</sub>/Si)-Perowskit-Silizium-Tandemsolarzellen aufgrund ihres Potenzials, die Umwandlungseffizienzgrenze von (c-Si)-Kristallsilizium-Einzelzellen zu einem vorhersehbaren, erschwinglichen Preis zu überschreiten, erheblich an Bedeutung gewonnen. Daher war es das Ziel des Projekts, die Testmöglichkeiten des SUPSI PVLab für die aufkommende Perowskit-Technologie zu bewerten, beginnend mit PK-Einzelmodulen. Es wurde eine Software geschrieben, um die Module unter STC-Bedingungen gemäß einem vom ESTI des Joint Research Centre (JRC) entwickelten Testverfahren sowie im Freien unter variablen Lichtbedingungen und unterschiedlichen Spannungs-durchlaufzeiten zu testen. **Die SUPSI hat ihre Testanlage für PK-Einzelmodule aufgerüstet. Der nächste Schritt wird die Aufrüstung für die Prüfung von Mehrfach-Junction-Perowskit-Modulen und die Optimierung von Algorithmen zur Nachführung des maximalen Leistungspunkts sein, die es der SUPSI in Zukunft ermöglichen würden, PK/Si-Module in die Technologie-Benchmark-Kampagnen im Freien einzubeziehen.**



# Content

<b>Summary .....</b>	<b>3</b>
<b>Zusammenfassung.....</b>	<b>5</b>
<b>Abbreviations.....</b>	<b>8</b>
<b>1      Introduction .....</b>	<b>9</b>
<b>2      Project Objectives and Approach .....</b>	<b>10</b>
<b>3      Activities and Results.....</b>	<b>13</b>
3.1      Procurement of test modules .....	14
3.1.1      Description of c-Si high efficiency modules .....	14
3.1.2      Description of perovskite modules .....	15
3.2      Initial Characterization of high efficiency modules.....	17
3.2.1      Capacitive effect on STC performance and temperature coefficient measurements .....	18
3.2.2      Initial classification according STC power and Electroluminescence (EL) .....	20
3.2.3      Initial stabilisation (light soaking) .....	22
3.2.4      Measurement of T-coefficients, irradiance dependency and spectral response .....	24
3.3      First Characterisation of Perovskite Devices .....	26
3.3.1      Indoor measurement of perovskite mini-module.....	27
3.3.2      Outdoor measurement of perovskite mini-module.....	31
3.4      Improvements in flasher measurements.....	33
3.4.1      Assessment of characterization methods for capacitive modules .....	34
3.4.2      Enhanced Dragonback® Measurement.....	36
3.4.3      Validation of enhanced Dragonback® measurement .....	38
3.5      Measurement Round Robins .....	43
3.5.1      Power Matrix measurements (IEC 61853-1) .....	43
3.5.2      Light and temperature induced degradation (LeTID).....	47
3.6      Outdoor Measurements (test cycle 14).....	49
3.6.1      Test stands configuration .....	51
3.6.2      Energy yield benchmarking (30° inclination reference stand) .....	52
3.6.3      Energy yield benchmarking (10° inclination test stand).....	54
3.6.4      Analysis of degradation rates.....	56
3.6.5      Technology specific degradation modes .....	58
3.6.6      Benchmarking for shading tolerance .....	62
<b>4      Conclusions &amp; Outlook .....</b>	<b>64</b>
<b>5      Dissemination .....</b>	<b>68</b>
<b>6      References.....</b>	<b>69</b>
<b>7      Annexes .....</b>	<b>71</b>
Ciclo 14 Dragonback Validation.....	71
Pm Matrix Dragonback Validation .....	75
Monthly Performance inter-comparison of test cycle 14.....	77
Indoor STC measurements test cycle 14.....	78
Indoor STC measured $P_{max}$ respect to nominal power test cycle 14.....	79



## Abbreviations

BAPV	Building Applied Photovoltaics
BIPV	Building Integrated Photovoltaics
BS	Backsheet
CO2	Carbon dioxide
DB	Dragonback®
EL	Electroluminescence
EVA	Ethylene-vinyl acetate
FF	Fill factor
Gpoa	Plane of array irradiance
GW	Gigawatt
HJT	Heterojunction cell technology
IBC	Integrated back contact
IEC	International Electrotechnical Commission
Isc	Short-circuit current
IV	Current-Voltage
LCOE	Levelised cost of energy
LeTID	Light and elevated Temperature Induced Degradation
MQT	Module quality test
PERC	Passivated Emitter and Rear Cell
PID	Potential induced degradation
Pm	Maximum power measurement at STC
PR	Performance ratio
PRcor	Temperature corrected performance ratio
PV	Photovoltaics
PVB	Polyvinyl butyral
ROI	Return of investment
STC	Standard test condition
STL	Seasonal and trend decomposition with LOESS
Tmod	Module operating temperature
TWh	Terawatt-hour
USD	United States dollar
UTC	Coordinated Universal Time
UV	Ultraviolet
VI	Visual inspection
Voc	Open-circuit voltage
WL	Wet-leakage
YoY	Year-over-Year



# 1 Introduction

In Switzerland alone, the goal of carbon neutrality by 2050, set by the Federal Council in August 2019, will cost around CHF 12.9 billion per year, of which CHF 1.2 billion will be spent on the energy sector alone, [1] through the application of new, reliable and long-lasting technologies. With the urgent need to decarbonize the planet, the photovoltaic Industry is taking the lead of the energy transition and, to do so, is more and more focused on two parallel targets. The first one embraces the utilities' point of view on large scale PV plants, with the aim of reducing at the minimum the Levelised Cost Of Electricity (LCOE) in order to be competitive with plants based on combustion of fossil fuels. The second target is focused on the integration of the PV generation in construction sector: Building Integrated Photovoltaics (BIPV) is still far from being a mass market, but it represents a fundamental instrument for energy decentralization and de-carbonisation, particularly in Switzerland, where the potential for production of energy from roofs and façades is set at 67 TWh/year [2].

For both objectives, the continuous increase in the efficiency of PV modules is crucial: contact passivation technologies at cell level (e.g. PERC/PERT/PERL, TOPCon, heterojunction), new module layouts (bi-facial cells/modules, half-cut cells, shingled cells, etc.), new materials and contact types are being commercialised at an ever faster rate, with the need to accurately assess their performance and safety through the development of new international standards, the number of which "has increased from 16 in 2012 to a total of 44 today, with 38 ongoing projects, either revisions or amendments of existing standards (21) or new documents (17)", according to a paper by T. Sample presented at the 35th PVSEC in September 2018 [3].

The update and validation of these standards lags behind the diffusion of these products on the market: e.g. the larger solar cells initially adopted for main stream modules will be later introduced in BIPV modules, with shorter strings and increased capacitance, posing a problem for the precise measurement of these products. More in general, the need to implement effectively the procedures set by technical committees goes together with experiments for new characterisation techniques to automate the measurement process and keep the competences of the SUPSI PVLab aligned with the other institutes of research.



## 2 Project Objectives and Approach

A number of technological innovations have entered the market in recent years, driven by the availability of larger and more efficient c-Si solar cells and the introduction of new module designs, materials and manufacturing processes. Furthermore, the development of next-generation solar cells based on (P<sub>k</sub>/Si) perovskite-silicon tandem has gained significant traction in recent years due to its potential to exceed the conversion efficiency limit of (c-Si) crystalline silicon single junction at a foreseeable affordable cost. Crystalline silicon based cell technology has evolved from aluminium backsurface field (Al-BSF) cells to p-type passivated emitter and rear cell (PERC), and currently to n-type tunnel oxide passivation contact (TOPCon) and new silicon heterojunction (SHJ) cell concepts, together with cut cells with little or no gap between cells and new contact technologies such as multi-busbar, multi-wire, shingled solar cells without busbars, tiling ribbons, combined with new series parallel/connection concepts. Manufacturers of these new c-Si PV module technologies claim higher energy yields due to either lower resistive losses, higher power density, lower temperature coefficients, reduced shading losses or improved resistance to light-induced degradation effects such as LID or LeTID.

However, the very rapid introduction and combination of several technological innovations at the same time has led to new failures in the field, which were not always detected in advance, and which may affect the long-term reliability of PV systems installed today [15]. The occurrence of PID and LeTID in recent years is a good example of the risk of lagging behind field experience and testing standards, and how long it can take to identify, understand and mitigate a new problem.

There are three main objectives that are pursued in this project.

1. Support R&D and industry with scientific field data and insights into the electrical performance and degradation rates of these new mainstream module technologies.
2. Support industry with innovative test solutions that accurately and efficiently test the electrical performance of all market relevant PV module technologies.
3. Keep the competences of the SUPSI PVLab in line with the technological evolution expected in the coming years.

The main research questions and the approach taken in the project are listed here.

**Efficient testing of capacitive modules:** Increasing cell size and efficiency and the resulting increase in cell capacitance leads to a well-known measurement artefact in pulsed solar simulators. Whereas in the past the market share of this type of module was small, today almost all new modules tested at SUPSI PVLab fall into the category of capacitive modules and require special and time-consuming measurement techniques to ensure the same measurement uncertainty as for non-capacitive modules. New methods for faster testing are therefore crucial both for the industry, by reducing the time and cost of testing, and for R&D, by allowing more detailed and frequent testing. Different measurement solutions to overcome capacitive effects and known from literature have been tested and compared within this project and the best for our case has been selected for implementation. Preliminary validations were carried out on the modules purchased for this project, including high capacitance HJT and IBC modules.

**Accurate performance testing under variable irradiance and temperature conditions:** The energy yield of PV modules is highly dependent on their response to changes in irradiance and temperature. Accurate indoor I-V curve measurements over the full range of environmental conditions are the basis for any technology benchmarking or energy yield prediction. In the past, larger deviations compared to STC have been observed in low irradiance and temperature coefficient measurements due to spectral mismatch, irradiance matching and inhomogeneities, leading to the need to improve solar simulators and test procedures. Over the last few years, SUPSI PVLab has continuously upgraded its PASAN solar



simulators and test procedures for I-V and spectral response measurements to reduce measurement uncertainty for all module technologies available on the market and over the full range of test conditions described in Part 1 and Part 2 of the IEC 61853 energy rating standard. Validation of previous upgrades as well as the improved method for capacitive modules in this project has been achieved through participation in the first international power matrix laboratory inter-comparison to our knowledge.

**Demonstration of technological differences in the field:** The measured energy yield of a module in the field is explained not only by the module characteristics described in Part 1 and Part 2 of the IEC 61853 Energy Rating standard, but also by the stability of the measured parameters over time. Degradation or metastability issues related to cell technology, module design or manufacturing quality also affect performance. To understand the technological differences claimed by manufacturers (e.g. better low irradiance performance, lower thermal losses, lower degradation rates) and their impact on energy yield, both indoor and outdoor measurements need to be performed. Outdoor measurements are generally performed on modules mounted in open rack conditions and oriented for maximum energy yield. However, deviations from optimal conditions can be useful to better understand the impact of cell and module design on energy production and degradation rates of modules mounted in unconventional conditions, such as buildings with PV facades or roof-mounted systems. One of the main objectives of this project was to investigate the advantages and disadvantages of various technological innovations introduced in recent years by monitoring them under optimal and sub-optimal 10° tilt conditions, representing typical rack-mounted flat-roof systems in Switzerland with reduced air circulation and increased soiling. The data collected is intended to show how technological differences are reflected in energy production and to identify any early degradation issues. A new measurement campaign "Test Cycle 14" was therefore initiated at SUPSI with a selection of commercial monofacial crystalline silicon PV module technologies that dominate or are expected to enter the European market very soon, representing the 4 main cell technologies available on the market today (PERC, TOPCon, HJT and IBC). Bifacial modules were excluded due to space constraints at the SUPSI campus test facility. In other projects, the purchase of more modules has been foreseen to perform tests under harsher or accelerated test conditions. In the future, Test Cycle 14 will also serve as a reference test for other projects. The limited number of technologies tested within the project does not allow generalisation to any specific technology, but represents case studies and provides the basis for accurate benchmarking and degradation studies.

**Accuracy of technology benchmarking and degradation rate determination:** Technology benchmarking is highly dependent on the choice of key performance indicator (KPI) used for ranking (e.g.  $Y_{rel}$  [kWh/Wp],  $Y_a$ [kW/m<sup>2</sup>]), the associated measurement uncertainties, the stability over time (e.g. initial degradation, metastability or long-term degradation), the time period considered (e.g. month, single year or multiple years) and the environmental conditions (e.g. tilt, ventilation, shading). Different methods are used in the PV community to calculate degradation rates, based either on indoor measurements or on outdoor monitoring data, and lead to different results, which can differ significantly from the derating claimed in warranty declarations. Different approaches will be compared and analysed to better understand the technological differences and the origin of degradation. Monitoring data will therefore be combined with punctual electrical power measurements such as low irradiance measurements and optical measurements such as electroluminescence and visual inspections. Stabilisation techniques will be applied and tested on modules purchased for this project, including PERC modules.

**Testing requirements for new generation perovskite modules:** Perovskite technology is severely affected by meta-stabilities and slow response times in the order of minutes, requiring the use of steady-state light sources to measure I-V curves and the adaptation of maximum power point tracking electronics for outdoor testing. Maximum power point trackers and IV tracers developed for c-Si modules need to be adapted at both HW and SW level to measure PK modules, and temperature control and simultaneous monitoring of all environmental parameters needs to be introduced. Within this project, SUPSI PVLab will continue to upgrade the existing test facilities with the support of the first laminated test



samples. The aim is not so much the accuracy of the measurements themselves, but rather to identify the limitations of the current test equipment, in particular the electronic loads, and to adapt it for outdoor testing.

As a result, the following outcomes are expected from the project:

- Support industry with high-precision, fast and cost-effective STC performance and energy rating measurements according to IEC 61853-1 for all market-relevant technologies, including high-capacitive modules.
- Foster innovation and encourage PV module manufacturers to optimise PV cell and module technology for energy yield and not just efficiency and STC performance.
- Monitor early degradation issues related to cell technology, module design or manufacturing quality.
- Contribute to improving the accuracy of long-term energy prediction models and warranty statements, and provide guidance on standardised quantification of degradation rates.
- Support standardisation bodies in the validation of new test methods for PV module characterisation (e.g. LeTID testing, shading losses).
- Support ongoing or future R&D projects with reference module field data and long-term scientific data.
- Provide the basis for future perovskite testing at SUPSI PVLab.



### 3 Activities and Results

**Background:** A large number of technological innovations entered the market over the last years driven by the availability of larger and more efficient solar cells and the introduction of new module concepts and materials as well as new manufacturing processes. Cell technologies changed basically from aluminium back surface field (Al-BSF) cells to p-type passivated emitter and rear cell (PERC) dominating the market at the start of this project, to emerging n-type tunnel oxide passivating contact (TOPCon) and new silicon heterojunction cell concepts (SHJ). On module level the trend went towards cutted cells with little or no gap between cells and new contact technologies as e.g. multi-bus bar, multi-wire, shingled solar cells without busbars, tiling ribbon technology, in combination with new series parallel/connection concepts. Manufacturers of these new c-Si PV module technologies claim higher energy yields due to either lower resistive losses, higher power density, lower temperature coefficients, or improved resistance to light induced degradation effects as LID or LeTID. The new cell-interconnection concepts promise reduced shading losses as well as lower risk of hot spots and an enhanced tolerance for mechanical loads. But as described by J. Zuboy, many of these technological trends introduce module reliability risks which has to be assessed [15]. Beside crystalline silicon modules, the development of next-generation solar cells based on (Pk/Si) perovskite-silicon tandem has gained significant traction in recent years, due to its potential of surpassing the (c-Si) crystalline silicon single-junction conversion efficiency limit with foreseeably an affordable cost, but did not reached the market until now.

**Scope:** SUPSI PVLab started already in the early 90s with the monitoring of commercial PV modules for the purpose of energy yield benchmarking and performance studies. The measurement campaigns (test cycles), each lasting 2-4 years, have tracked the evolution of crystalline silicon PV modules with first generation HJT and IBC technologies entering the market, followed by the new thin-film technologies (12th test cycle in 2011), coloured and bifacial technology (13th test cycle in 2018). The recent and fast transition to new cell and module technologies described above, motivated the initiation of a new measurement campaign. The aim is to test mainstream technologies recently appeared on the market and to collect first experience with perovskite prototypes. The test modules chosen for the 14th test cycle are here described in more detail.

**Results:** The focus of test cycle 14 was set on commercial monofacial crystalline-silicon PV technologies dominating or foreseen to enter the European market very soon. Bifacial modules were excluded for reasons of space on the test facility of the SUPSI Campus. The original idea for the selection of technologies has evolved toward the adoption of 7 different module types with 4 types of high efficiency cells (PERC, TOPCon, HJT, IBC), different cell dimensions, including third cut solar cells from 210mm wafer, different contacting methods (multi-bus bar, smart-wire, back contact, shingled solar cells without busbars) and a new module layout with a single diode per cell representing shadow resistant modules. The n-type TOPCon technology was still difficult to retrieve at that time of the project start and p-type had to be chosen instead. 4 out of 7 modules (PERC half-cut, HJT half-cut, IBC and PERC shingled) were furthermore included into another project dealing with the reliability testing of building integrated modules. The outdoor facility (test cycle 14) is so dealing as reference system. The unavailability of (Pk/Si) perovskite-silicon tandem modules for outdoor testing leaded to the decision to focus on the preliminary testing of single junction mini-modules from a Swiss manufacturer.



### 3.1 Procurement of test modules

#### 3.1.1 Description of c-Si high efficiency modules

The market offers a large range of different c-Si products which can differ in performance and reliability. Figure 1 and Table 1 shows the characteristics of the 7 commercial monofacial PV module technologies chosen for test cycle 14: 4 different PERC modules (half-cut, third-cut, five-cut shingled and full-cell modules with integrated bypass diodes), 1 TOPCon half-cut, 1 IBC full-cell and 1 HJT half-cut module technology. The idea was to test the mainstream cell technologies which aims in increasing either efficiency or reduce the cost of solar energy.

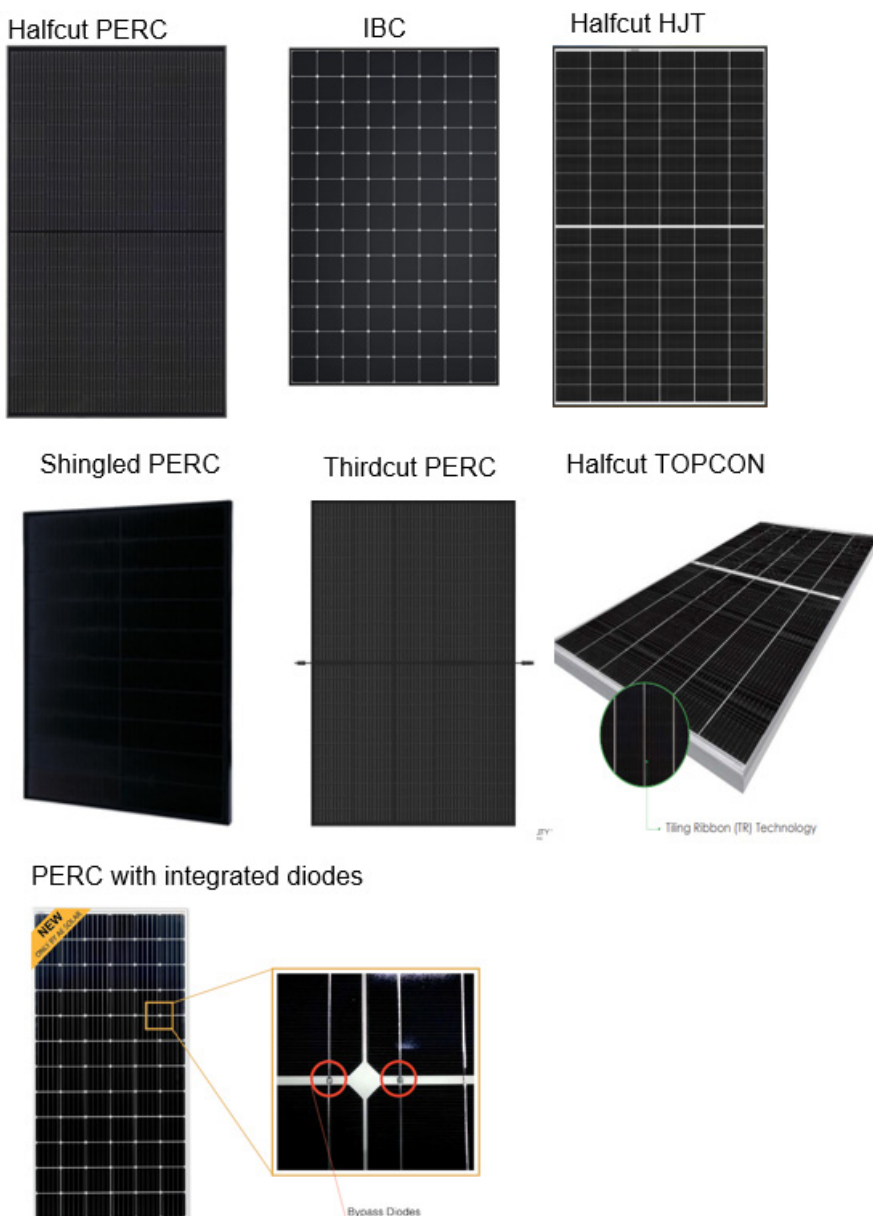


Figure 1: pictures of the different technologies selected for ATTRACT



Label	Cell technology	Wafer size	Cell cuts	Contact technology	Name-plate power	n° test modules (ATTRACT / REBI / REF)
Tech 1	mono p-type PERC	M6	half-cut	365	365 W	15 (5/8/2)
Tech 2	mono p-type PERC	M12	third-cut	9 BB	385 W	4 (3/-/1)
Tech 3	mono p-type PERC	M2	5-cut	shingled	365 W	10 (5/3/2)
Tech 4	mono p-type TOP-CON	M6	half-cut	tiling ribbons	470 W	4 (3/-/1)
Tech 5	mono n-type IBC	M2	full size	back contact	400 W	15 (3/8/4)
Tech 6	mono n-type HJT	M2	half-cut	smart wire	375 W	15 (3/8/4)
Tech 7	mono p-type PERC	M2	full size	5 BB, 60 diodes	320 W	4 (3/-/1)

Table 1: Overview of module technologies and number of modules purchased within the project.

The last column in Table 1 reports the number of modules procured in the frame of the project. Some of the modules are also part of the REBI-PV project co-funded by SNF/BFE, (IZ-COZ0\_182976/1;SI/501982-01) dealing with the reliability testing of building integrated PV modules. A minimum of 1 reference/type is stored in the dark for the purpose of stability control or as spare modules.

### 3.1.2 Description of perovskite modules

Beside mainstream c-Si modules, the project envisaged the procurement of some innovative module technologies. The device selected for this activity was a single junction perovskite mini-module, provided by the Swiss company Solaronix and shown in Figure 2. The device consists in a single junction perovskite mini module encapsulated with hot-melt thermoplastic film and polysobutylene (PIB) edge sealant. The device has been realized with a focus on the stability of the active material rather than the efficiency of the module.

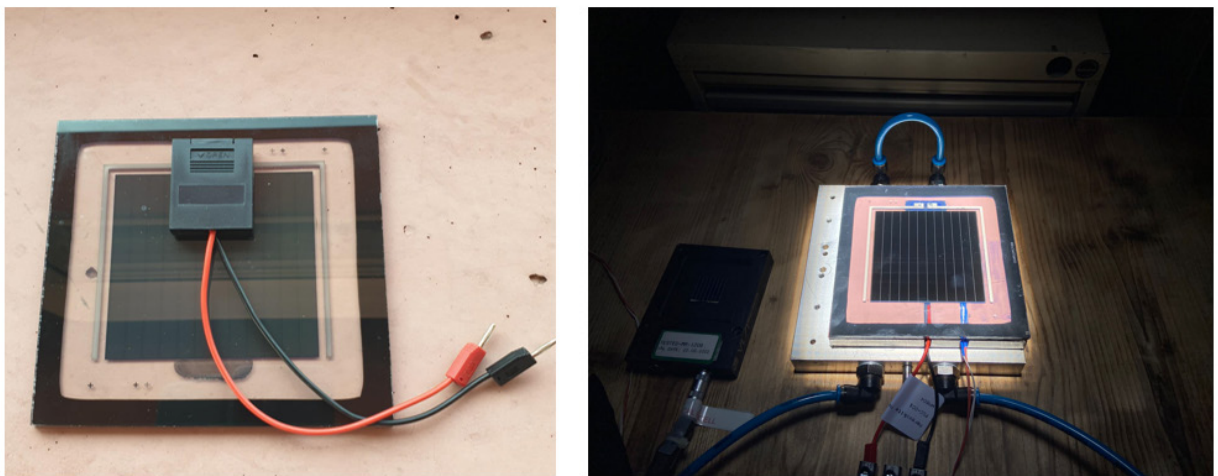


Figure 2: Encapsulated mini-module with hot-melt thermoplastic film and a polysobutylene (PIB) edge sealant



The specifications of the mini-module is shown in Table 2. The electrical parameters of the device are presented as indicative values due to the fact that the device did not undergo a full certification and the testing activities performed on this technology were limited to the quality check performed by the manufacturer.

Datasheet	
<b>Manufacturer</b>	Solaronix
<b>Size</b>	12.5 x 12.5 cm <sup>2</sup>
<b>Active Area</b>	56.79 cm <sup>2</sup>
<b>V<sub>oc</sub></b>	~11 V
<b>I<sub>sc</sub></b>	~100 mA

Table 2: Solaronix single junction perovskite mini-module datasheet



## 3.2 Initial Characterization of high efficiency modules

**Background:** An adequate inter-comparison of different PV technologies is only possible if the STC power and its uncertainty are known. The nameplate or nominal power  $P_{nom}$  as declared by the manufacturer is generally considered as the less adequate for an inter-comparison, because it differs from the real power due to manufacturing tolerance, measurement uncertainty and commercial labelling strategies. Modules which are not stabilized before measuring the STC power can furthermore lead to misleading results. The IEC 61215 standard defines both, the stabilisation procedures as well as power declaration requirements.

To understand over- or under-performance of one technology with respect to another under specific climatic conditions, the individual sources of loss with respect to the power under standard test conditions have to be quantified. The IEC 61853-1 and 61853-2 describes the procedures to measure the effects of temperature, irradiance, spectrum, angle of incidence and environmental conditions (as wind speed and mounting configuration) on the output power of a PV module.

**Scope:** The scope of the initial characterisation of test cycle 14 modules is:

- to quantify the impact of module capacitance on the I-V measurement with a 10ms pulsed solar simulator and to set the methodology for the measurement of all consecutive measurements
- to stabilise the modules before outdoor exposure and quantify any initial light induced degradation rates which could affect energy rating benchmarking
- to measure the real installed STC power of the modules to be used as reference value for the calculation of the specific energy yield or performance ratio
- to assess module parameters influencing the energy yield (e.g. irradiance, temperature and spectral dependency).
- to assess the initial conditions (electrical and visual performance) of the modules as reference to measurements after outdoor exposure, later used to detect and analyse degradation
- to identify any damaged or low quality modules to be excluded from the technology benchmarking study in the field
- to assess the conformity of the manufacturer declarations

**Results:** According to the internal procedure of SUPSI PVLab all 7 module types resulted to be affected by capacitive effects in such way to require the multi-flash approach to be used instead of the faster standard I-V sweep method. The PERC modules are very little affected compared to the high efficiency technologies, with IBC and HJT showing errors around 10%. It was demonstrated that temperature coefficient measurements are also affected by the module capacitance. As next multi-flash measurements and EL images were performed and used to qualify the modules. 4 out of 7 products resulted to have average STC power below the tolerance limit of the minimum nameplate power specified by the standards. The EL images highlighted some minor visual defects in PERC shingled modules and 1 IBC module with some minor cell cracks, both not affecting performance. Except for a few outliers, the pre-conditioning tests performed under artificial light demonstrated minor initial degradation rates not exceeding -0.6%. The HJT showed a technology specific increase in power of around 0.8%. Once stabilised the modules underwent a full electrical characterisation to quantify the irradiance, temperature and spectral dependency of each technology. As expected, the  $P_{max}$  temperature coefficients depends on cell technology and ranges from  $-0.26\text{%/}^{\circ}\text{C}$  to  $-0.38\text{%/}^{\circ}\text{C}$ , with HJT and IBC having the lowest temperature coefficients, whereas low irradiance performance depends mainly on the manufacturing process with some differences and larger intra-batch variations for shingled and diode integrated modules. Spectral response differences in the UV and IR range are observed in the modules.



### 3.2.1 Capacitive effect on STC performance and temperature coefficient measurements

It is well known that the cell diffusion capacitance in high-efficiency solar cells generates transient loss (or gain) of power when these products are electrically characterized with fast voltage sweeps. Different possibilities are available to overcome this issue, but each of them brings important differences in terms of measurement flexibility, time required, precision and feasibility.

In SUPSI PVLab the procedure to reduce the uncertainty related to the measurement of highly capacitive modules is performed through a multi-flash method based upon the results of a preliminary capacitance test as illustrated in the picture below. The multi-flash method represents one of the most accurate measurement techniques for the electrical characterisation. It is mainly used by metrology or ISO17025 accredited laboratories (due to its time-consuming nature) and it consists in measuring the I-V by sampling it in different step, where the voltage level is kept constant, and the current has enough time to stabilize and compensate the capacitive effect. The difference between the single flash measurement performed with a direct forward sweep and the multi-flash measurement determines which method to use. The threshold is set to a 0.5% difference between the two.

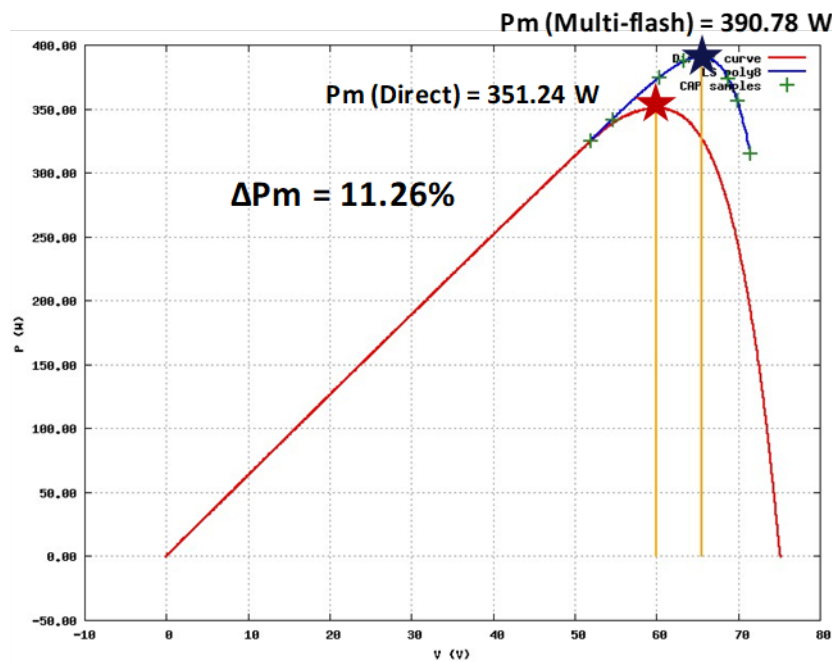


Figure 3: Result of the capacitance test (I-V single sweep in red, points sampled for the cap test in green)

In the following table, we can see the classification of the ATTRACT modules according to the difference in  $P_{max}$  between the single flash and multi-flash measurement. As expected, the highest capacitive effect is shown by the n-type IBC and HJT technologies, followed by TOPCon and by the mono PERC family, having lower module capacitances related to the cell area and module layout (number of cells in series  $N_s$  and parallel  $N_p$ ), following the formula [3]:

$$C_{eff,mod} = \frac{N_p}{N_s} \cdot C_{eff,cell}$$



Cell Technology	Wafer size and cell area [cm <sup>2</sup> ]	No. of cells in series / parallel	SUPSI-PVLab				
			ΔP%	P <sub>m</sub> [W]	V <sub>oc</sub> [V]	I <sub>sc</sub> [A]	FF [%]
Mono p-type PERC	M6 (Halfcut) 137.7	60/2	<b>0.51</b>	356.5	40.93	10.95	79.5
Mono p-type PERC	(Shingled-5cut) 46.5	4(18)/5	<b>0.51</b>	349.1	48.1	9.28	78.2
Mono p-type PERC	M12 (Thirdcut) 147	60/2	<b>1.07</b>	382.1	41.064	11.73	79.4
Mono p-type PERC	M2 245.71	60/1	<b>1.36</b>	301.3	40.671	9.82	75.5
Mono p-type TOPCon	M6 (Halfcut) 137.7	78/2	<b>4.43</b>	470.2	54.778	10.68	80.4
Mono n-type HJT	M2 (Halfcut) 127.44	60/2	<b>8.94</b>	359	44.358	10.19	79.4
Mono n-type IBC	152.7	104/1	<b>11.3</b>	388.8	75.981	6.34	80.5

Table 3: Initial measurements and capacitive test results (ΔP% - difference between single flash and multi-flash measurement)

One of the test activities where a fast and precise electrical performance measurement is very important, is the determination of the temperature coefficients: in this activity, the time needed for a multi-flash approach is struggling with the temporal stability and uniformity of the temperature inside the thermal box, particularly at the higher temperatures, that are also the most important for the evaluation of real performances on the field. In Figure 4 some results of the comparison between temperature coefficients determined with a single flash and with multi-flash method are reported. As it can be seen from the difference between the two values, the temperature dependency of the module capacitance is leading to an error in the determination of the P<sub>max</sub> temperature coefficients (9), which is increasing with increasing module capacitance. Multi-flash measurements have been therefore chosen for the final determination of the P<sub>max</sub> temperature coefficients (see 4.2.2).

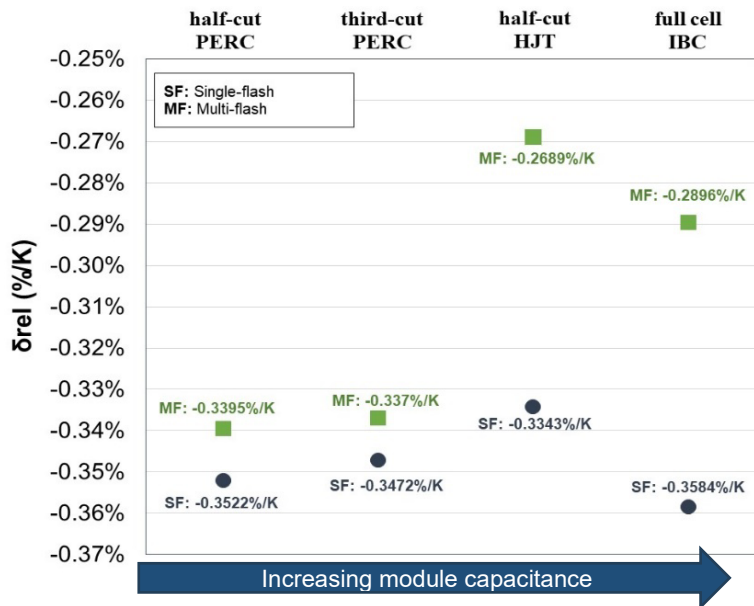


Figure 4: Temperature coefficients and impact of capacitance

### 3.2.2 Initial classification according STC power and Electroluminescence (EL)

Before installing the modules outdoors, an intensive campaign for the characterization of the whole batch of modules was carried out using of the highest precision IV curve characterization method, corresponding to the multi-flash method. The table below shows the results with the categorisation according to the IEC 60215-1:2021 criteria for the product qualification. All the modules fell in category B or C, and in most cases did not fulfil the minimum requirements specified in the IEC norm. The TOPCon modules could here not be classified because of the unavailability of data sheets values.

<b>A+:</b> $P_m > \text{Rated power} + \text{measurement uncertainty}$	<b>B:</b> $P_m > \text{Rated power} - (\text{measurement uncertainty} + \text{min. declared power tolerance } t_1)$
<b>A:</b> $P_m > \text{Label nominal PMAX independently on measurement unc. and tol.}$	<b>C:</b> $P_m < \text{B class limit}$

Cell Technology	Pm [W]		Module Class. (IEC 61215-1:2021)			
	SUPSI (mean)	Datasheet	A+	A	B	C
Mono p-type PERC	355.1	365 (0/+5 W)	-	-	8.3% [1]	91.7% [11]
Mono p-type PERC	350.5	365 (0/+3%)	-	-	-	100% [6]
Mono p-type PERC	380.9	385 (0/+5 W)	-	-	100% [4]	-
Mono p-type PERC	301.1	320 (0/+5 W)	-	-	-	100% [3]
Mono n-type Ntopcon	470.2	-	No DS	No DS	No DS	No DS
Mono n-type HJT	359.9	375 (0/+5 W)	-	-	-	100% [4]
Mono n-type IBC	387.5	400 (0/+5 W)	-	-	-	100% [12]

Table 4: Classification of modules according to IEC 61215-1:2021 (gate1) Legend: [number of tested modules].



Cell Technology	EL – Module Classification (IEA PVPS T13)			
	A+	A	B	C
Mono p-type PERC	100% (15)	-	-	-
Mono p-type PERC	-	-	-	100% (6)
Mono p-type PERC	100% (4)	-	-	-
Mono p-type PERC	100% (4)	-	-	-
Mono n-type Ntopcon	15% (1)	75% (3)	-	-
Mono n-type HJT	80% (12)	20% (3)	-	-
Mono n-type IBC	26.7% (4)	66.7% (10)	-	6.6% (1)

Table 5: Classification of modules according to IEA Task 13 criteria for electroluminescence. Legend: (number of tested modules).

The analysis of electroluminescence (EL) images highlighted some further problems related to shingled modules and IBC ones, as reported in the table and figures below:

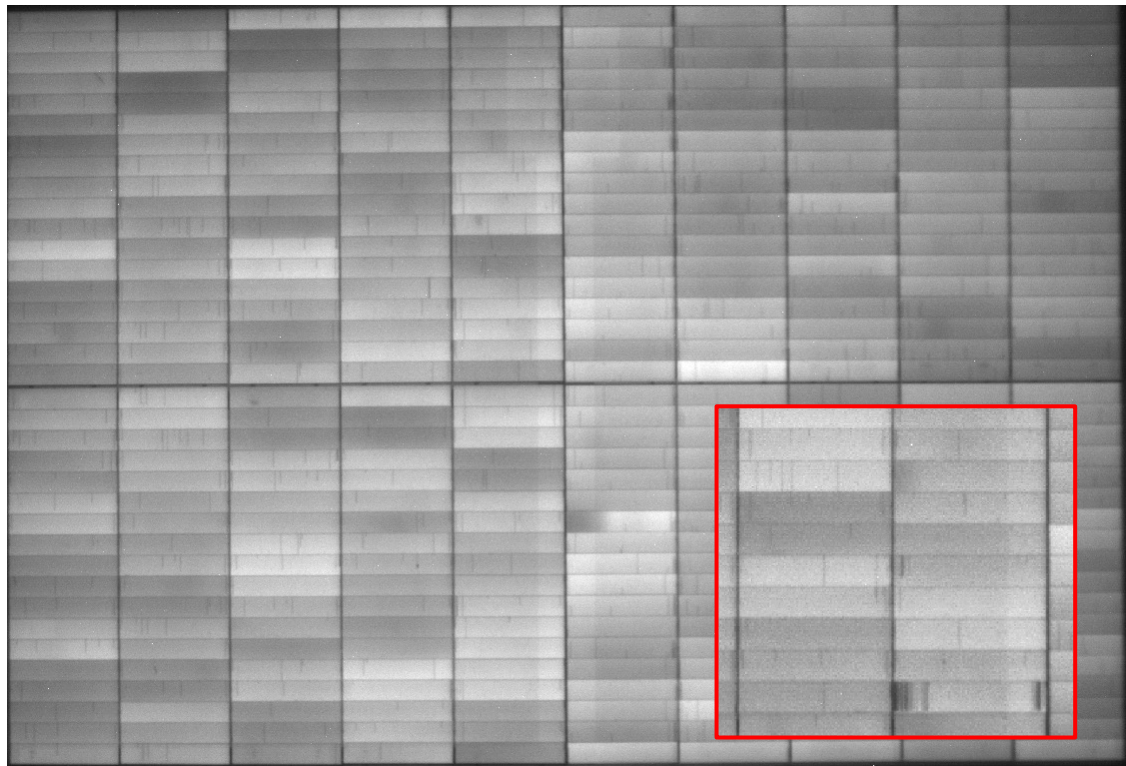


Figure 5: Defects of shingled PERC modules: mismatched cells and grid fingers problems

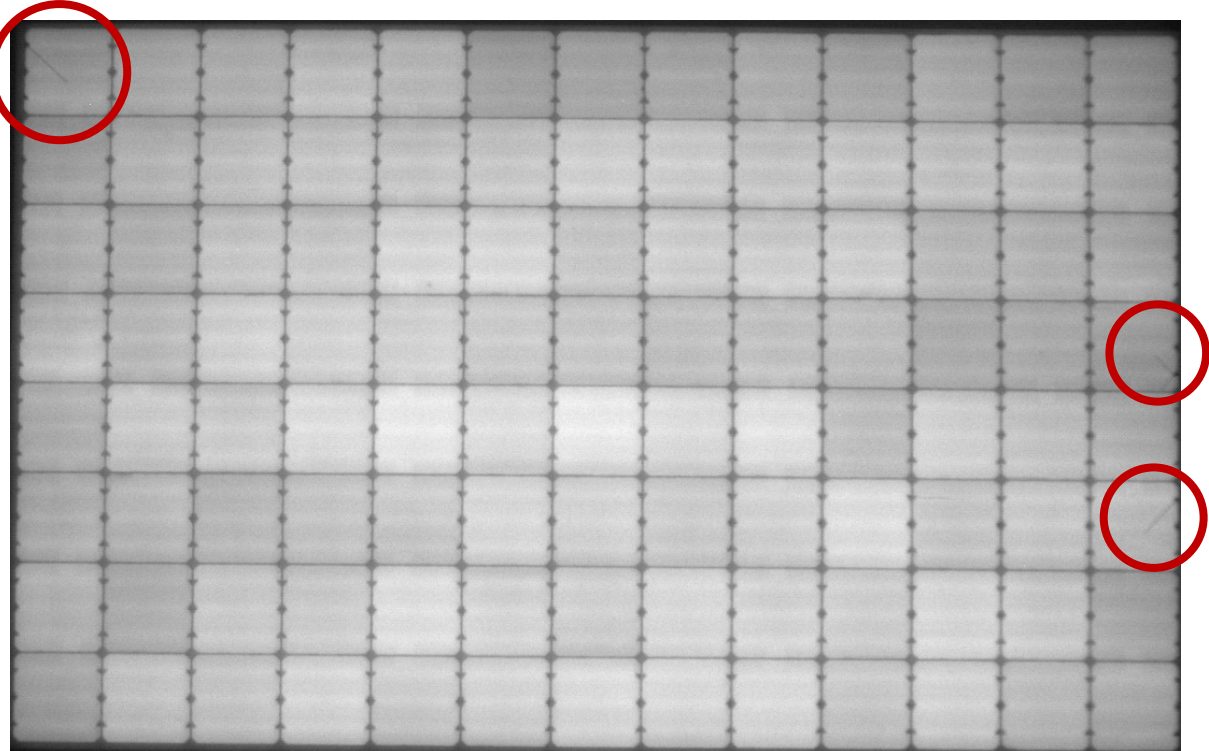


Figure 6: IBC module, cracks from cells interconnectors

### 3.2.3 Initial stabilisation (light soaking)

Before being classified (see chapter 3.2.2) all modules were stabilised. Different techniques were employed in order to properly stabilise the modules. For the reference ones, to be stored in dark as witnesses, the procedure included in the IEC 61215 standard was applied with the results illustrated in the Figure 7.

The STC power of the modules was measured before and after stabilization. The modules, stabilized under a steady state simulator, were therefore connected to a MPP-tracker and the temperature was maintained in the range of  $50 \pm 10^\circ\text{C}$ . Figure 7 shows the results of the power measured at the begin and after the first (LS1) and second light soaking step (LS2) consisting each in at least  $5 \text{ kWh/m}^2$ . The first number in the figure gives the degradation rate of the reference module, whereas in brackets are reported the mean and standard deviation of degradation rates of the other tested modules. The number of tested samples is represented by the last value. A significant variability within the same module types is observed, with HJT and TOPCon showing a positive trend whereas the others are generally characterized by slight negative trends of maximum  $-0.6\%$ . The only exception are the shingled modules showing slightly higher degradation rates up to  $-1.36\%$ , with no clear stabilization even after three light soaking periods. In general, we can say that:

- Mono p-type PERC shows very low degradation.
- IBC n-type, shows a decrease in power of  $-0.53\%$  (decrease in  $\text{Voc}$   $(-0.25\%)$ ,  $\text{Isc}$   $(-0.17\%)$  and  $\text{FF}$   $(-0.12\%)$ )
- HJT shows an increase in power and fill factor, most probably due to improvement in surface-passivation [4], [5], [6]

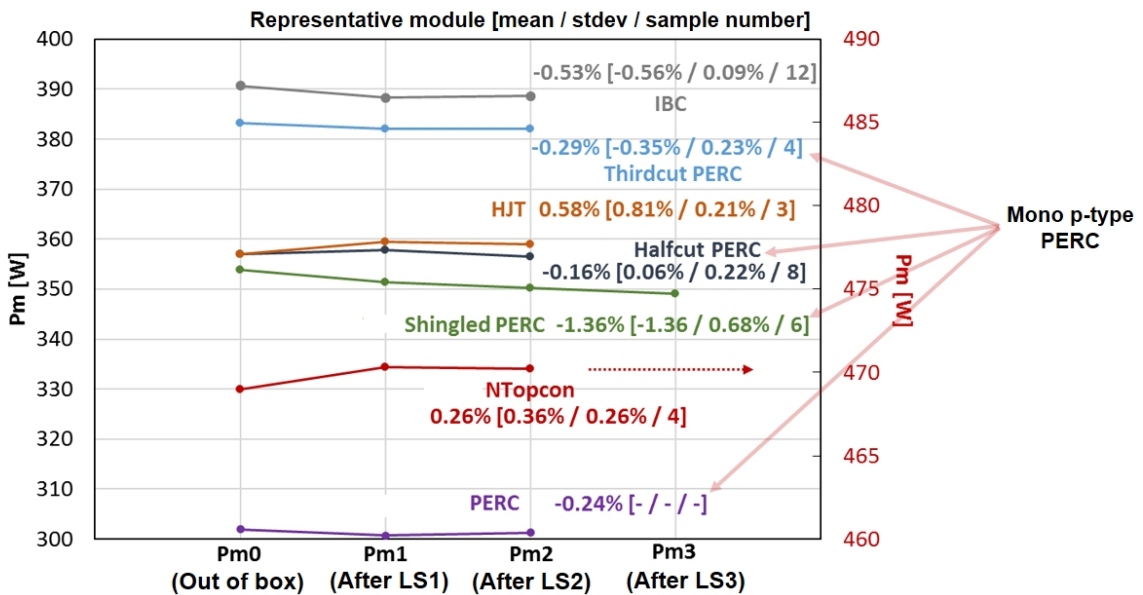


Figure 7: Stabilisation paths of the different technologies

In order to speed up the stabilization activities and compare the outdoor exposure to indoor setup, some modules were exposed outdoor, in two separate steps or in a single one: we found some differences, shown in Figure 8. Investigations about the origin of the higher degradation under outdoor conditions are still ongoing.

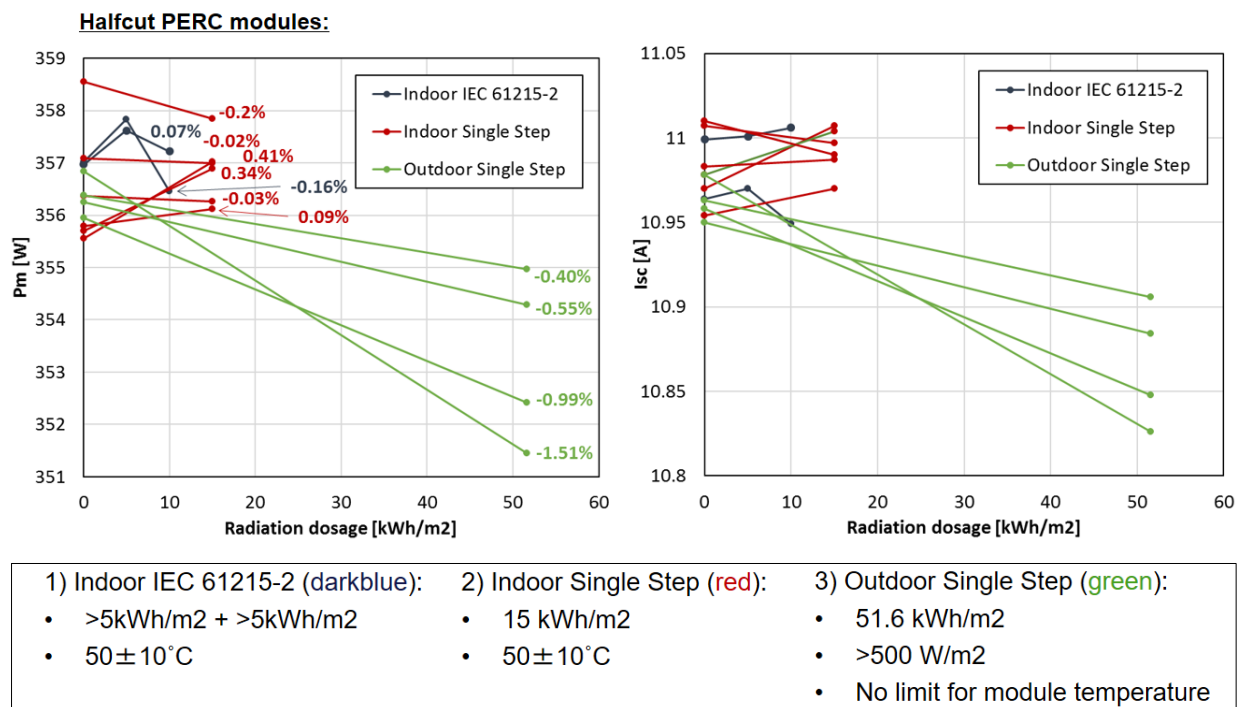


Figure 8: Stabilisation paths indoor vs outdoor for halfcut PERC modules

### 3.2.4 Measurement of temperature coefficients, irradiance dependency and spectral response

Afterwards, the previously stabilised modules underwent a full electrical characterisation to quantify the irradiance, temperature and spectral dependency. To save time and due to the to be expected low variation within a test batch, the last two (temperature coefficient and spectral response measurements) were limited to 1 module/type, whereas the irradiance dependency was measured for all modules.

The measured temperature coefficients of  $P_{max}$  and respective data sheet values are depicted in Figure 9. The datasheet values are all within the limits of the PVLab measurement uncertainty. The TOP-Con module couldn't be measured because exceeding the size of our thermal chamber.

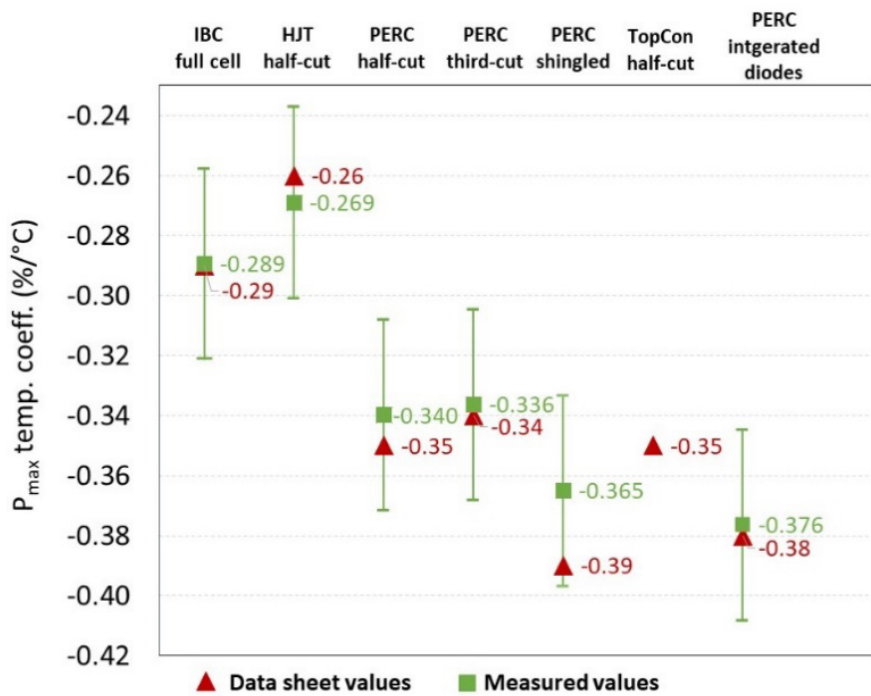


Figure 9: Measured temperature coefficients respect to data sheet values

The relative efficiency change with irradiance of all modules is shown in Figure 10. The modules with integrated bypass diodes and shingled cells shows a higher variation within the tested batch. The electrical performances at low light give important feedback on the quality of solar cells and inter-connections, highlighting the presence of local and border shunts. The good performances of the “hotspot free” PERC module with integrated diodes (1 diode per cell) is due to an increase of the series resistance caused by the bypass diodes. At the same time, this results in lower STC and FF power, which is reflected in lower efficiency compared to the other PERC module types. The shingled PERCs modules present the worst performance, confirming the quality issues detected also through electroluminescence images.

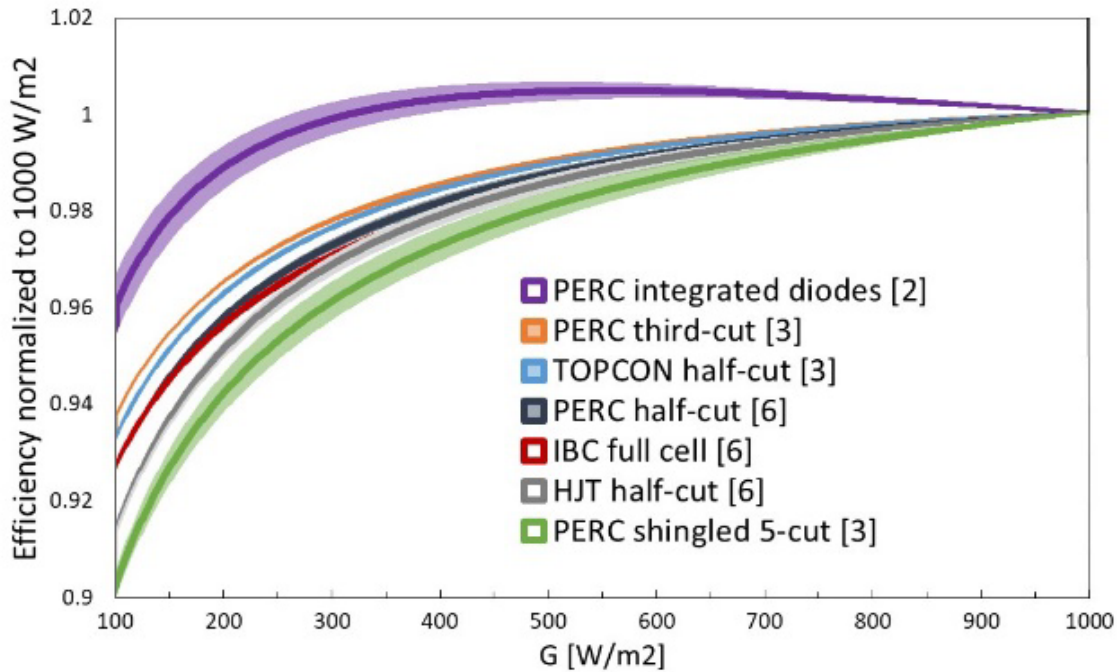


Figure 10: Irradiance dependency of relative module efficiency, measured at 25°C, for all 7 module technologies, together with the variability within the module batch (sample numbers are in brackets).

For completeness, the relative spectral response (SR) of all 7 module technologies were measured. The measurements were performed with a class AAA solar simulator equipped with 28 spectral bandpass filters. Figure 11 shows the normalised SR curves. The curves are normalized respect to its maximum. Differences in SR are mainly driven by the cell technology and the front layers. The differences concentrate in the UV range and in minor extend in the infrared. The HJT module shows the largest deviation which will lead to the largest deviations when operating under variable spectral conditions in the field.

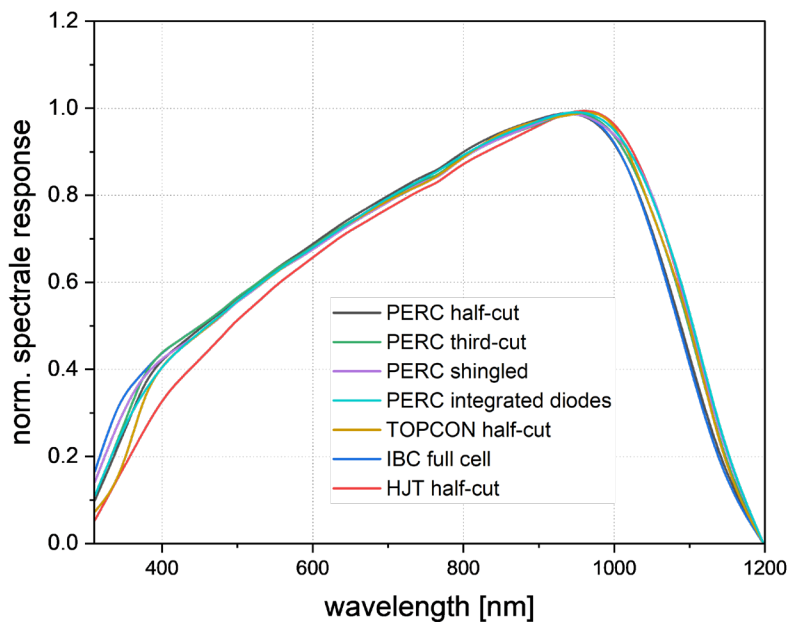


Figure 11 : Normalized spectral response curves of test cycle 14 technologies.



### 3.3 First Characterisation of Perovskite Devices

**Background:** Perovskite PV modules represent a cutting-edge advancement in solar energy, this is due to the fact that these devices have shown a great potential in terms of high efficiency and cost effectiveness. However the intrinsic metastability of the active material, the long term stability, the degradation under real world conditions and the maturity of the technology bring challenges regarding their electrical characterisation. A standard procedure for the characterisation of these devices has not yet been determined, however some laboratories have proposed their own methodology and the research in this topic is quite active. Determine the most accurate and stable characterisation method is a key task in order to guarantee the development of this technology and address the critical barriers to mass adoption of this technology in the solar energy market.

**Scope:** This task aims to enhance the capabilities of SUPSI PVLab in the field of perovskite PV modules. The scope includes upgrading the current hardware to support advanced research and experimentation with perovskite PV technologies. The objective is to conduct a comprehensive study to identify and implement the most effective characterization methods for these devices, based on the current status of the research, and to assess the precision and reliability of acquired data. Additionally, the project involves developing a first preliminary outdoor monitoring system to evaluate the real-world performance of perovskite PV devices and gather the knowledge required to perform a long-term outdoor measurement campaign.

#### Results:

- After the procurement of single junction perovskite modules SUPSI has started the research activities related to the electrical characterization of this type of devices. After attending some conference and discussing with other research institutes the activity has started and a first indoor electrical characterization has been performed.
- The I-V curve of the device has been measured by using a Xenon lamp based solar simulator and two different acquisition systems: MPPT3000 and Keithley 2612a. Both trials were successful and the I-V curve of the device has been obtained by using the measurement procedure developed by the ESTI research centre at JRC [10]. The data obtained have been analysed and the results compared with the one reported by JRC. Some discrepancies were noted, especially in terms of maximum power and open circuit voltage. This could be related to the fact that the device has been measured after 3 months of dark storage so an analysis on the preconditioning tests needed for the stabilisation, or the assessment of the stability of the device, should have been performed.
- For the outdoor measurement a LabVIEW® software has been developed in order to control the Keithley 2612a and acquire the I-V curve with a slow voltage sweep. The irradiance has been recorded with a pyranometer and the temperature with a PT100 sensor.
- The voltage sweep time and number of samples acquired was changed in order to define the best output result. The sweep time has been varied from 250s to 600s with a number of sampling points that was increased from 25 to 30. The 600s (10 min) long voltage sweep was the one that presented the best results. Hysteresis effects are mitigated by the long voltage sweep.
- The algorithm for the maximum power point tracking needs to be further developed in order to perform long-term outdoor measurement campaigns.



### 3.3.1 Indoor measurement of perovskite mini-module

This chapter describes the measurement performed on the perovskite module that has been introduced in paragraph 3.1.2. The datasheet of the test sample provided by the manufacturer contains approximate values because the sample was not characterized in a certified laboratory. At the current status a standard procedure for the determination of the main parameters of a perovskite module does not exist in the IEC standards [9]. Every laboratory measures the modules following their own procedure for the electrical characterization. In order to perform an outdoor measurement it has been decided to first fully characterize the mini-module at STC in controlled indoor environment.

After visiting the JRC ESTI laboratory it has been decided to follow their procedure [10] for the indoor characterization. The proposed testing procedure by JRC can be simplified as follows:

- a) Initial I-V sweep
- b) Definition of  $P_m$
- c) Change the voltage step-wise towards  $I_{sc}$
- d) Move back to  $P_m$
- e) Change the voltage step-wise towards  $V_{oc}$
- f) Move back to  $P_m$
- g) Repeat the sequence (b)-(f)
- h) Final I-V sweep for comparison

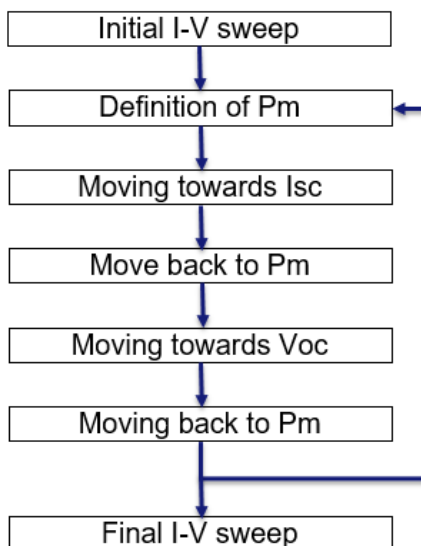


Figure 12: Proposed measurement method by JRC to measure perovskite modules.[10]

The procedure is a long and iterative method where it is possible to assess the stability of the sample by repeating the measurement multiple times in order to find a stable value for the maximum power. Degradation mechanisms and metastability processes might occur in the device, meaning that the measurement of the I-V curve of perovskite modules is a quite challenging task.

Before starting the measurement an analysis on the most suitable light source has been performed. Perovskite materials have a slow light response, meaning a pulsed simulator is not suitable for the characterization. The only option for measuring these devices is using a steady-state simulator.



At SUPSI PVLab two options are available, a Xenon lamp simulator (Oriel) and a LED simulator (Alfartec Blue Sky MT100). The two simulators and their light spectrum are shown in Figure 13. The LED simulator has a wavelength range from about 380 nm to 800 nm, which is suitable for the device, on the other hand the Xenon lamp simulator has a full range wavelength in line with the IEC specification for STC characterization.

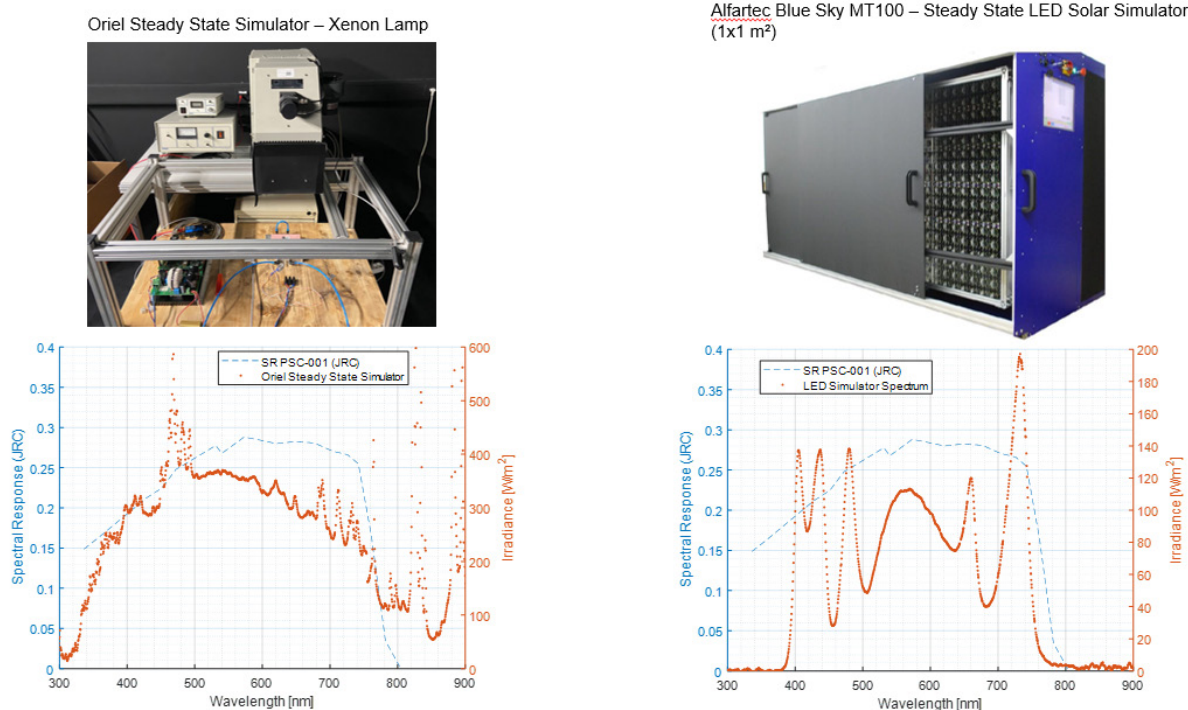


Figure 13: Solar simulator available at SUPSI PVLab

For the test it has been decided to use the Oriel steady state simulator due to the fact that the thermal management of the lamp is working better compared to the LED simulator, especially for many hours of continuous illumination. The setup prepared for the LED simulator is shown in Figure 14.

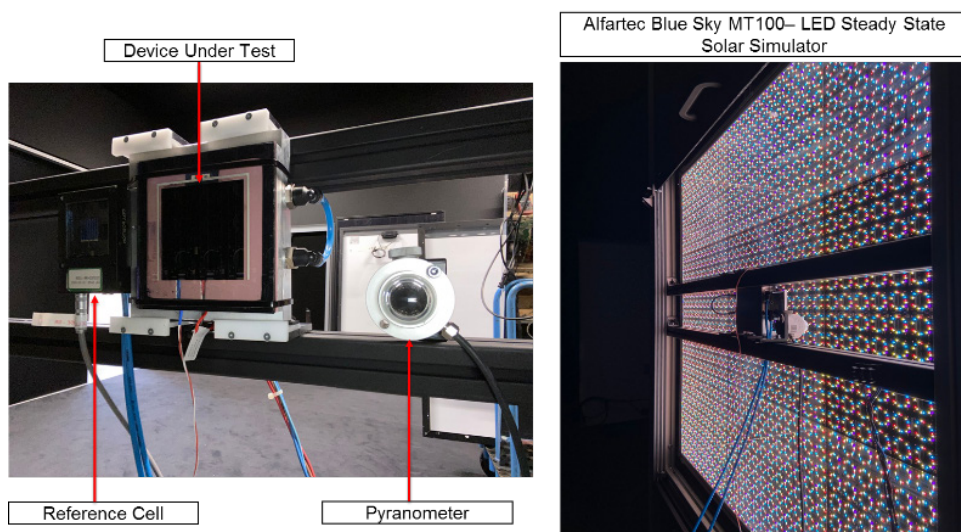


Figure 14: LED solar simulator measurement setup



In order to acquire the electrical parameters of the module the MPPT3000 has been modified for reading low currents and a long sweep time was implemented. However due to license problems it was not possible to modify the firmware of the device so the maximum sweep time is about 60 seconds. The setup for the measurement is shown in Figure 15.

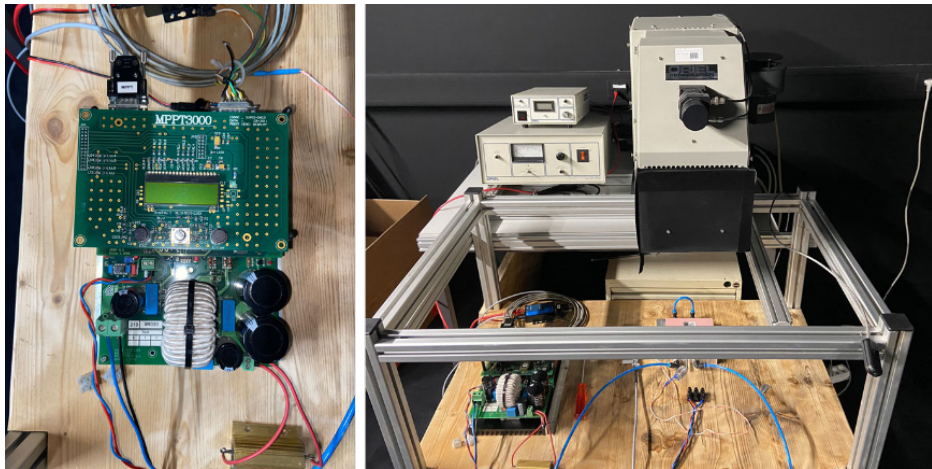


Figure 15: (Left) Modified MPPT3000 for perovskite. (Right) ORIEL – Steady state solar simulator.

In Figure 16 are shown some of the most important steps of the measurement. On the left there is the first initial I-V sweep, where the module is characterized right after a first initial stabilization obtained through light exposure. The sweep time used for this first I-V curve was 10 seconds. We can clearly see that sweep time is not enough to obtain a correct I-V curve due to the slow response of perovskite devices. In the middle is shown the step C of the procedure; after finding the maximum power point of the device the voltage set by the MPPT3000 is decreased stepwise towards  $I_{sc}$ . After this step the voltage is set back at the maximum power level and a second measurement is made in order to verify that the maximum power point was not changed. On the right is shown the step E, where the voltage is increased stepwise towards  $V_{oc}$ .

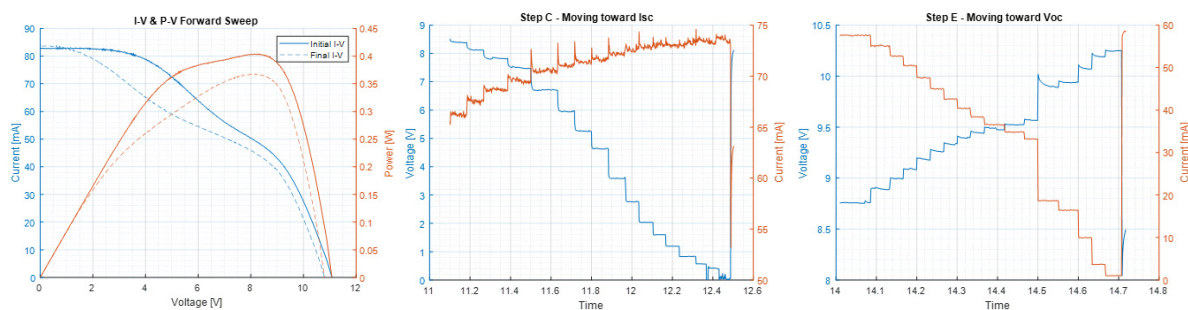


Figure 16: (Left) The initial step of the procedure. (Middle) Step C of the procedure. (Right) Step E of the procedure.

As shown in Figure 17, the mini-module's temperature was within  $25 \pm 0.5$  °C during the whole measurement. This was able by using a cooling plate (visible in Figure 2) connected to a chiller. The whole measurement procedure required almost 7 hours to be completed.

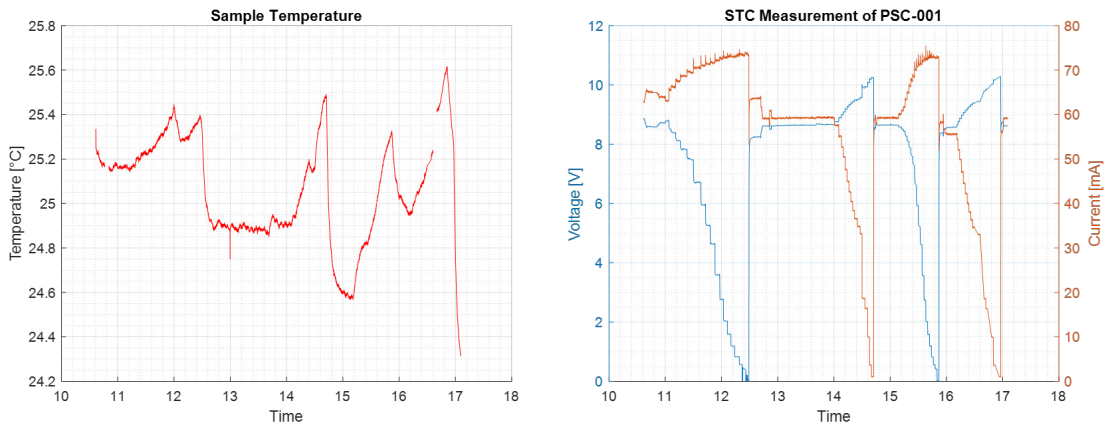


Figure 17: (Left) Temperature during the measurement procedure. (Right) Voltage and Current profiles during the measurement procedure.

After the first measurement with the MPPT3000 has been decided to carry out another measurement at STC using a second device, the Source Measurement Unit (SMU) Keithley 2612a. This device has a current range of 100 nA to 10A and high accuracy for low currents. The whole measurement procedure has been repeated with this second device and the results of the indoor characterization are shown in Table 6 and the I-V curves in Figure 18.

	JRC	SUPSI (MPPT)	SUPSI (Keithley)	$\Delta\%$ (MPPT)	$\Delta\%$ (Keithley)
I <sub>sc</sub>	75.58 mA	72.98 mA	75.46 mA	-3.44%	-0.15%
V <sub>oc</sub>	10.89 V	10.25 V	10.4 V	-5.90%	-4.50%
P <sub>m</sub>	0.61 W	0.52 W	0.55 W	-14.80%	-9.84%
I <sub>m</sub>	68.78 mA	63.35 mA	64.6 mA	-7.90%	-6.08%
V <sub>m</sub>	8.95 V	8.27 V	8.5 V	-7.64%	-5.03%

Table 6: Indoor measurements summary

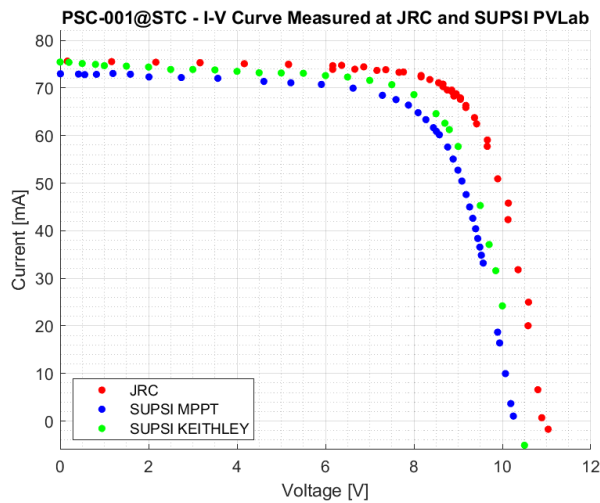


Figure 18: I-V curves indoor measurements.

The device has been measured for the first time (MPPT3000) after 3 months of dark storage. This type of device is particularly sensible to the conditions of storage and the discrepancies with the JRC measurement might be caused by this or due to the device stability. The results of the round-robin on perovskite measurements carried out by the METRO-PV project partners will provide more information about the stability of the device.

### 3.3.2 Outdoor measurement of perovskite mini-module

The Keithley SMU has proven to be a very flexible device and due to the firmware issues of the MPPT3000 it has been decided to use it for the outdoor measurements. A LabVIEW® software has been implemented in order to control the SMU and acquire the I-V curves automatically. With this unit the sweep time for measuring the I-V curves can be set without limits, some tests have been performed in order to find the most effective time and accuracy combination.

The perovskite mini-module have been mounted with a tilt angle of 30° and an Azimuth of 0°. The structure has been moved during the day in order to track the sun, a temperature sensor has been placed on the back of the module and the irradiance has been measured with a pyranometer. The outdoor measurement setup is shown in Figure 19.

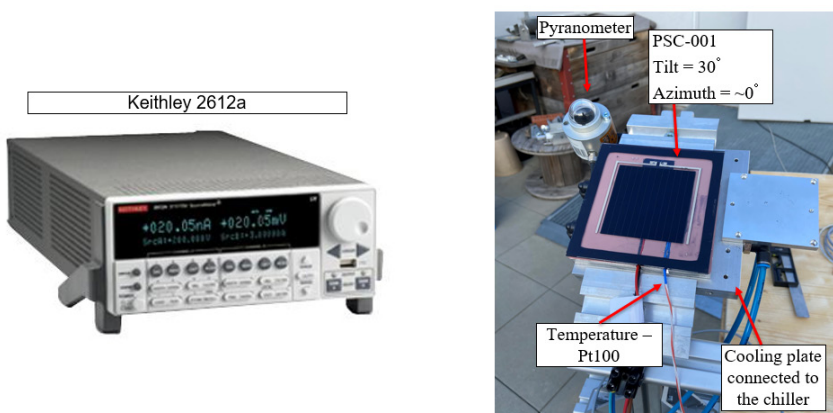


Figure 19: Outdoor measurement setup



The device has been measured using different combination of parameters such as sweep time and number of sampled points. The sweep time has been gradually increased in order to identify the best compromise between time and curve shape. The algorithm implemented in LabVIEW® set a voltage level and keep it constant for a period of time that is related to the number of points and the sweep time:

$$t_p = t_{sweep}/n_{points}$$

The summary of the outdoor test performed is shown in Table 7. The I-V curves have been irradiance corrected in order to have a significant comparison between them and defining the most suitable combination of sweep time and points. With a sweep time of 600s and 30 points every voltage step is kept at a constant level for 20 seconds. The I-V curve shape has lower hysteresis effects compared to the other tests, however a 10 minutes long measurement becomes challenging for an outdoor campaign. This is due to the fact that the weather conditions can change quite fast in this time period so a major correction is needed and this introduce a higher uncertainty to the data recorded.

Test	Sweep Time	N° Points	G avg	T avg
Test 1	250s	25	850 W/m <sup>2</sup>	21.5
Test 2	250s	25	885 W/m <sup>2</sup>	22.3
Test 3	300s	30	905 W/m <sup>2</sup>	22.7
Test 4	600s	30	942 W/m <sup>2</sup>	22.8

Table 7: Outdoor measurements parameters

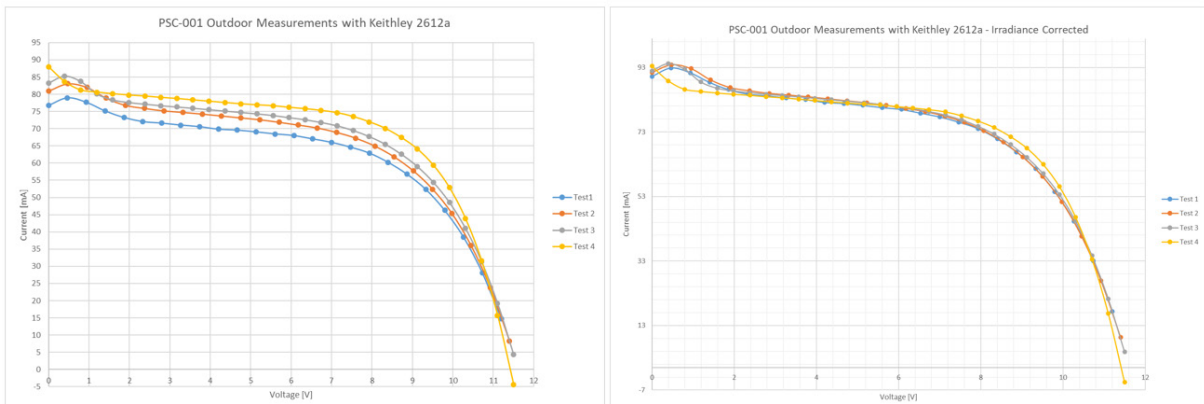


Figure 20: (Left) Perovskite outdoor measurement (Right) Perovskite outdoor measurement, irradiance corrected

A strategy for the future measurements might be focusing more on the maximum power tracking of the device rather than all the parameters of the I-V curve. The ones that are more affected by the sweep time are the voltage levels close to  $I_{sc}$  and the short circuit current itself.

Developing a new hardware specifically made for perovskite outdoor measurements would overcome all the challenges encountered during this project. Research on the most appropriated algorithm needs to be performed and then tested on different perovskite devices in order to tune it for various stability and metastability behaviours.



### 3.4 Improvements in flasher measurements

**Background:** In the recent years the industry have faced an increase of capacitive module in the market. This trend has reached a point where the majority of modules arriving at our laboratory require testing methods that specifically account for capacitive behavior. While the current multi-flash (MF) approach provides accurate results, it is both time-consuming and hardware-intensive. In collaboration with SUPSI PVLab in 2012 PASAN developed the dragon-back® method which allows to measure capacitive modules in production environment where high throughputs are required, but with practical limitations for test laboratories. The challenge is even more pronounced when testing small modules with only a few cells in series. These modules, often used for product optimization/prototyping purposes, exhibit increased capacitance in conjunction with lower voltages, making accurate measurement particularly difficult.

This situation imposes substantial limitations on research and development efforts due to the high costs and complexities associated with testing. Although new LED simulators present a potential alternative for testing, due to their long pulse (flash) that compensate the capacitive behavior, they come with their own set of challenges. These simulators are not only expensive but also introduce issues related to spectrum adjustment and thermal stability, which can further complicate the testing process. As a result, the industry and in particular our laboratory face a pressing need for more efficient, cost-effective, and reliable testing methods to keep pace with the evolving characteristics of PV modules.

**Scope:** The scope of this task is improving the overall efficiency and precision of the laboratory by: Comparing different techniques for the testing of a capacitive modules on a PASAN solar simulator and select the most effective for the laboratory while maintaining a good measurement uncertainty. The focus is on finding the most time effective solution due to the time consuming nature of the current approach (multi-flash) for the electrical characterization of PV modules. - Overcoming the measurements issues brought by modules with low voltage and high capacitive effects through a fine tune of the multi-flash recipe.

#### Results:

- An analysis regarding the electrical characterization method for high efficiency modules has been conducted. A adapted dragon-back (DB) method has been selected as potential alternative approach among all the candidates (capacitance correction, multi-sectional and DB). A software has been developed in order to deal with the raw data analysis and interpolations required by the method.
- The whole matrix measurement using the DB method has been performed on different modules, resulting in an effective measurement time reduced by 10 times (limited to the electrical characterisation only), compared to the multi-flash approach (7 hours for a full matrix with MF respect to 45 minutes for DB).
- The measurement of low voltage capacitive modules was implemented through a precise tuning of the measurement recipe. A standard recipe for module with low open circuit voltage ( $V_{oc} < 10$  V) have been created. This guarantees a fast and accurate characterisation of prototypes or samples coming from the industry using the multi-flash approach.



### 3.4.1 Assessment of characterization methods for capacitive modules

Various measurement methods (multi-flash, Dragonback®, multi-sectional, dark IV translation, etc.) have been introduced over the years to solve capacitive induced measurement artefacts. One of the most accurate and straightforward methods for capacitive modules, applicable also with 10ms pulsed solar simulators, is the multi-flash approach, in which multiple measurements are performed at fixed voltages. The data from each flash are interpolated to have the complete current-voltage (I-V) curve. However, since about 23-25 flashes are necessary, this method takes around 15 minutes, while a single flash takes less than 1 minute. The measurement of the power matrix requires 22 I-V curves at different irradiance and temperature conditions ranging from 100-1100 W/m<sup>2</sup> and 15-75°C. With the multi-flash method, the effective measurement (without considering the time needed to stabilize the temperature) can take more than 5 hours. A faster measurement of a complete power matrix is strategic for the test laboratories and industry.

In order to define the most time and cost-effective characterization method for the I-V curve measurement few methods have been taken into consideration and analysed. The summary list of the characterization techniques can be found in Table 8. The following methods have been selected as main candidates: 1) Capacitance correction 2) Dark I-V 3) Multi-sectional 4) Dragonback®.

approach	description	applicability	limitations	use within ATTRACT
Single I-V sweep	Fast voltage sweep from Isc to Voc within single flash.	Non-capacitive modules	Underestimates the power of capacitive modules.	Worst case REFERENCE measurement.
Multi-flash measurement	Fixed voltage within multiple flashes.	Most capacitive modules.	Time consuming and high usage of lamp. Non standard modules (e.g reduced number of cells, ultra large cells, ...) are more complex to be measured with the PASAN SW.	Best case REFERENCE measurement for standard high efficiency modules. Optimization for non-standard modules. To be verified for ultra-high capacitive modules.
Steady state measurement	Slow voltage sweep with a steady state solar simulator.	All modules	Requires a Class A+ steady state solar simulator.	Best case REFERENCE measurement. To be performed on a selected number of modules with external simulators (e.g SPF LED simulator by applying spectral correction or JRC large area Xenon steady state simulator).
Triangular pulse	Forward and backward measurement within single flash.	Determination of the presence of capacitive problems (YES/NO).	Under or overestimates the power of capacitive modules.	To be implemented as CAP TEST in alternative to current approach and for the testing of OPTION 3
Multi-sectional measurement	Reduced voltage sweeps within multiple flashes.	Low capacitive modules.	A reconstruction of the I-V curve is required.	TESTOPTION 1 for low capacitive modules.
Dragon back method	Single saw tooth like voltage ramp within single flash.	Most capacitive modules. Mainly for in-line testing in production.	Complex procedure for the determination of the appropriate saw tooth parameters.	TESTOPTION 2 only for repetitive measurements and with an optimization of the parameter setting procedure.
Dark I-V method	I-V curve correction based on steady state and transient dark I-V curves.	To be validated for different technologies.	Accuracy is limited by the accuracy of the series resistance Rs used for the correction.	TESTOPTION 3 to be validated. Very attractive because of the need of a single flash only.
I-V curve correction method	I-V curve correction based on theoretical models and additional measurements (e.g dark impedance)	To be validated for different technologies.	Accuracy is limited by the accuracy of the correction parameters.	TESTOPTION 4 to be validated. Alternative or in combination with OPTION 3.

Table 8: Summary of the characterization techniques under investigation.

The first that has been tested is the capacitance correction. This method uses a single triangular sweep or two flashes in order to have two I-V curves. The first I-V curve is the one obtained from the forward sweep (from Isc to Voc) while the second one is obtained from the reverse sweep (from Voc to Isc). If the module has high capacitive effects the I-V curve obtained with reverse sweep will have a severe overshoot near the maximum power. A correction is then applied to the two curves in order to calculate the final I-V curve that takes into account the capacitive behaviour of the module.

This method has shown good results for low capacitive modules, however for technologies such as HJT or IBC it has been proven to be not the most effective approach. This is due to the fact that the correction is more accurate for pulse length higher than the laboratory's flasher capability (>10 ms). As shown in Figure 21 the correction is not working for high capacitance modules.

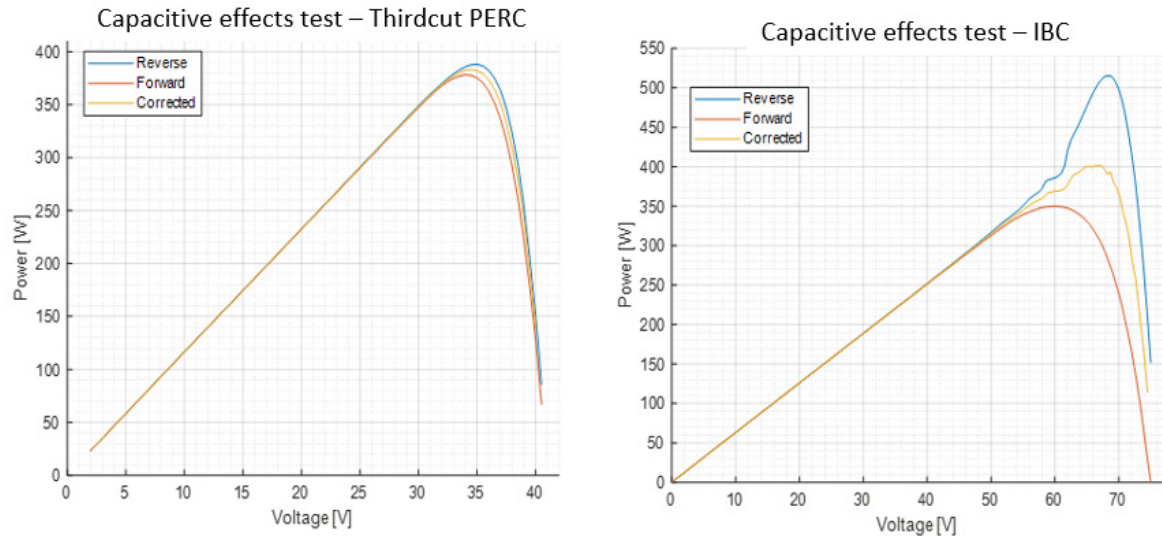


Figure 21: Capacitance correction (Left) Third-cut PERC, low capacitive effects (Right) IBC, high capacitive effects

The dark I-V method have been partially implemented during the project, however some issues with the electronic load from PASAN have been encountered. At the current status is not possible to set the sweep time resulting in an underestimation of the maximum power of the module.

The multi-sectional method has shown great potential in terms of precision and time. However the voltage sweep for every section needs to be set precisely. This initial calibration of the recipe might require some time and several trials might be needed in order to find the most accurate measurement.

As shown in Figure 22 for a sectional measurement of an IBC module at least 4 flashes are needed in order to obtain an I-V curve, however we can clearly see that some parts of the curve are missing meaning that an interpolation is needed in order to recreate the full I-V curve.

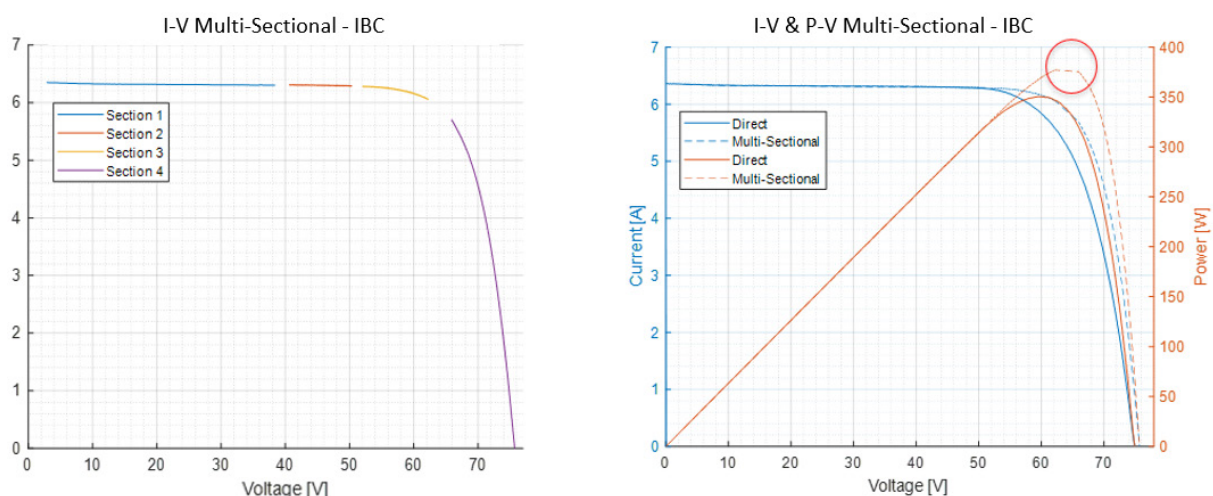


Figure 22: Multi-sectional measurement



This method has been discarded because of the time constraints, even though it has been proven to be a potential candidate for replacing the multi-flash measurement. For high capacitive modules the multi-sectional approach leads to an underestimation of the maximum power and finding the most suitable combination of flashes becomes challenging. The underestimation of the maximum power can be avoided by increasing the number of flashes, however this strongly reduces the advantage of this method. In addition to this, a multi-flash measurement is needed in order to calibrate the recipe meaning that this method can be more suitable for measuring a batch of modules rather than just a single measurement.

By considering all the previous points it has been decided to focus more on other characterization methods that use a different approach and a reduced number of flashes, such as the Dragonback® method.

### 3.4.2 Enhanced Dragonback® Measurement

The DB approach has been identified as the most promising and time efficient characterization method for capacitive modules. Following the guidelines given in [3][7] some experiments have been carried out. This characterization method consists in applying a customized initial voltage sweep that consists in short stationary steps where  $dV/dt=0$ . Different configurations of the initial voltage sweep have been tested as shown in Figure 23 and the most effective one has been identified as a combination of 3 flashes: one direct sweep (from -3.5V to  $V_{oc}$ ) and two DB flashes. This configuration has been proven effective on both low and high capacitive modules at STC and different irradiance values. Compared to the other two versions of the initial sweep an increased number of stable points can be obtained easily by adjusting the voltage of the last two sweeps in order to fine-tune it for the maximum power and open-circuit voltage.

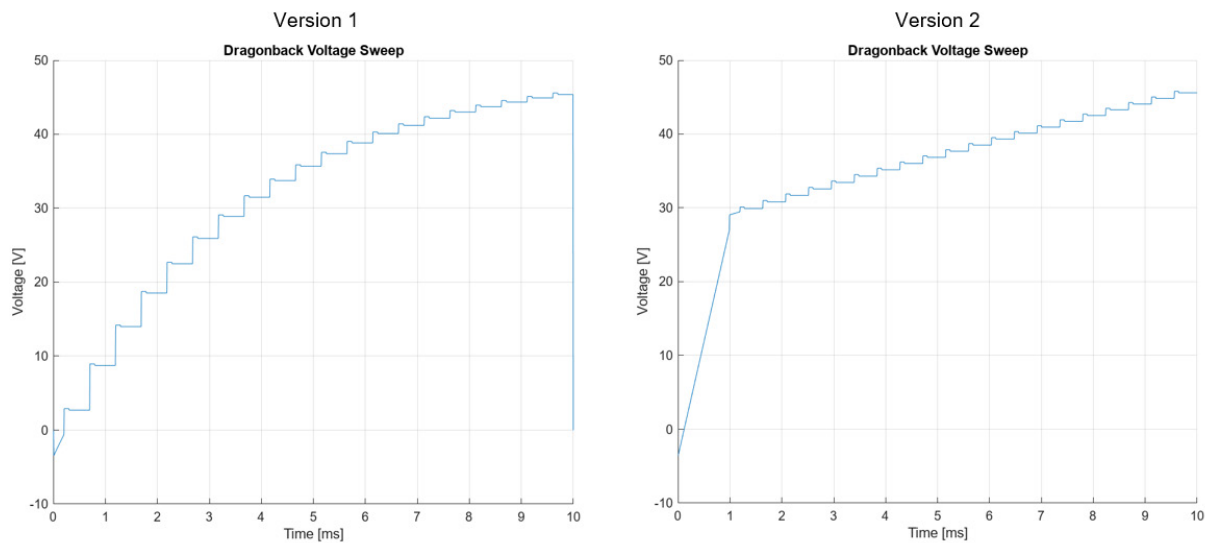


Figure 23: DB voltage sweep profiles (v1 and v2)

After the definition of the initial sweep an analysis on the results is required. In order to have the I-V curve of the module the data needs to be filtered to define the stable points that correspond to the voltage and current values for the stationary part of the sweep. After the selection of the stable points the results are interpolated and the I-V curve of the module is obtained.

Considering that the first part of the I-V curve is not affected by the capacitive behaviour of the module, it has been decided to use the results obtained with the first direct voltage sweep in order to obtain the



data used for the interpolated I-V curve. This is also due to the fact that few stable points are obtained in this section of the curve and often the results are outliers that have a huge impact on the curve shape and final results.

The approach used consists of three flashes where the first one is a direct I-V sweep and is used in order to find the values from  $I_{sc}$  to  $0.7 \cdot P_{max}$ . The second flash is a DB sweep and is used in order to find all the stable point near the maximum power point. The last DB flash is finally used to determine the values around  $V_{oc}$ , which is one of the parameters most affected by the capacitive behaviour of the module. The composition of the I-V curve and the final results are shown in Figure 24 and Figure 25.

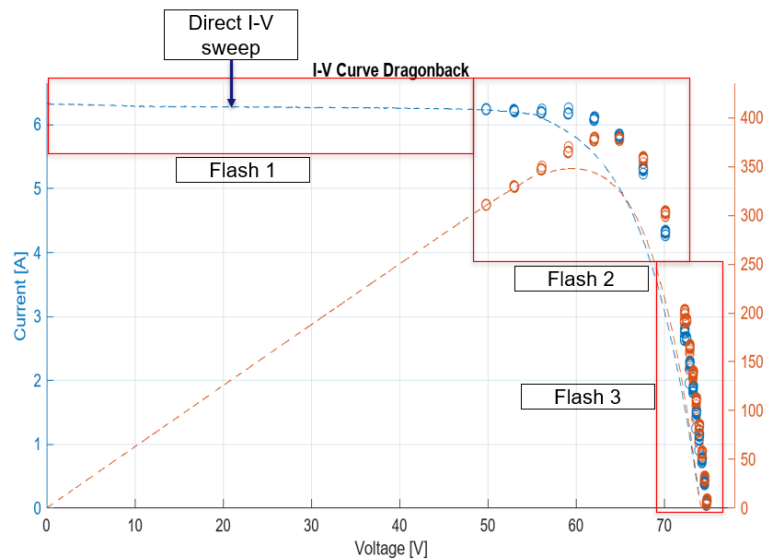


Figure 24: DB 3 flash measurement results

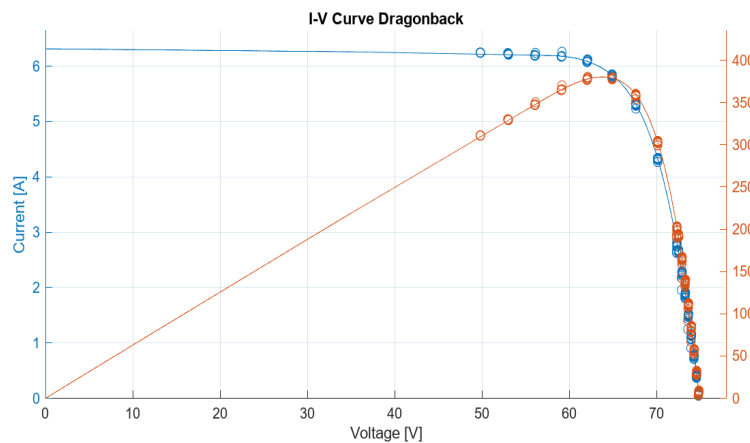


Figure 25: DB I-V curve

In order to perform the data analysis a software has been developed using MATLAB® programming language. The software has been organized in two tabs, where in the first one is possible to easily generate the initial voltage sweep and in the second tab the analysis of the results can be performed. The data can also be exported in a format compatible with the current requirements of the laboratory in



terms of data storage. This means that the data can actually be uploaded on the SUPSI PVLab web tool and used by the researchers in the same way as the multi-flash measurement. An overview of the main panel of the software is shown in Figure 26.

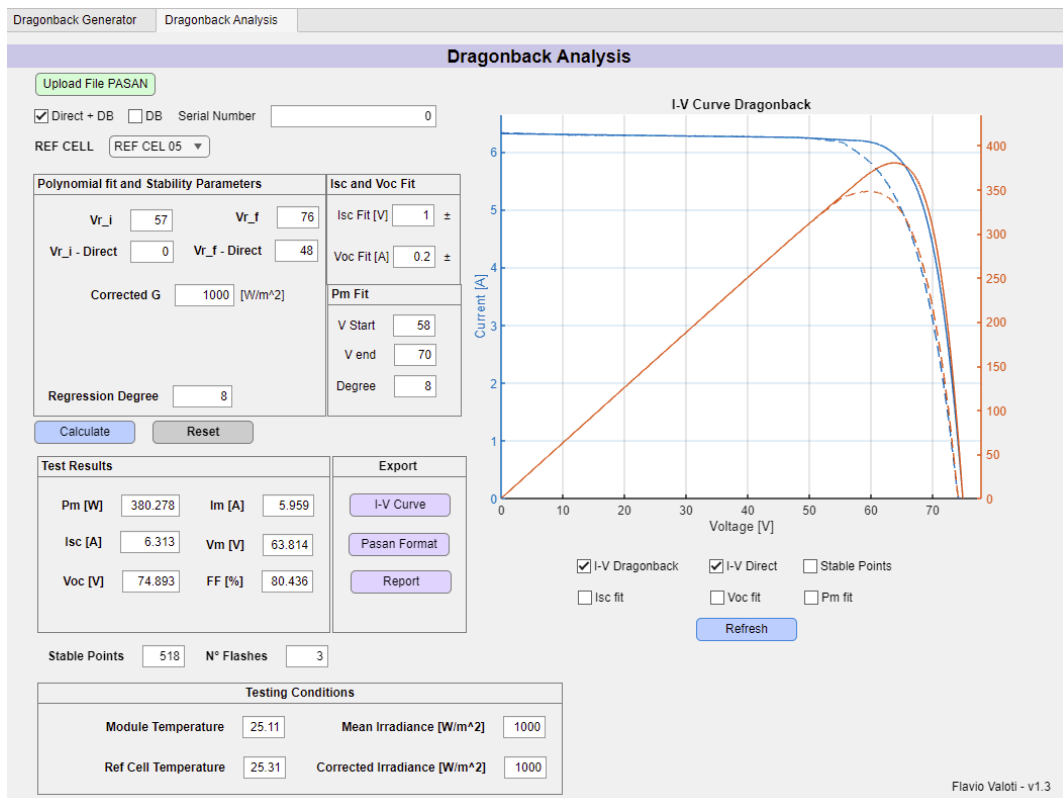


Figure 26: DB Software developed using MATLAB®

The software offers the possibility of adjusting the regression parameters for the I-V curve and the three regression's parameters performed by the SUPSI PVLab web tool: short circuit current, open circuit voltage and maximum power. The values are then corrected for the irradiance level and reference cell temperature.

The three flashes approach requires a total measurement time of about 90 seconds which is clearly a huge improvement when compared to the laboratory standard procedure for capacitive modules that takes about 15 minutes.

In order to implement this characterization method in the daily activities of the laboratory a validation is required. The validation has been carried out by comparing the results obtained with this new procedure and the multi-flash measurement under different conditions such as module equivalent capacitance, irradiance levels and temperature set-points.

### 3.4.3 Validation of enhanced Dragonback® measurement

The DB measurement has been performed on the test cycle 14 modules after one year of outdoor exposure. The measurement has been carried out in parallel with the standard procedure for capacitive modules, meaning that a multi-flash measurement has been also performed on the modules.



In order to optimize the time for the measurement only one module out of four has been measured with the two methods, the other three modules have been characterized by using only the DB approach. On these modules a full measurement at different irradiance levels (GCO) has been performed with the multi-flash and DB methods. Table 9 summarizes the modules selected for the DB validation.

Module Label	Technology	Power [W]	$\Delta P\% \text{ (MF-Direct)}$
21-C14-A	PERC Halfcut	365 W	0.7%
21-C14-B	IBC	400 W	11.26%
21-C14-C	Halfcut HJT	375 W	8.94%
21-C14-D	Thirdcut PERC	385 W	1.07%
21-C14-E	Thirdcut Shingled	365 W	0.51%
21-C14-F	Integrated diode PERC	320 W	0.71%
21-C14-H	NTopcon		4.43%

Table 9: CICLO 14 modules selected for the DB validation

**The detailed measurement results of the CICLO 14 modules can be found in the attachments of this document.**

At the end of the indoor measurements for the CICLO 14 modules an analysis on the advantages and disadvantages of this characterization method has been performed. First of all, the DB method has been proven to be the most time efficient for the laboratory, especially for the measurement at different irradiance levels. This is due to the fact that this measurement does not involve any other factors that might affect the measurement time, such as temperature, meaning that the actual time effort for the test corresponds to the measurement time. As shown in Table 10 this results in a time effort reduced by ten times.

Test	Multiflash	Dragonback®	$\Delta t \text{ (DB-MF)}$
PM_STC	900s (15 min)	90s (1.5 min)	810s (13.5 min)
GCO	4500s (75 min)	450s (7.5 min)	4050s (67.5 min)

Table 10: Multi-flash - DB, measurement time comparison

However, this remarkable result comes with a lower precision, especially at low irradiance levels (below 400 W/m<sup>2</sup>). In Figure 27 is shown the trend of the percentage error of the DB measurement compared to the multi-flash, which has been used as reference for the validation. The mean error for each irradiance level has been summarized in Table 11.



	Mean Error [%]					
	Pm	Isc	Voc	Vm	Im	FF
<b>1000 W/m<sup>2</sup></b>	0.024981	-0.05376	-0.01755	0.063999	-0.03795	0.095384
<b>700 W/m<sup>2</sup></b>	-0.0042	-0.14628	-0.01489	0.03355	-0.04228	0.154933
<b>400 W/m<sup>2</sup></b>	-0.01743	-0.07186	-0.03833	0.147981	-0.09955	0.065374
<b>200 W/m<sup>2</sup></b>	0.306219	-0.01338	-0.05524	-0.02257	0.335611	0.360419
<b>100 W/m<sup>2</sup></b>	0.698233	0.196984	-0.32795	0.158714	0.533303	0.86705

Table 11: Mean error for each irradiance level for the CICLO 14 modules

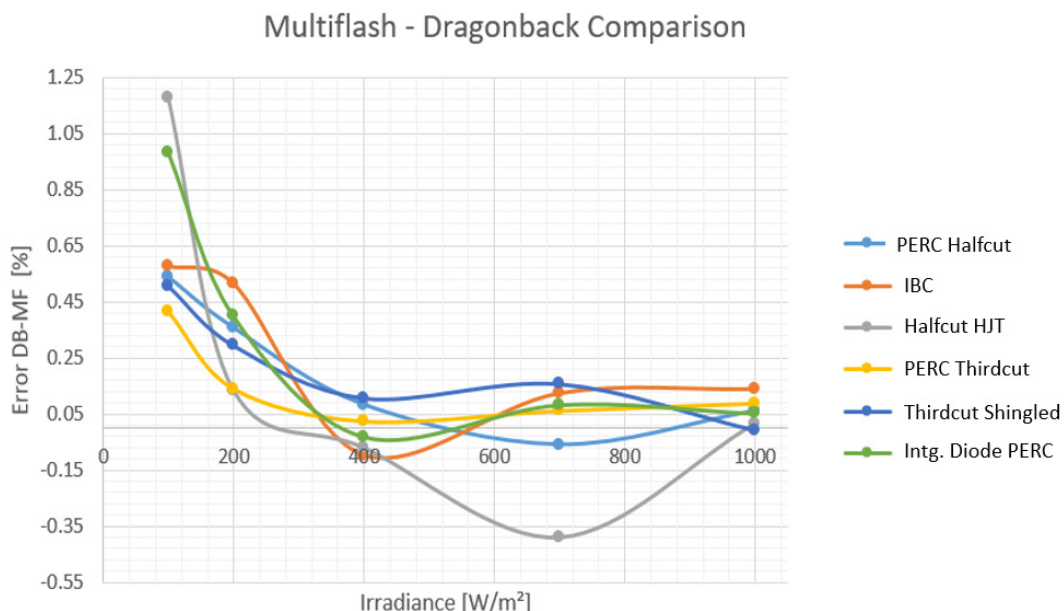


Figure 27: DB maximum power error trend for different technologies and irradiance levels

As final result of this first validation process it has been found that the DB approach can be successfully used in order significantly reduce the measurement time especially when measuring a batch of modules. In the case of a single module the multi-flash approach is suggested in order to increase the accuracy of the measurements. This suggestion is also due to the fact that in order to prepare the voltage sweep for the DB 2-3 minutes of time effort are required. The same amount of time might be also required for the data analysis, depending on the operator experience. Considering these two points and the accuracy the multi-flash approach remains the suggested procedure for a single module.

On the other hand when dealing with a large number of modules the multi-flash approach requires a huge time commitment that results in increased costs for the laboratory. Considering this, the DB method is the most time and cost-effective solution.

The power matrix is a long measurement that might require up to one entire week of testing, this is due to the fact that a large number of irradiance and temperature levels are required. Another problem that arises during the measurement is related to the temperature uniformity of the climate chamber used in order to stabilize the module at a certain temperature. The machine works perfectly and is quite precise, however having a temperature uniformity below 2 °C requires a lot of time (for the measurement at 75 °C this might take up to 4 hours). Having a measurement method with a reduced amount of flashes (when compared to the standard procedure) is then fundamental in order to reduce the time needed to perform



the whole power matrix. This have a huge impact on the laboratory budget because a lot of measurement time can be saved and, by using a method that has a reduced number of flashes, it is possible to increase the lifetime of the flasher's lamps. For this reason, the DB have been selected as main candidate for replacing the multi-flash during the power matrix measurement.

As final validation the DB measurement has been used for the electrical characterization at different irradiance and temperature of two PV modules.

Two modules have been tested within the frame of the European METRO-PV project, where a round-robin for the power matrix measurement has been carried out in order to assess the comparability and validate the uncertainties of the involved test laboratories. The DB method has been performed after the multi-flash characterization for every temperature and irradiance set point for the PERC module and for two temperature set points for the HJT module.

Module Label	Technology	Power [W]	$\Delta P\%$ (MF-Direct)
METRO-PV-F	PERC	360 W	0.95%
METRO-PV-G	Halfcut HJT Smart Wire	380 W	9.35%

Table 12: Modules selected for the power matrix DB validation

**The detailed measurement results of the power matrix round-robin can be found in the attachments of this document.**

The plots of the two modules' error at different temperatures are shown in Figure 28. As for the CICLO 14 modules the error is higher at low irradiance levels.

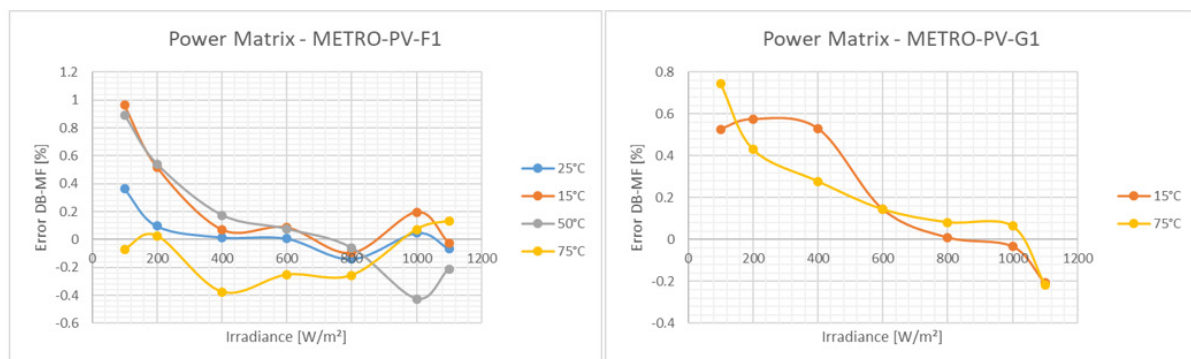


Figure 28: Power matrix measurement error, (Left) PERC, low capacitive effects (Right) HJT, high capacitive effects

The DB method had a huge impact on the time budget of the measurement, leading to a measurement time reduced by ten times. This results in at least one day of measurement saved, making it possible to potentially measure two modules in one week. This improvement will have a positive impact on the laboratory activities allowing the laboratory to perform the power matrix measurement more often.



Test	Multiflash	Dragonback®	Δt (DB-MF)
PM_STC	900s (15 min)	90s (1.5 min)	810s (13.5 min)
GCO	4500s (75 min)	450s (7.5 min)	4050s (67.5 min)
POWER MATRIX	25200s (420 min)	2520s (42 min)	22680s (378 min)

Table 13: DB - Multi-flash measurement time

#### Improvements in the capacitive measurements for low voltage modules

One of the main issues encountered when measuring high capacitive modules was the definition of the correct measurement recipe for low voltage modules ( $V_{oc} < 10$  V). This is due to the fact that the electronic load that is acquiring the current values has a voltage offset. This offset is a difference in terms of absolute value from the level specified by the user and the one imposed by the electronic load. This problem becomes more important when dealing with modules that have an open-circuit voltage close to this value. However, through a fine tuning of the recipe, applied during the analysis of the different measurement approaches, the problem has been drastically improved, as it can be seen in the picture below.

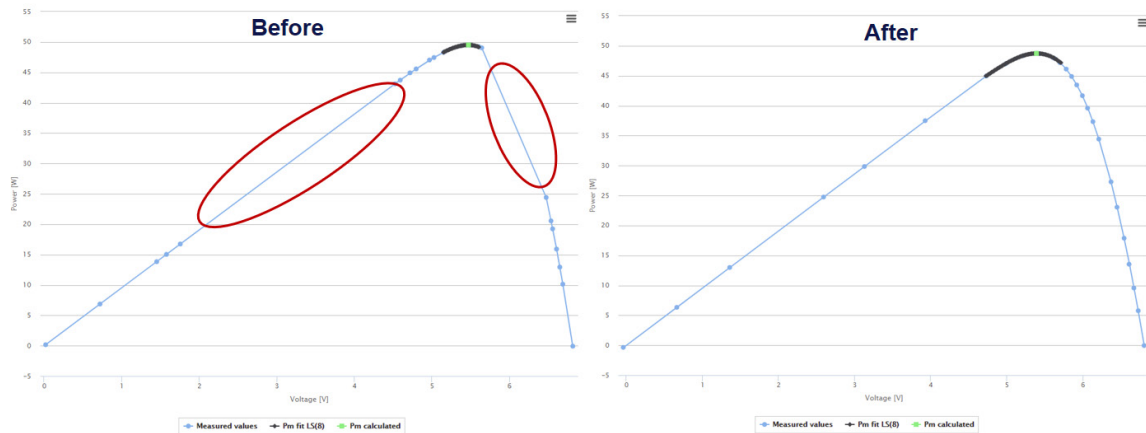


Figure 29: improvements in the multi-flash electrical performance measurement at low voltages

The recipe has been corrected and a template has been created, meaning that low voltage capacitive measures are no longer challenging for the laboratory.



### 3.5 Measurement Round Robins

#### **Background:**

A round robin test is an interlaboratory comparison, obligatory for ISO 17025 accredited laboratories, used to qualify test procedures and its implantation at test laboratories. Each participating laboratory receives identical or comparable samples and instructions of how to perform the tests. The inter-comparison allows to validate the implementation of existing or new test procedures and the respective measurement uncertainties. SUPSI PVLab is participating regularly to international round robins with other accredited test laboratories to validate new test procedures or to re-confirm existing test procedures especially in case of hardware changes or technological changes of the device under test.

#### **Scope:**

In the frame of this project SUPSI participated at two round robins:

- Power matrix measurement round robin of capacitive and not capacitive modules organised in the frame of the European project METRO-PV. With this the I-V curve measurements at different irradiance and temperatures according to IEC 61853-1 applying all three available methods (single I-V sweep, multi-flash (MF) and enhanced dragonback (DB)) were validated and further improved.
- LeTiD round robin organised in the frame of the IEC working group developing the new Technical Specification IEC TS 63342:2022 “c-Si photovoltaic (PV) modules - Light and elevated temperature induced degradation (LETID) test – Detection”.

#### **Results:**

The power matrix measurement round robin, coordinated by TÜV Rheinland, allowed SUPSI PVLab to demonstrate and validate the accuracy of their electrical performance measurements including high capacitive HJT modules and over the whole range of irradiance and temperatures defined by the IEC 61853 Energy Rating standard and to extend its accreditation with a new and faster test procedure for high efficiency modules. Independent of the module technology and measurement method the deviations of the SUPSI measurements respect to the average value of the 6 involved test laboratories remained well below the SUPSI PVLAB measurement uncertainties, suggesting a revision of the measurement uncertainties for c-Si PV modules and in particular for measurements without spectral mismatch correction.

The LeTiD round robin allowed SUPSI to implement and test the forthcoming standard technical specification for LeTiD testing of PV modules, IEC TS 63342 Ed1, but due to reasons of time it was not possible to apply it to the modules of test cycle 14.

#### 3.5.1 Power Matrix measurements (IEC 61853-1)

The DB method was furthermore validated within a round robin (RR) between 6 European PV test laboratories performed within the European research project 19ENG01 ‘Metrology for Emerging PV Applications’ (Metro-PV), which preliminary data were published at the 40<sup>th</sup> EUPVSEC [SUPSI 1]. The testing laboratories taking part in this round-robin campaign were the following: TÜV Rheinland Solar (Germany), Fraunhofer ISE (Germany), SUPSI-PVLab (Switzerland), Institute for Solar Energy Research GmbH (Germany), Physikalisch-Technische Bundesanstalt (Germany) and the European Solar

Test Installation of JRC (Italy). The measurements were performed using different test equipment's representing a broad range of testing solutions: 2 different types of pulsed Xenon solar simulators, 1 LED and 1 steady state solar simulator.

The RR was divided into 2 phases. A second batch of modules were tested because of some stability problems with the high efficiency HJT module within the first run. Two new modules were therefore tested. Throughout the whole RR, the analysis consisted in the evaluation of the measured electrical parameters  $I_{sc}$ ,  $V_{oc}$  and  $P_{max}$ , extracted from the I-V curves of partner. The collected data were compared by calculating for each parameter the average value of all laboratories and for each temperature-irradiance set point and by plotting then the percentage deviation of each point against the average.

Figure 30 shows the results of the measurements of the stable multi c-Si module performed at SUPSI, within the first phase. The measurements were here performed with the best matched reference cell and without applying any spectral mismatch correction. More details and results about the round robin can be found in the publication of G. Bardizza (see chapter 5). Except for a few  $V_{oc}$  values at 75°C all other values lie within the limits of the declared measurement uncertainty [ $u\% ; k=2$ ] of SUPSI PVLab without mismatch correction (2.6% for  $P_{max}$ ; 2.5% for  $I_{sc}$  and 0.4% for  $V_{oc}$ ). Very similar results, not shown here, are obtained when applying a spectral mismatch correction. The deviation of  $V_{oc}$  is related to the difficulty to stabilise the chamber at so high temperatures. Further improvements are foreseen in future.

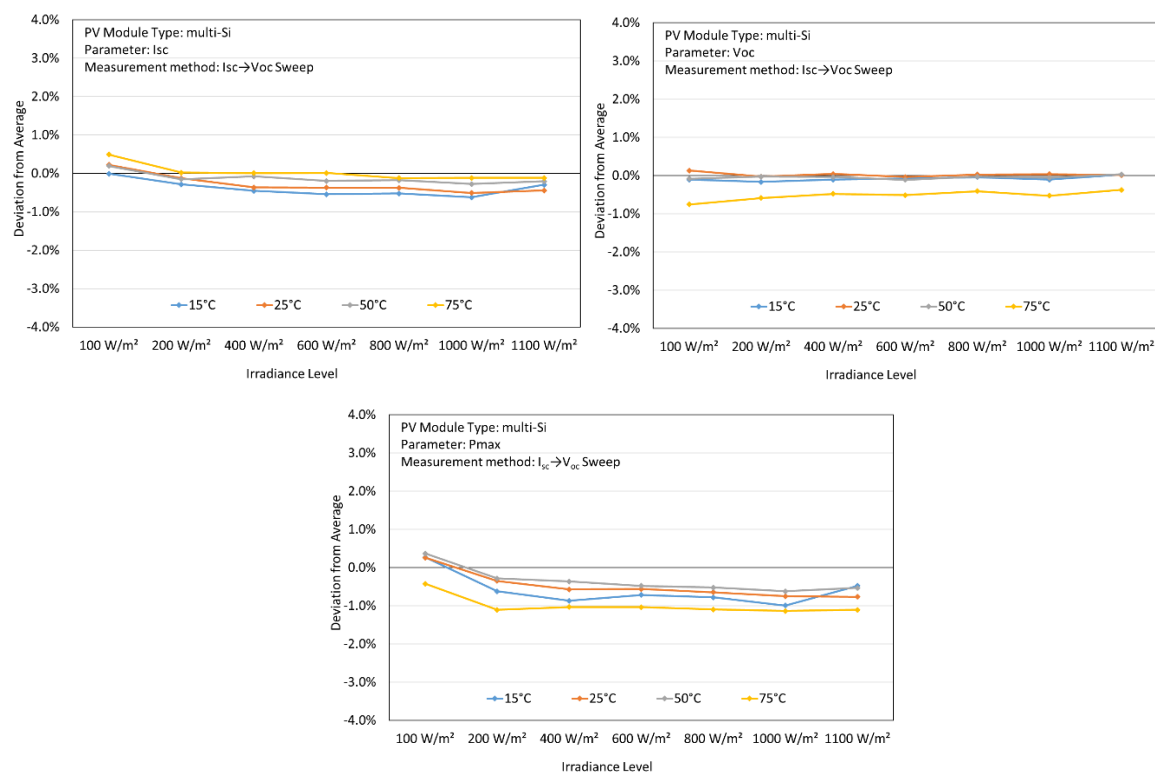


Figure 30: Deviation of  $P_{max}$ ,  $I_{sc}$ ,  $V_{oc}$  measured at SUPSI from the average of 6 test laboratories for a non-capacitive multi c-Si module.

In phase 2 of the RR two different modules were added: 1 low capacitive PERC module and 1 high capacitive HJT module (see Table 12: Modules selected for the power matrix DB validation). Measurements have been performed both with multi-flash and the enhanced DB method. For reasons of time on



the HJT module the DB method was limited to 15°C and 75°C. Figure 31 and Figure 32 shows the respective results for the two modules.

As for phase 1, the values lie all within the limits of the declared measurement uncertainty at SUPSI, independently of the applied measurement method. Minor issues were observed in the determination of  $V_{oc}$  at low irradiances related to the test recipes both for multi-flash as well as the DB method, leading to a further adaptation of the method as shown in chapter 3.4. The temperature dependency observed in the  $I_{sc}$  deviation will be further analysed to better understand its origin.

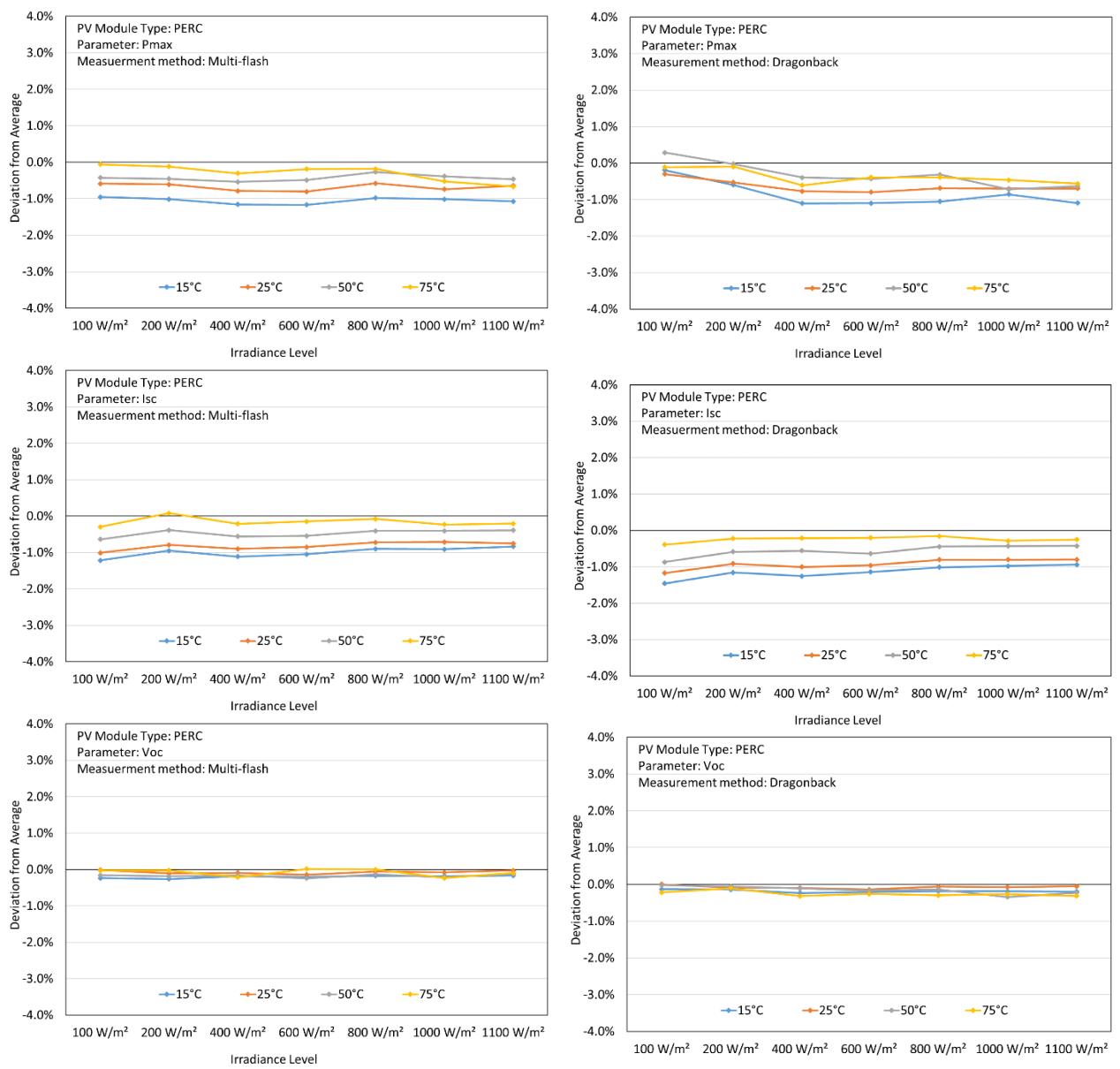


Figure 31: Deviation of  $P_{max}$ ,  $I_{sc}$ ,  $V_{oc}$  measured at SUPSI from the average of 5 test laboratories for the module METRO-PV-F.

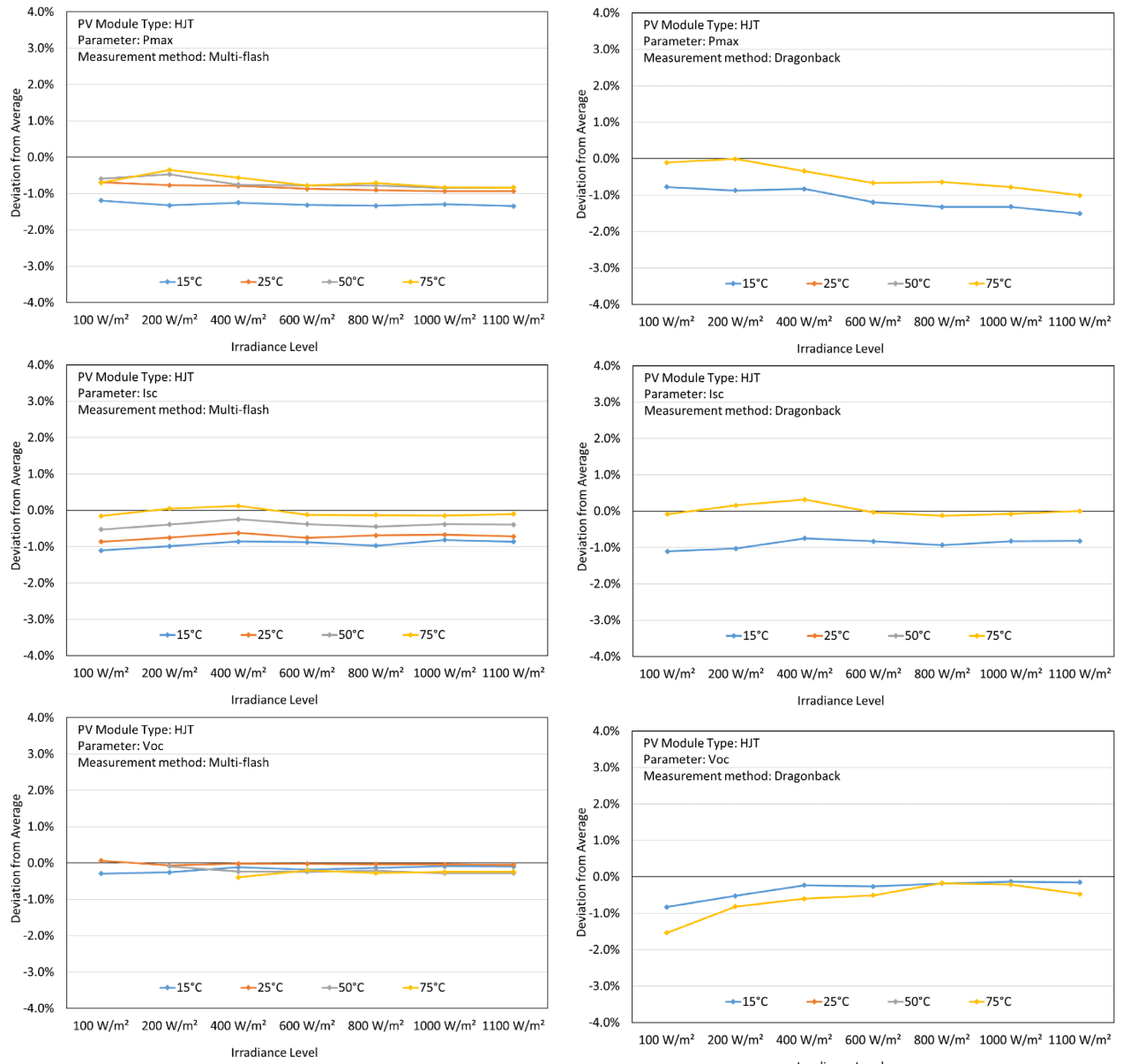


Figure 32: Deviation of  $P_{max}$ ,  $I_{sc}$ ,  $V_{oc}$  measured at SUPSI from the average of 5 test laboratories for the module METRO-PV-G.



### 3.5.2 Light and temperature induced degradation (LeTID)

During the project, SUPSI-PVLab has participated to an international round robin proposed by NREL, in the framework of the development of the Technical Specification IEC TS 63342:2022 “C-Si photovoltaic (PV) modules - Light and elevated temperature induced degradation (LETID) test – Detection”, having the following main goals:

- Evaluation of the proposed LeTID test procedures (as laid down in the draft Technical Specification 82/1771/NP)
- Evaluate practicality, clarity of the test procedure, stop criteria, ways to streamline test, etc.
- Check reproducibility of two proposed methods (dark current injection and artificial light exposure method): do different test labs get similar results on the same product?
- Perform LeTID regeneration (even if not required in the draft technical specification), to separate LeTID from other degradation modes.

The round robin measurements were performed with the dark current injection method only (climatic chamber + current injection), from September 2019 to June 2020, on one PV module which was initially classified as “Special LeTID-sensitive module”.

Figure 33 shows the results obtained by SUPSI PVLab and submitted to the round robin coordinator.

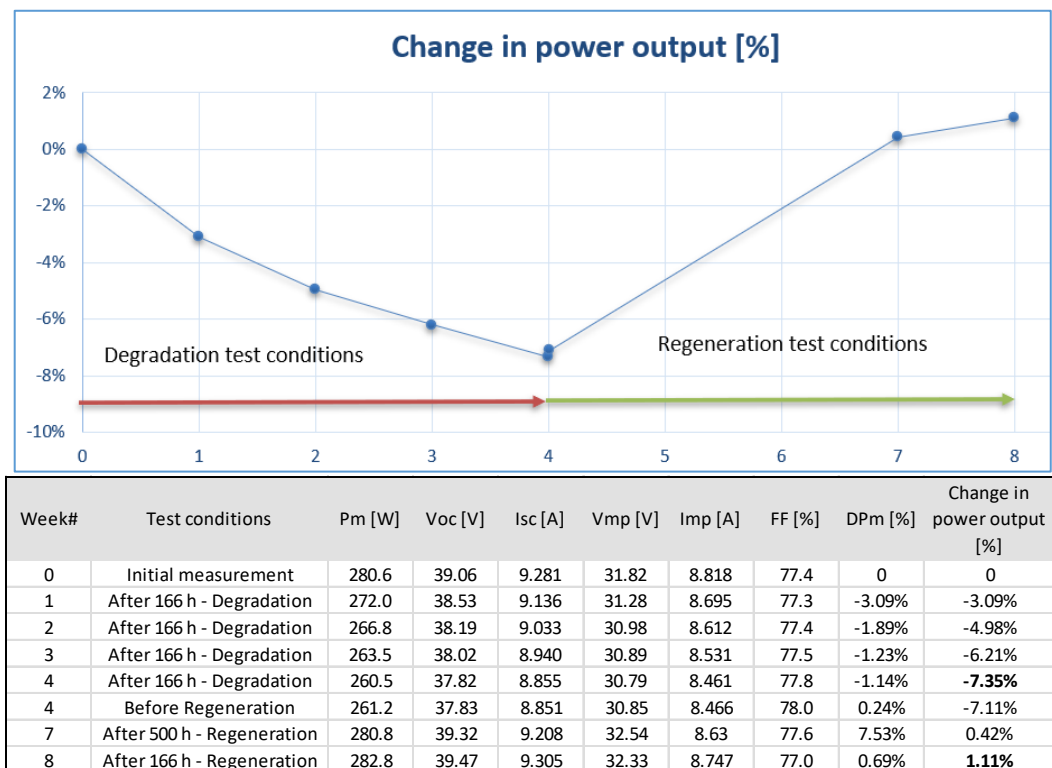


Figure 33: Trend of  $P_{max}$ , measured at SUPSI during the 8 weeks of LeTID testing (4 weeks in degradation test conditions and 4 weeks in regeneration test conditions).



The results of the round robin among the 6 participating laboratories can be found in the final publication of J. Karas and co-authors [SUPSI 5]. The outcomes are here summarized as follows:

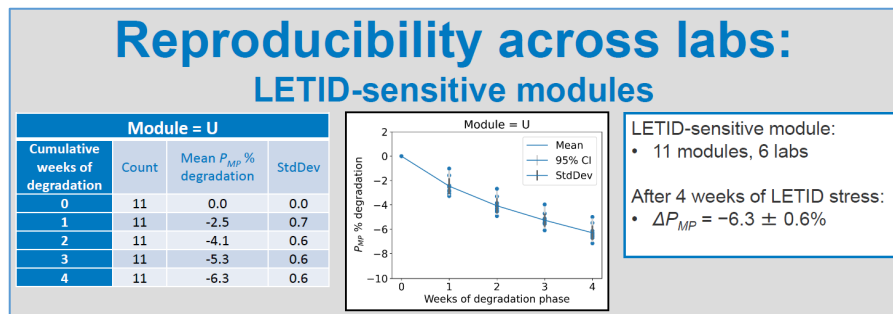
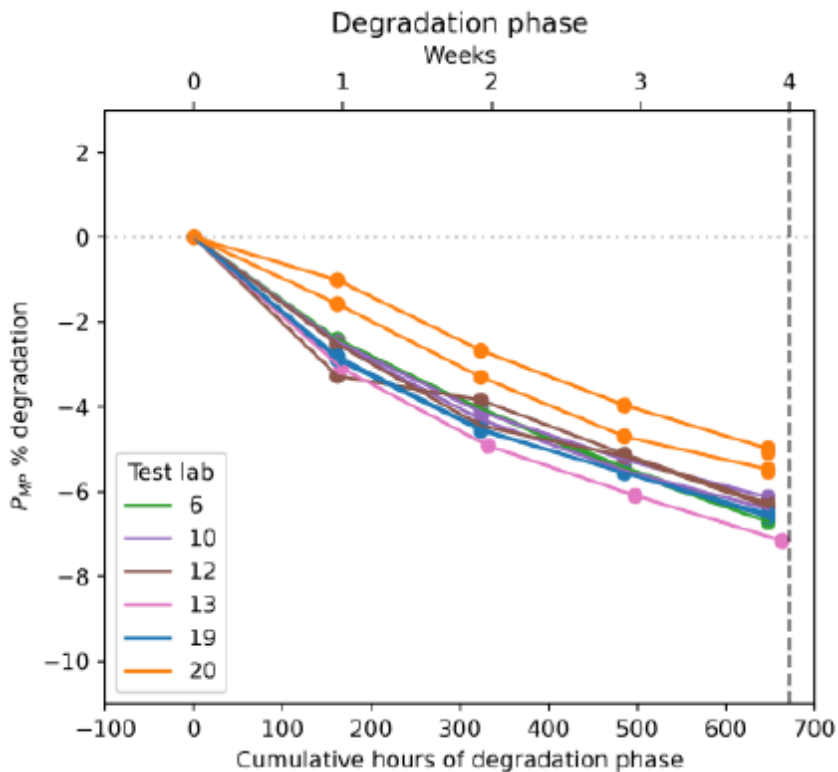


Figure 34: LeTID round robin results of a LeTID sensitive module within 6 test laboratories.

As shown in Figure 34, in intentionally engineered LeTID-sensitive modules, the mean degradation after the prescribed detection stress is roughly 6%  $P_{MP}$ . In other module types the LeTID sensitivity is smaller, and in some we observe essentially negligible degradation attributable to LeTID. In LeTID-sensitive modules, both open-circuit voltage ( $V_{oc}$ ) and short-circuit current ( $I_{sc}$ ) degrade by a roughly similar magnitude. We observe, as do previous studies, that LeTID affects each cell in a module differently. An investigation of the potential mismatch losses caused by nonuniform LeTID degradation found that mismatch loss is insignificant compared to the estimated loss of cell  $I_{sc}$ , which drives loss of module  $I_{sc}$ . Overall, this work has helped inform the creation of a forthcoming standard technical specification for LeTID testing of PV modules, IEC TS 63342 Ed1, and should aid in the interpretation of results from that and other LeTID tests.



### 3.6 Outdoor Measurements (test cycle 14)

**Background:** The main aim of outdoor measurements of PV modules is the assessment of the performance and reliability under real operating conditions and to get inside into technological differences claimed by manufacturers (e.g. better low irradiance performance, lower thermal losses, lower degradation rates). To guarantee fair inter-comparisons with the highest accuracy module level side by side inter-comparisons has to be performed by following existing best practice guidelines. Technology benchmarkings are generally performed on modules mounted in open-rack and optimally oriented. However, deviations from optimal conditions are useful to better understand the impact of cell and module design on the energy production and degradation rates of modules mounted in unconventional conditions as e.g. in buildings with PV facades or roof mounted systems. Different methods are used in the PV community to calculate degradation rates, based either on indoor measurements or outdoor monitoring data and leading to different results which can significantly deviate from the derating claimed in warranty declarations.

**Scope:** One of the main scopes of this project was to investigate the advantages and disadvantages of different technological innovations introduced over the last years by monitoring them under optimal and sub-optimal 10° tilt conditions, representing typical rack mounted flat roof systems in Switzerland with reduced air circulation and increased soiling. The collected data aims to demonstrate how technological differences reflect in energy production and to identify any early-stage degradation issues related to cell technology, module design or manufacturing quality. The study of these degradation rates is essential to improve the accuracy of long-term energy prediction models and warranty statements, and to provide guidance for standardised quantification of degradation rates. The limited number of technologies tested here does not allow to generalise on a specific technology but represents case studies and sets the basis for accurate benchmarking and degradation studies.

**Results:** In December 2021 SUPSI launched a new outdoor measurement campaign 'test cycle 14' with 7 commercial monofacial PV module technologies including 4 different PERC modules (half-cut, third-cut, five-cut shingled and full-cell modules with integrated bypass diodes), 1 TOPCon half-cut, 1 IBC full-cell and 1 HJT half-cut module technology (Fig.35). Energy production and performance ratios for the first 22 months were analyzed on a daily, monthly and total basis, whereas the degradation behaviour was studied by the mean of punctual indoor measurements and the processing of outdoor monitoring data. The main results are here listed.

- Under optimal conditions (open-rack 30° tilt) the PR difference measured over 22 months of the PERC, TOPCON and IBC modules were in the range of  $\pm 0.9\%$  with TOPCON and IBC having the highest module PR (Fig.39). The HJT modules were not considered because of a manufacturer related degradation problem. At a lower inclination of 10° tilt the PR spread increased to  $\pm 2.1\%$  and a change of the ranking order was observed (Fig.40). TOPCon had still the highest PR whereas IBC was moving down in the ranking. The reason for it is related to a lower performance during the winter months, when the angle of incidences exceeded 50°. This highlights the importance of performing a full characterization of PV modules according to IEC 61853 part 1 and part 2. In the case of a technology benchmarking according the area specific energy yield (Fig.38), the spread increases up to  $\pm 7.0\%$  with IBC outperforming the other technologies due to the higher module efficiency (22.6%).



- The 3 HJT modules tested within test cycle 14 were affected by a strong degradation in FF and  $P_{max}$  and minor in  $I_{sc}$  and  $V_{oc}$  (Fig.42), leading to the lowest PR within the technology inter-comparison (Fig.36). The main cause of the failure is to be attributed to a poor bill of material, which do not prevent the penetration of the humidity through the backsheet, as confirmed by electroluminescence images showing the moisture penetration along the cell edges and grid finger defects (Fig.46 and Fig.47), in addition to higher series resistance visible in the electrical indoor measurements (Fig.48). A non-linear  $P_{max}$  degradation of -5.75 %/year in the first year and -1.57 %/year in the second year have been observed for the worst module (Fig.45).  $I_{sc}$  and  $V_{oc}$  losses are lower and stabilizes over time. The last could be related to other degradation mechanisms as e.g UV induced degradation of the cells. The sensitivity to humidity of HJT is already known from literature and is generally mitigated by an appropriate BOM and module manufacturing.
- The IBC modules showed a degradation in  $P_{max}$  exceeding the 2% of the first-year warranty declaration. Beside  $P_{max}$  also  $V_{oc}$  is affected, but in minor extend, whereas  $I_{sc}$  is stable. The origin of this degradation is still under investigation. The 4 PERC technologies showed  $P_{max}$  degradations in the range of 0.5-2.5% within the first 22 months, increasing from 2-cut, 3-cut to 5-cut shingled technology. TOPCon half-cut and the PERC module with integrated diodes resulted to be stable (Fig.42).
- The calculation of the degradation rates depends also on the applied method (Fig.44) with advantages and disadvantages for each. Both here applied approaches looks at the drop in STC power, measured either indoor or extracted from outdoor data. As demonstrated by the analysis of low light performance (Fig.48), the consideration of STC performance only, is giving an incomplete picture of the ongoing degradation and to be expected energy production loss.
- Looking in more detail at the seasonal variation of PR (Fig.37), for some of the technologies, particularly PERC third-cut and PER shingled, differences were observed between modules of the same type, suggesting manufacturing related batch variations and ongoing stabilisation processes.
- The modules mounted at low tilt angle (10°) were additionally affected by higher soiling at the bottom of the modules (Fig.39), which even if very small, leaded to power losses which extend depends on the frame type, cell distance from frame and cell-interconnection typology. As expected, the PERC module with cell-level integrated diodes showed here the highest PR (Fig.40), which is due to the lowest shading losses and better low light performance: the last is due to the high series resistance caused by the cell level integrated diodes. This leads at the same time to a lower STC performance and module efficiency which is reflected in a lower area specific energy yield. The advantages of this type of module are so limited to systems with repeated and significant shading conditions.
- A short measurement campaign was performed to quantify the shading resistance of the 7 module technologies under different shading scenarios. The modules were classified according to a rating procedure, going from A to D, developed within the European collaborative project METRO-PV (Fig.52). As expected, the module with integrated diodes resulted to be independent from the shading type and consistently classified as B. The IBC module with full cells was the only one to reach the class A under long side shading conditions.

### 3.6.1 Test stands configuration

Figure 35 shows the three outdoor test facilities installed in December 2021 and operational since January 2022. The outdoor measurements are performed in two south facing configurations, (1) standard open-rack mounting conditions at 30° inclination without significant shading and (2) in low 10° inclination to reproduce the typical conditions of flat roofs in Switzerland, with reduced air circulation and increased soiling. The aim is to study the sensitivity of the different technologies to optimal and sub-optimal test conditions.



Figure 35: Pictures of the test stands mounted in Mendrisio (Switzerland): (top) 30° open-rack (bottom left) 10° open-rack and table of the technologies tested within test cycle 14.

The table included in Figure 35 shows the seven technologies mounted on the test stands. More details about the single module types can be found in chapter 3.1.1. The table summarizes some of the most important module parameters measured in the laboratory and described in Chapter 3.2: the initial stabilized power  $P_{ref}$ , the  $P_{max}$  temperature coefficient measured at 1000 W/m<sup>2</sup> and the low irradiance performance, here expressed as efficiency loss at 200 W/m<sup>2</sup>. The power of the modules is in the range of 300 to 700 Wp, whereas the temperature coefficients of PERC and TOPCon varies from -0.34 %/°C to -0.38 %/°C and -0.27 %/°C to -0.29 %/°C for the two high efficiency modules. The efficiency losses at 200 W/m<sup>2</sup> are strongly technology dependent and varies between -1 % to -5.3 %.

Except for the PERC technology with integrated diodes, where only one module is measured on the 10° facility, for all other technologies three modules are monitored: two at 30° mounted in landscape orientation and positioned one on top of the other and a third one at 10° mounted in portrait configuration.

Each PV module is connected to a MPPT3000 test unit which is composed of a maximum power point tracker and an I-V tracer. Additionally, to the maximum power point values ( $I_m$ ,  $V_m$ ), in-plane irradiance ( $G$ ) and module temperature ( $T_{mod}$ ) are monitored in 1-minute intervals. The irradiance is measured with some calibrated pyranometers, whereas the temperature with two PT100 sensors attached on the rear of the module. The I-V curves are recorded every 5 minutes. The measurements are combined with data from a close by meteo station. The test facility is built according to the recommendations provided in the best practice guideline IEA-PVPS T13-11:2018 [8].

Due to the above-listed technological differences, variations in energy yield are to be expected. The following paragraphs gives some insight into different technology benchmarkings.



### 3.6.2 Energy yield benchmarking (30° inclination reference stand)

The ranking is here performed by comparing the performance ratio (PR) of the modules for the period April to August 2023 (17 months). The first months of exposure had to be excluded due to some missing data. The equation describing the performance ratio is  $PR = \sum P_m \cdot G_{stc} / \sum G \cdot P_{ref}$ , with  $G_{stc}$  being equal to the reference irradiance of 1000 W/m<sup>2</sup>,  $P_m$  and  $G$  being the power and irradiance measured in 1-minute intervals and  $P_{ref}$  the stabilized STC power, as measured in the laboratory. Data affected by close by shading are filtered out for all modules, to exclude wrong PR values and to have comparable module data.

Figure 36 shows the PR of the 6 module technologies (2 modules per type) mounted at 30°, together with the relative deviations respect to the best module.

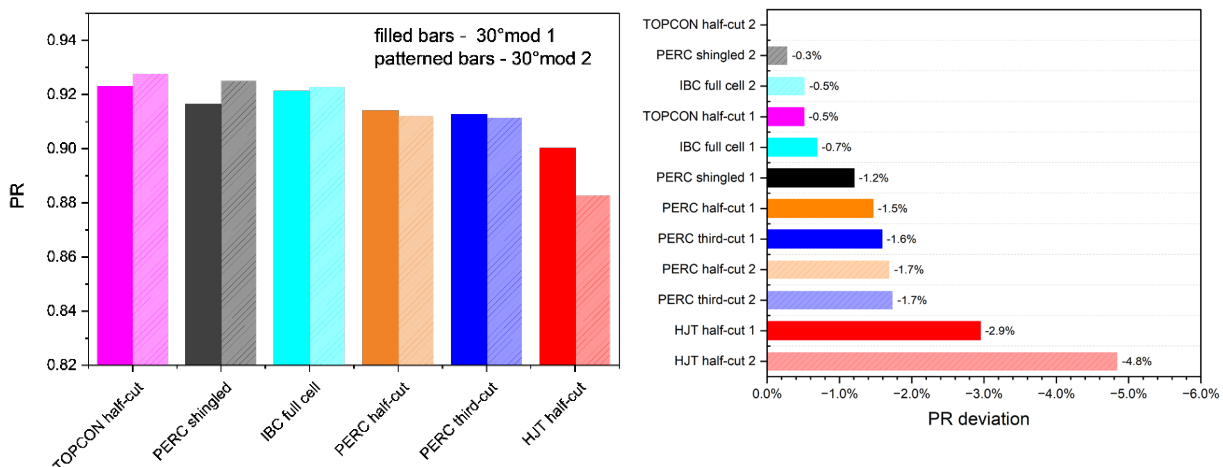


Figure 36: Comparison of the total performance ratio (left) and relative deviation (right) of the 12 modules (6 different technologies/2 modules per type) mounted on the 30° tilted test stand. Legend: Table 1 – module mounted on the top row, Table 2 - bottom module.

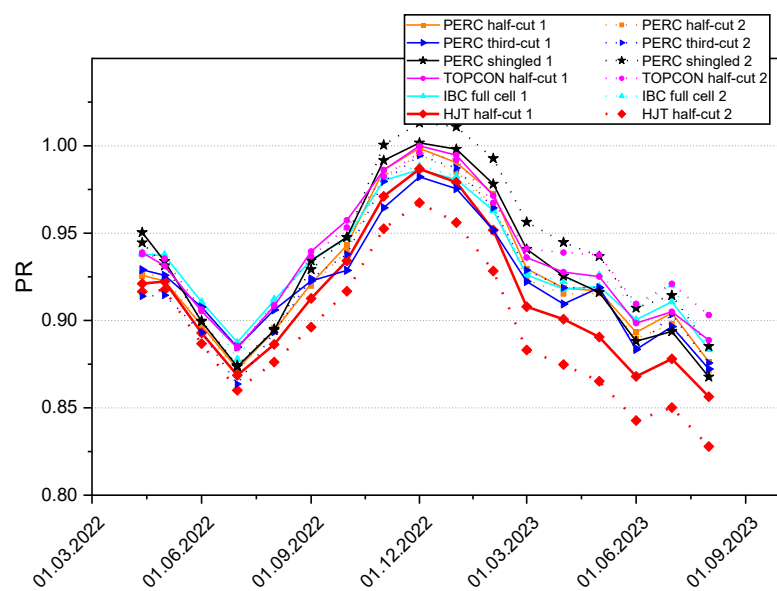


Figure 37: Monthly performance ratio of the 12 modules (6 different technologies) mounted on the 30° tilted test stand.



When excluding the two HJT modules, which are clearly affected by degradation effects, the PRs for the first 1,5 years of operation are all in the range of  $0.92 \pm 0.9\%$ . Except for the shingled PERC technology, modules of the same type showed consistent results with very close PRs with TOPCON and IBC having the highest PR and PERC half-cut and PERC third-cut modules slightly higher deviations respect to the best module. Considering a relative measurement uncertainty for PR in the range of  $\pm 1.5\%$  as described in the best practice guideline IEA-PVPS T13-11:2018 [8], the differences have to be considered as not significant.

However, to get a better inside into technological differences, the evolution of PR over time must be analysed. Initial minor degradation effects and seasonal variations are hidden when integrating the PR over the full period. Figure 37 shows the monthly PR of all modules for the same period. The degradation of the two HJT modules, leading to the lowest PR (-2.9% and -4.8% lower respect to the best module), is clearly visible. Module 2 seems to be more affected. A closer look to the seasonal trend of the other technologies shows that for some technologies there are differences between the modules of the same type, suggesting some ongoing stabilization processes or manufacturing related batch variation. This is particularly true for PERC third-cut and PERC shingled. Technology specific graphs of the monthly PR are given in Annex 3.

Another approach of technology benchmarking looks at the energy yield normalized respect to the module area. This approach is of particular interest for building integrated PV, where the space for the installation of PV modules is limited. Figure 38 shows the ranking of the 6 module technologies respect to the best module technology but calculated with the area specific energy yield measured in kWh/m<sup>2</sup>. As expected, the IBC modules with a declared module efficiency of 22.6% outperforms the others. Despite its second-best module efficiency (21.4%), the two HJT modules underperform due to their degradation. The second-best module technology in the ranking is instead the TOPCon technology, which has an efficiency of 20.9% and the best low irradiance performance (see Figure 10 ), whereas the PERC half-cut module with the lowest efficiency (19.5%) is at the last position. PERC shingled and PERC third-cut with both 20% declared module efficiency performs the same and are in-between the others. One of the shingled modules shows a different behaviour which is still under investigation.

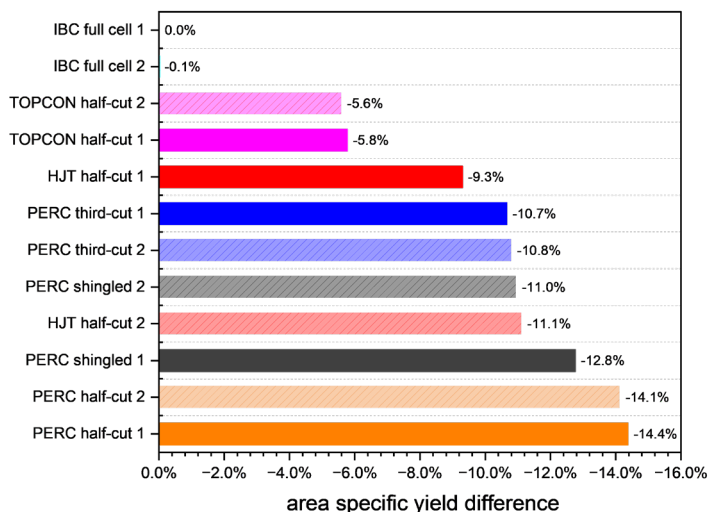


Figure 38: Comparison of the are specific yield differences of the 12 modules (6 different technologies/2 modules per type) mounted on the 30° tilted test stand respect to the best module.

Even if the module efficiency in case of building integrated PV systems is one of the main criteria for module selection, it has also to be considered that BIPV modules are very often mounted in non-optimal

conditions like in facades or flat roofs or with bad rear ventilation, where other module parameters can have a major influence. The angle of incidence response and temperature coefficient should for example be considered as well when optimization for the energy yield. The next paragraphs give an example of how the ranking is influenced by a low inclination.

### 3.6.3 Energy yield benchmarking (10° inclination test stand)

The modules mounted on the 10° test stand, representing typical flat roof PV systems in Switzerland, are exposed to different conditions compared to the 30° test facility. Figure 39 shows the distribution of (1) in-plane irradiance, (2) module temperature, (3) angle of incidence and (4) a picture of typical soiling conditions for modules mounted at 10°.

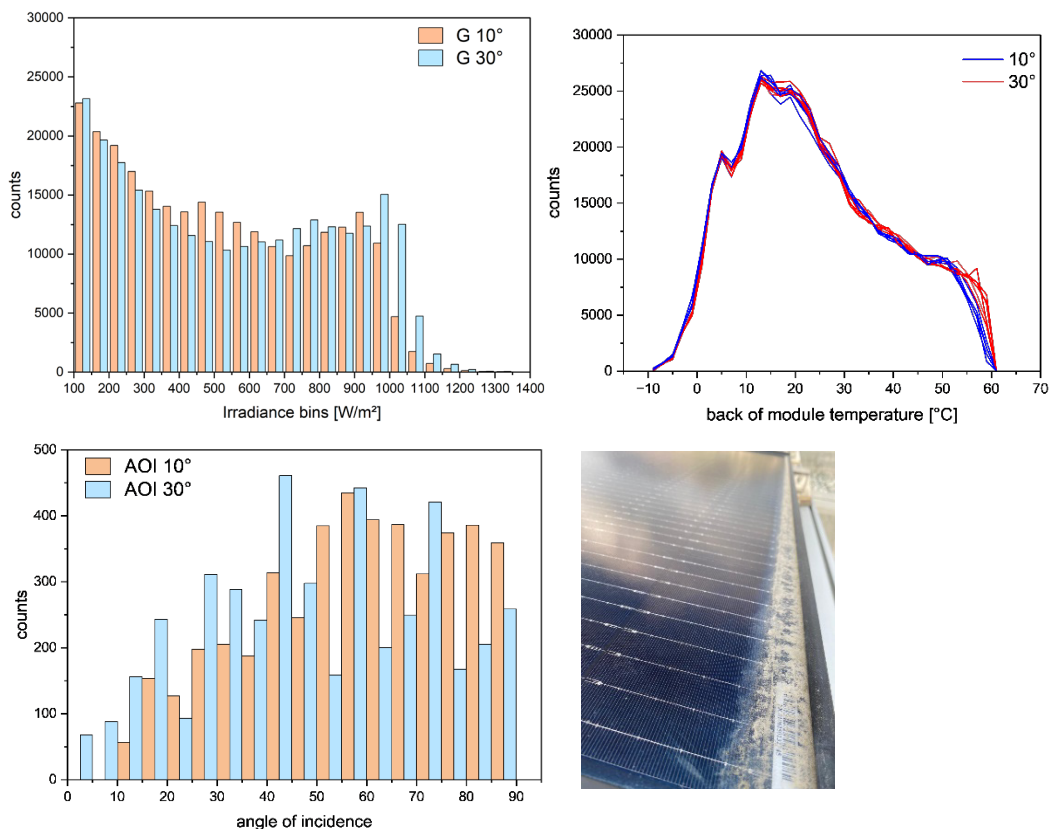


Figure 39: Test conditions present on 10° and 30° test stands.

Respect to 30°, at 10° inclination intermediate irradiances between 200 to 600 W/m<sup>2</sup> are occurring with a slightly higher frequency, whereas high irradiances above 950 W/m<sup>2</sup> occurs less. The distribution of module temperatures shows respectively less events above 55°C compared to 30°. The most significant difference is seen in the distribution of the angle of incidence, with a higher frequency of AOI>50°, which occurs mainly in the winter months, including noon time when the irradiance is the highest. Furthermore, the modules mounted at 10° are affected by more soiling. All modules have frames which generally increases the accumulation of soil at the bottom part.

How these different test conditions affect PR is shown in the following graphs. Figure 40 depicts the absolute and relative PR ranking for the 6 technologies as mounted on the 30° test stand plus the one shading resistant PERC module with integrated diodes.

Overall, the lower inclination led to an increase in the spread of PR from  $\pm 0.9\%$ , observed on the  $30^\circ$  test stand, to  $\pm 2.5\%$  ( $\pm 2.1\%$  excluding the HJT module) and a change of the ranking order. TOPCON and PERC with integrated has the highest PR. The good PR of the last is to be attributed to the good low light performance, originating from the high series resistance caused by the series connection of the diodes. IBC is moving down in the ranking despite its better temperature coefficients. As shown in Figure 41, the reason for this is the lower PR of the IBC module in the winter months, when the angle of incidences exceeds  $50^\circ$ . An angle of incidence measurement will be performed in later stage to verify if the IBC has effectively a lower angle of incidence response. The HJT module shows again the lowest PR, but also PERC third-cut seems to be affected by higher losses.

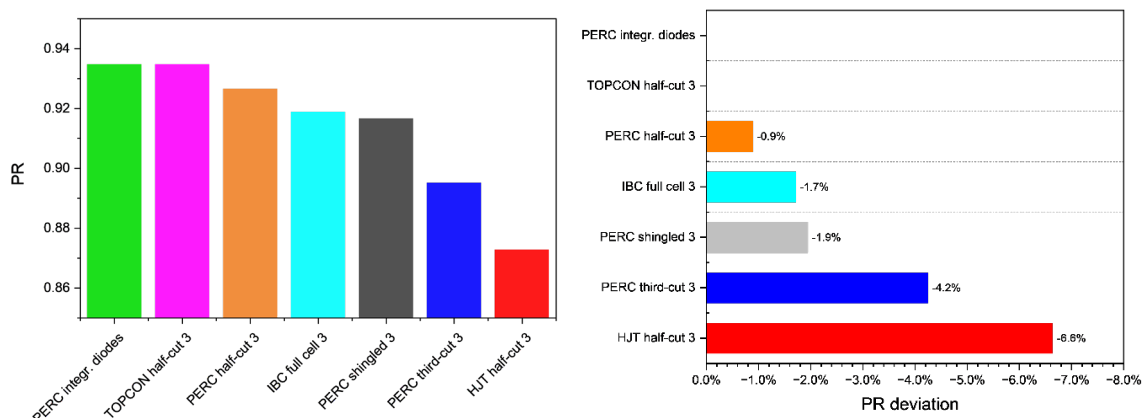


Figure 40: Comparison of the performance ratio (left) absolute PR and (right) relative deviation respect to the best of the 7 modules mounted on the  $10^\circ$  test stand.

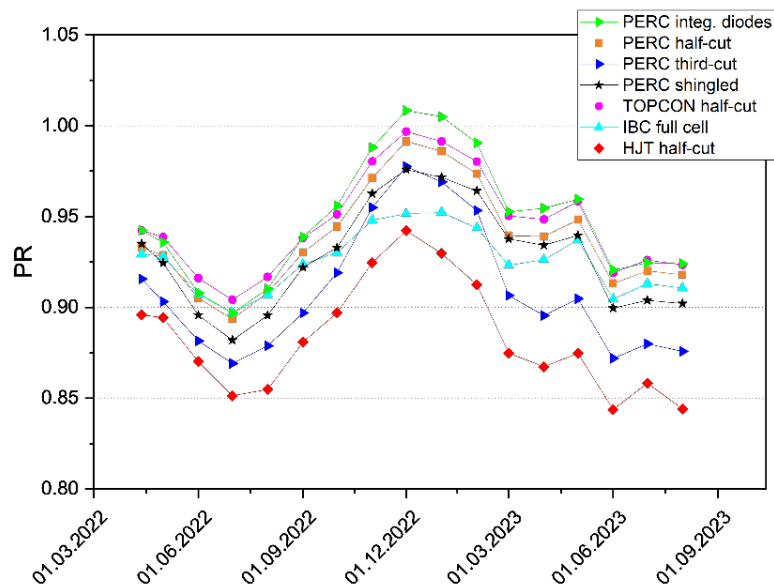


Figure 41: Monthly performance ratio of the 7 modules mounted on the  $10^\circ$  tilted test stand.

The general increase in the PR spread is to be attributed to the different impact soiling has on the modules with different cell arrangements, inter-connections and module designs (glass type and cell distance from frame). In particular, the edge effect has an impact because there are modules with cells very close to the frame, such as the third-cut PERC module, which are more affected by the persistent



dirt on the lower frame. The TOPCON module has the largest edge, making it much less susceptible to performance degradation from border. This edge effect is obviously design dependent and not cell technology dependent. Beside this the angle of incidence response and low irradiance performance have a major impact at low inclination. The single contributions will be quantified in the next months.

The following chapter will focus on the quantification of the degradation rates and its effect on the technology benchmarking.

### 3.6.4 Analysis of degradation rates

A common approach for the determination of degradation rates or annual performance loss rates (PLR), are based on the PR [11]. However, all the described methods require at least 4 years of data to be applicable. As having less than 2 years of data available until now, two different alternative approaches have been applied here: (1) an indoor approach, consisting in the dismantling of the modules from the test stand and the measurement of the electrical performance in the laboratory, and (2) an outdoor approach, consisting in the correction of filtered outdoor data to fixed irradiance and temperature conditions. The results of the two approaches are here presented and compared to each other.

### Indoor measured degradation:

Figure 42 shows the results of the STC measurements performed on the new modules (out of the box) and after 22 months of outdoor exposure. The relative change in  $P_{max}$ ,  $I_{sc}$  and  $V_{oc}$  is shown for all outdoor exposed modules and its respective reference module stored in dark and measured at the same time as the outdoor exposed modules. The observed differences of the outdoor modules include, both initial light induced degradation as LID or LeTID, as well as natural aging caused by the environmental conditions. The reference modules have been stabilized and then stored in the dark. A Table and Figures summarizing all indoor measurements, including the measurement done after stabilization, can be found in Annex 4 and Annex 5.

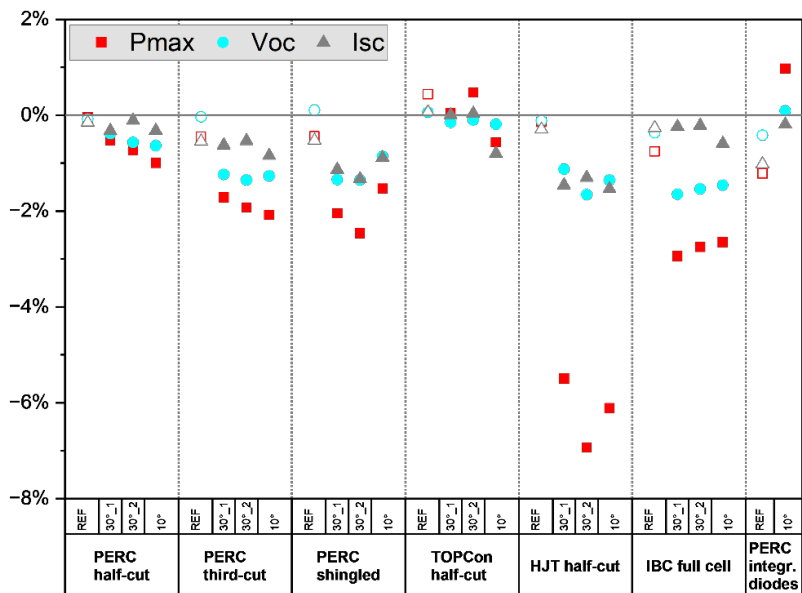


Figure 42: Degradation of STC values after 22 months of outdoor exposure.

In Figure 42 it can be seen that the degradation of the 4 PERC technologies is in the range of 0.5-2.5%, increasing from 2-cut, 3-cut to 5-cut shingled technology. TOPCon half-cut and the PERC module with

integrated diodes resulted to be the most stable technologies, whereas the HJT and IBC modules are affected by some degradation. IBC in minor extend for  $P_{max}$  and  $V_{oc}$ . The HJT half-cut modules had instead a strong degradation in FF and  $P_{max}$  and in minor extend in  $I_{sc}$  and  $V_{oc}$ .

It has to be highlighted that the degradation rates measured in the first years can exceed the annual degradation rates as stated by the manufacturers. Especially in the new generation modules the stabilization processes can take months or even years to be completed. Results from an extended measurement campaign presented by Theristis et al. [12], where modules have been measured indoors every 6 months showed stabilisation periods of around 3-4 years before reaching stable annual degradation rates as stated in the warranties. Much higher or even positive rates were measured.

Furthermore, indoor measurements do not say anything about when the degradation occurred and with which tendency (linear, exponential, saturating, abrupt, miscellaneous) as described within the technical IEA report on failure modes [13]. More frequent measurements would be needed, but with the disadvantage of losing outdoor data caused by the time needed to dismantle and measure the modules in the laboratory.

#### Outdoor measured degradation:

To avoid the interruption of the measurement campaign, outdoor data were here analysed to detect any early degradation. The linear interpolation of the daily average temperature and irradiance corrected power  $P_{corr}$  is therefore plotted against time. The power is first filtered around  $G_{ref} \pm 50\text{W/m}^2$ , then corrected to  $G_{ref}$  and  $T_{ref}=25^\circ\text{C}$  by using the measured temperature coefficient and the measured back of module temperature and daily averages are calculated at the end. Only daily averages with at least 10 data points of clear sky days are used for the linear interpolation. Figure 43 shows the linear trend of the 18 modules (6 technologies). The high uncertainty related to the correction of outdoor data together with the unavailability of valid data for the first winter months makes it difficult to detect small degradations or non-linear trends. Significant degradation as the one observed in the 3 HJT modules are however well detected, and they are close to the one calculated from indoor measurements. The positive trend observed for one of the PERC shingled modules (see Figure 43) is still unclear.

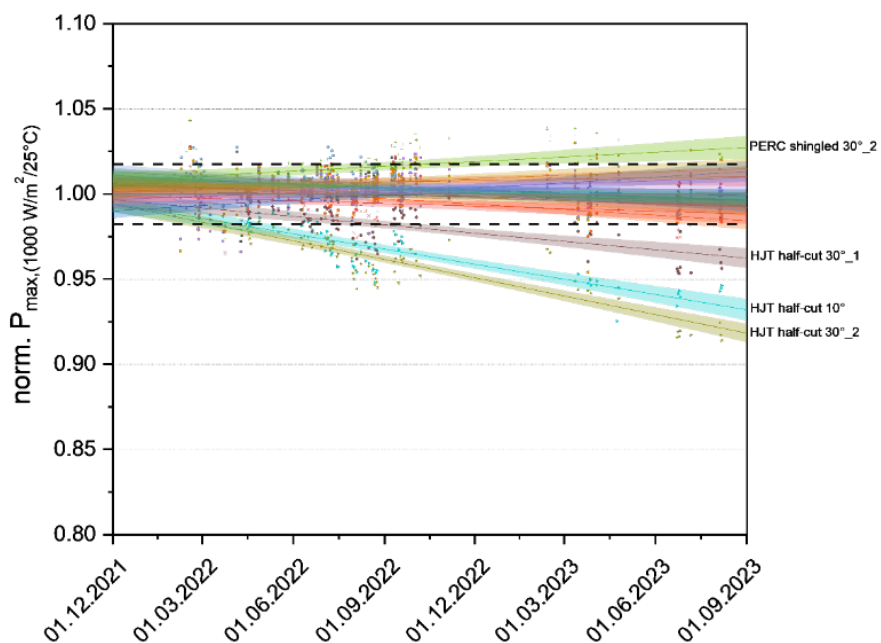


Figure 43: Degradation rates obtained from temperature and irradiance corrected outdoor data (applied filter: clear days,  $1000 \pm 50\text{W/m}^2$ , early morning/afternoon data affected by shading)

Figure 44 compares the total degradation obtained from both, indoor and outdoor data. Higher degradations above 2%, as observed for HJT, IBC and PERC shingled (10° and 30°) modules are detected with both approaches. The others are generally overestimated with the outdoor approach.

The three technologies showing minor or major degradation are described in more detail in the next chapter.

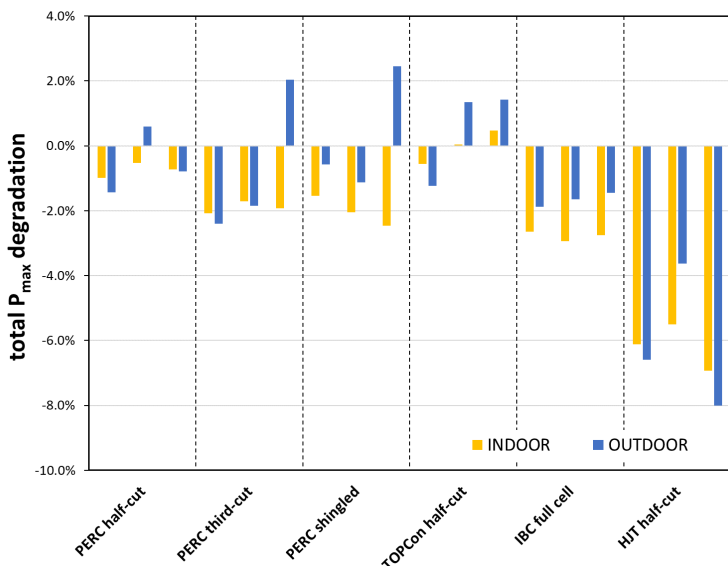


Figure 44: Inter-comparison of the  $P_{max}$  degradation obtained from indoor and outdoor data for all 6 technologies.

### 3.6.5 Technology specific degradation modes

#### HJT half-cut technology

Because of the fast degradation of HJT modules intermediate indoor measurements were performed on all three outdoor exposed modules. The following figure shows the change in  $P_{max}$ ,  $I_{sc}$  and  $V_{oc}$  after 10 and 22 months of outdoor exposure. The first two points corresponds to the initial measurement performed on the new modules (out of the box) and after stabilization according to IEC 61215 (MQT 19.1). The here given degradation rates are calculated respect to the first measurement. From the graphs it is visible that the degradation is non-linear, with a faster  $P_{max}$  degradation of -5.75 %/year in the first year and -1.57 %/year in the second year in the worst case. In the first 10 months,  $I_{sc}$  and  $V_{oc}$  showed losses of -2.3 %/year and -1.35 %/year respectively, which later stabilized.

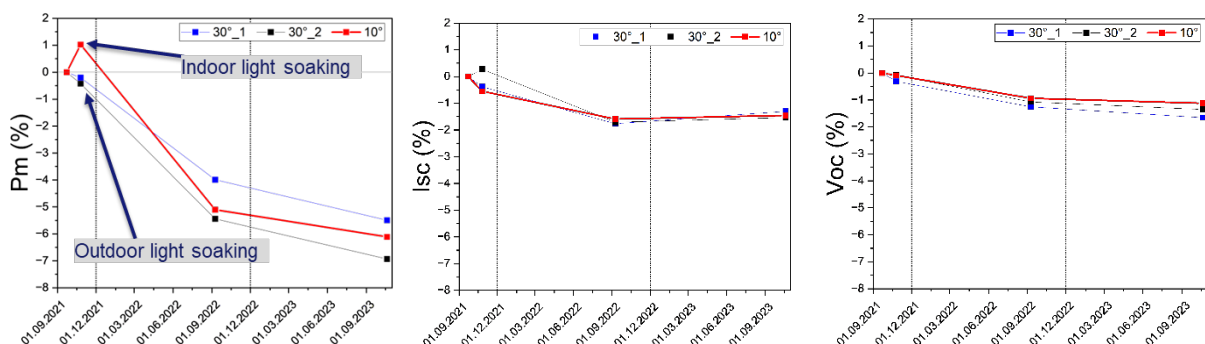


Figure 45: Normalised IV parameters measured indoor at STC after 10 and 22-months of outdoor exposure for the 2 HJT modules mounted at 30° and 1 modules at 10°.



As shown in the first graph, on two modules the initial stabilization has been performed outdoors whereas on the other two indoors. More information about the general stabilization approach and results can be found in chapter 4.2.5. The indoor stabilization under artificial light shows an increase of approx. 1%, which is typical for HJT modules and can be explained by an improvement of surface passivation [4]. Once exposed outdoors the modules started immediately to degrade, hiding the initial gain. Considering the stabilized power instead of the initial value would in this case lead to even higher degradation rates.

To better understand the origin of the degradation the electroluminescence (EL) images of the modules have been analysed (Figure 46) over time.

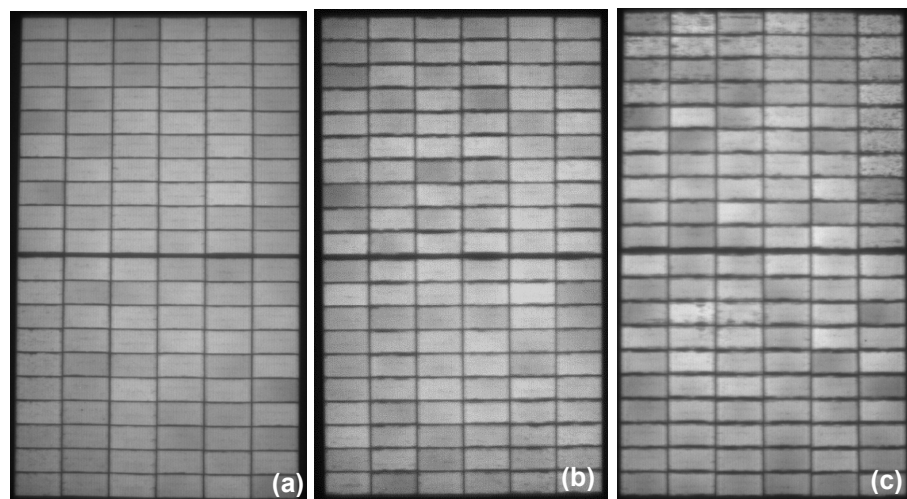


Figure 46: EL pictures of one of the HJT modules (a) at the begin, (b) after 10 months and (c) after 22 months of outdoor exposure.

The EL image of the new module, depicted in Figure 46, shows no defects, whereas the EL image after 10 months of outdoor exposure, shows first moisture penetration along the cell edges and damaged fingers, with an increase of failures after 22 months.

Figure 47 shows a zoom-in of the figure failures.

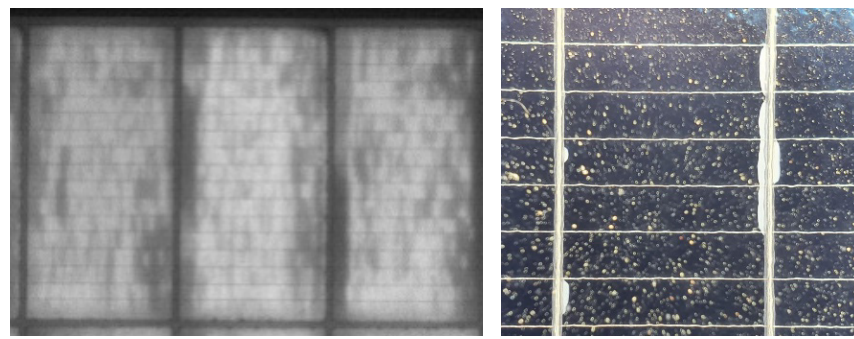


Figure 47: Zoomed EL and visual image showing the finger failures.

The probable cause of the failure is attributed to the poor bill of material, packaging structure or manufacturing process of these specific modules, which do not prevent the penetration of the humidity through the backsheet. One of the primary reasons of the  $P_{max}$  degradation seems to be related to the increase of series resistance caused by the humidity induced finger damages, observed also as Fill factor loss.

The reduction of  $V_{oc}$  is a typical consequence of UV induced degradation, mechanisms which are caused by the deterioration of the UV exposed front passivating layers. A more detailed discussion about different degradation mechanisms occurring in HJT modules can be found in the work of E. Özkalay, who investigated the performance of the same modules under harsher outdoor and indoor test conditions [PhD thesis to be published on repository of EPFL and SUPSI]. To gain a deeper understanding of how these failures affects the energy yield, the low light performance of the modules was also analysed.

Figure 48a shows the indoor measured relative efficiency curve measured at 25°C in dependence of irradiance of the 3 unexposed HJT modules and after 22 months of outdoor exposure. The here observed change in the shape of the efficiency curve is typical of an increase of series resistance. The better low light performance is the reason for the lower degradation rates extracted from outdoor data corrected to  $G_{ref}=500\text{W/m}^2$  (see Figure 48b) and the reason why the energy losses are not directly proposal to the STC power loss.

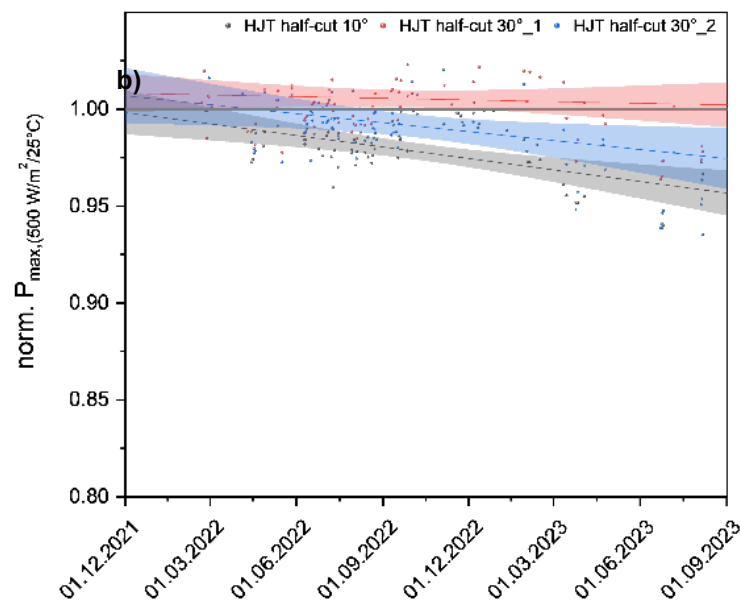
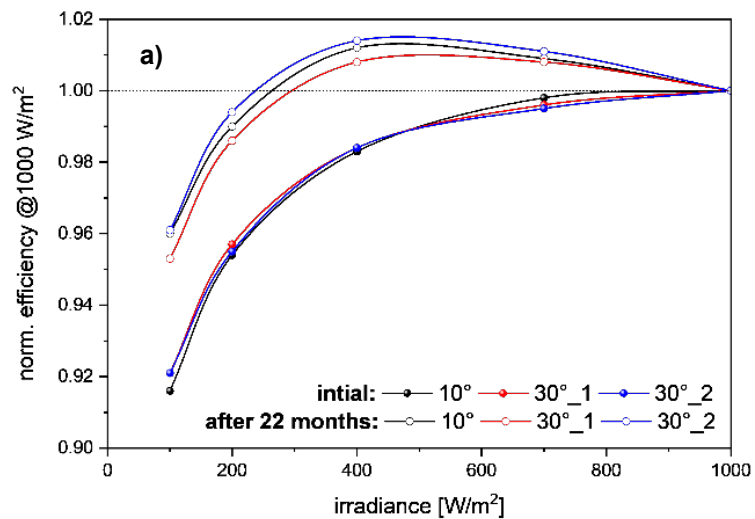




Figure 48: (a) Change in indoor measured relative efficiency curve @25°C after 22 months of outdoor exposure for the 3 open-rack mounted HJT modules and (b) temperature and irradiance corrected outdoor data of the same modules (applied filter: clear days, 500±50W/m<sup>2</sup>, early morning/afternoon data affected by shading)

#### IBC full cell technology

The visual inspection of the three outdoor exposed IBC modules revealed no major defects that could explain the observed degradation in  $P_{max}$  and  $V_{oc}$ . The EL images of the modules performed before and after 22 months of outdoor exposure, shown in Figure 49, highlighted a cell mismatch and a non-uniformity on cell-level, which could suggest UVID, but the origin is still under investigation.

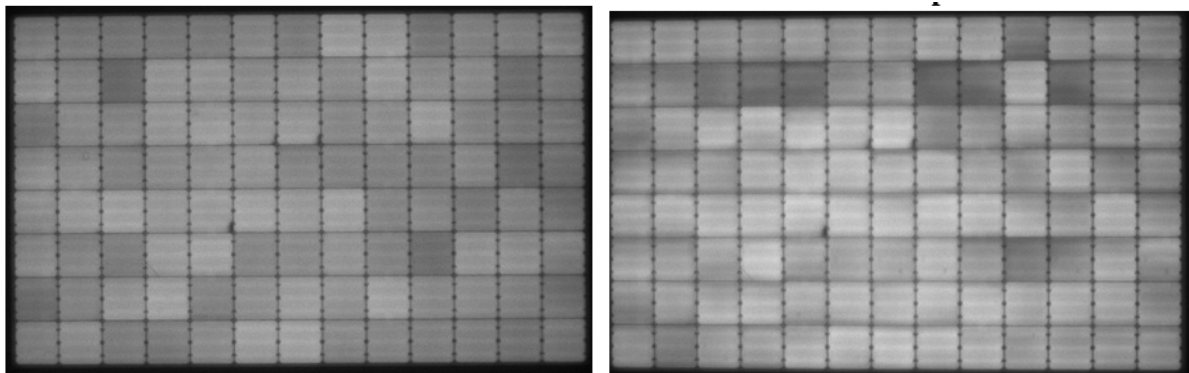


Figure 49: EL pictures of new and aged IBC modules. (left) Initial (right) after 22 months of outdoor exposure.

#### PERC shingled modules

The 5-cut shingled PERC modules, which showed lower performance ratios in both test stands, also showed some meta-stable behaviour in the field and during some thermal cycling tests, which results are still under investigation. The EL pictures of new modules showed some evidence of cell mismatch and grid finger problems (Figure 50). The light soaking tests performed at the begin highlighted already slightly higher degradation rates of up to -1.36%, with no clear stabilization even after three light soaking periods (see in 4.2.2).

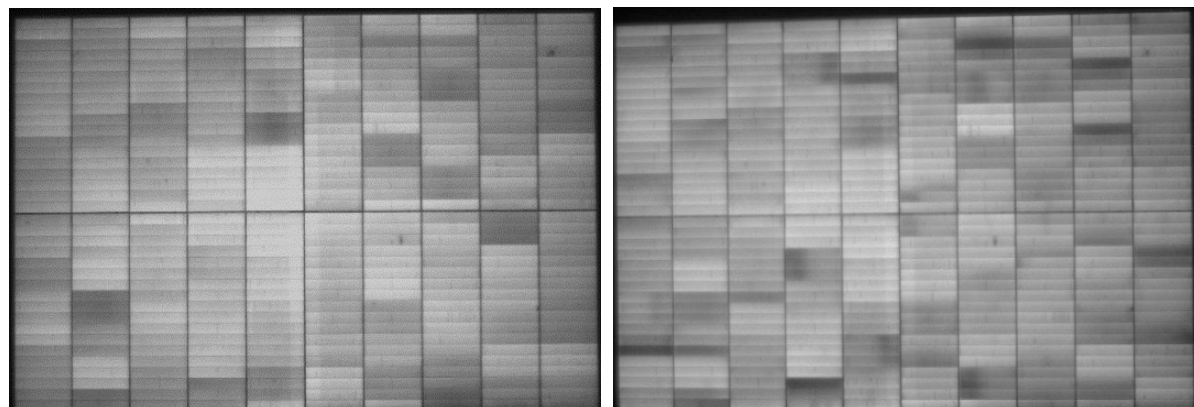


Figure 50: EL pictures of new and aged PERC shingled modules (a) Initial (b) after 22 months of outdoor exposure.



### 3.6.6 Benchmarking for shading tolerance

It is evident that innovative module designs are often marketed for their improved shading resistance. However, comparing different module technologies and designs becomes problematic when shading resistance as a characteristic of a photovoltaic (PV) device is not clearly defined and there are no standardised methods for evaluating the shading resistance of a PV module compared to common technologies. In the European project METRO-PV, a classification scheme that assesses the power loss of a PV module under different shading patterns was proposed [14].

The methodology assumes that the power loss is entirely dependent on the shaded area of the PV module, and that an ideal device would experience a power loss equivalent to the size of the shaded area. For instance, if 20% of the module area is shaded, a perfect shading-resistant device would only experience a 20% reduction in power output. Any additional loss (AL) beyond this anticipated loss is primarily due to the circuit design of the PV module. The additional loss is calculated as the difference between the actual power loss and the expected power loss based on the size of the shaded area.

$$AL = \left( 1 - \frac{P_{mpp,shaded}}{P_{mpp}} - \frac{A_{shaded}}{A_{total}} \right) \times 100\%$$

where  $P_{mpp,shaded}$  is maximum power under shadow,  $P_{mpp}$  is maximum power without shadow,  $A_{shaded}$  is shaded area and  $A_{total}$  is total module area. The best case is  $AL = 0\%$  meaning that the shading does not reduce the power generation of the unshaded part of the module. Although a variety of shading scenarios have been explored in literature, we focused on three stationary shading scenarios in this study (see Figure 51):

- 1) Shading along the long side of the PV module
- 2) Shading along the short side of the PV module
- 3) Spot shading within one solar cell

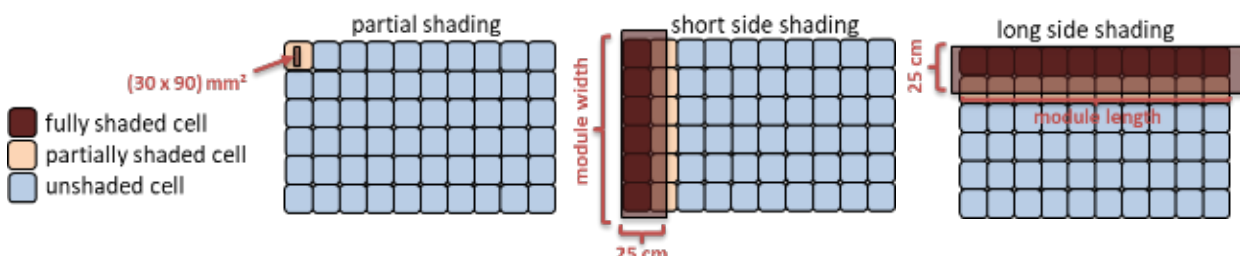


Figure 51: Shading scenarios on a standard 60-cell PV module.

Table 14 provides a classification of PV modules based on their additional loss (AL) for various shading scenarios. Four classes are identified ranging from A (very good) to D (very bad). It is worth noting that the long and short side shadings exhibit similar characteristics and thus, share the same class limits. In contrast, spot shading results in significantly lower AL values compared to the other patterns, leading to distinct class limits for this shading type.

Class	Long side shading [%]	Short side shading [%]	Spot shading [%]
<b>A</b>	$AL < 5$	$AL < 5$	$AL < 2$
<b>B</b>	$5 \leq AL < 25$	$5 \leq AL < 25$	$2 \leq AL < 5$
<b>C</b>	$25 \leq AL < 50$	$25 \leq AL < 50$	$5 \leq AL < 10$
<b>D</b>	$AL \geq 50$	$AL \geq 50$	$AL \geq 10$

Table 14: Classification scheme for the shading resistance depending on the additional loss (AL).

#### Outdoor shading measurements:

As part of a laboratory measurement inter-comparison of the METRO-PV project, SUPSI examined the shading tolerance of all 7 module technologies of test cycle 14. The tested modules, depicted in Figure 52, offer different mitigation approaches to increase their shading resistance for certain shading patterns. The classification of the shading resistance was done according the before described approach and was based on outdoor measurements.

The outdoor measurements were carried out using the maximum power point tracker (MPPT3000) developed by SUPSI. In each module type, two modules were used. One PV module was utilized as the reference, while the other module was shaded using three shading patterns (as shown in Figure 51). Opaque material was used for the shading of the modules. The measurements for the long and short side shadings of the module were repeated separately for both sides. For the spot shading, four measurements were performed on different solar cells within the module. The measurements were conducted only under close to clear sky conditions. As the test and reference module may have different powers in the unshaded case, the power of both modules was measured simultaneously without shade, and the power ratio was calculated and used as an additional correction factor.

Figure 52 illustrates the shading classification for all the types of modules that we evaluated, along with their module layout. In terms of long side shading, only the IBC full-cell module is categorized as Class A, while PERC shingled is classified as Class C, and the remaining modules are categorized as Class B. However, for short side shading, the IBC full-cell module is classified as Class D, while PERC shingled and PERC integrated diode modules are classified as Class B. The remaining modules are categorized as Class C. For spot shading, all modules, except for PERC half-cut, are classified as Class B.

The results of the round robin, which was part of the METRO-PV project will be presented at the 41<sup>st</sup> EUPVSEC conference [SUPSI 4]. Both indoor as well as outdoor results were here analysed.

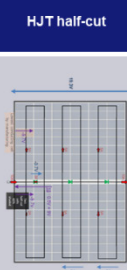
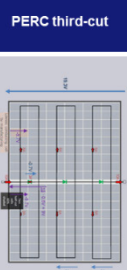
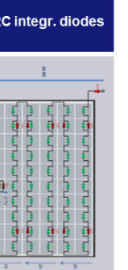
	PERC half-cut	IBC full cell	HJT half-cut	PERC third-cut	PERC shingled	TOPCon half-cut	PERC integr. diodes
Module layout							
Shading class	Long side: B Short side: C Spot: C	Long side: A Short side: D Spot: B	Long side: B Short side: C Spot: B	Long side: B Short side: C Spot: B	Long side: C Short side: B Spot: B	Long side: B Short side: C Spot: B	Long side: B Short side: B Spot: B

Figure 52: Shading classification of the modules together with their module layout.



## 4 Conclusions & Outlook

### Technology benchmarking and related uncertainties

As part of the ATTRACT project, SUPSI has launched the 14<sup>th</sup> outdoor measurement campaign, focusing on the analysis of the performance and reliability of some of the new cell technology changes that have come onto the market in recent years. Seven representative commercial mono-facial PV module technologies, including 4 different PERC modules (half-cut, third-cut, five-cut shingled and full-cell modules with integrated bypass diodes), 1 p-type TOPCon half-cut, 1 IBC full-cell and 1 HJT half-cut module technology, were selected within the in 2021 available products. The analysis of the first two years of outdoor data showed that 6 out of 7 technologies had very close specific energy yields ( $Y_f$ ) expressed in kWh/W<sub>p</sub> or performance ratios (PR), all within  $\pm 0.9\%$ , when installed under optimal conditions: open-rack for reduced thermal losses and south-orientation with 30° tilt for high irradiance gains. This shows that under optimal mounting conditions the technological differences of the test cycle 14 modules are close to negligible. The main technological differences are to be found in the efficiency of the modules and, as a consequence, in the energy yield produced per square meter.

Accurate PR based technology benchmarking relies on the **knowledge of the real STC power** of the modules. SUPSI is therefore measuring the STC power of each module in the laboratory with the highest possible measurement uncertainty of  $\pm 1.6\%$  before installing them in the field. Modules are furthermore affected by initial light induced degradation effects as LID and LeTID, which should be taken into account by module manufacturers when rating their modules. SUPSI is therefore stabilising all modules according to the procedures described in the IEC 61215 standard. The initial stabilisation of the test cycle 14 modules showed no major degradation issues, but it was observed that most module manufacturers were reporting higher STC power than the measured. The use of nameplate power instead of real stabilised STC power would so lead to higher deviations in the technology benchmarking, to the detriment of the manufacturer who overstates the module power. The consequences are unrealistic module performance data and wrong energy expectations, with a higher risk of underperforming systems. Accurate technology benchmarking, based on high precision indoor and outdoor measurements, fosters instead innovation and stimulate PV module manufacturers for optimizing PV cell and module technology with respect to energy yield and lifetime and not just efficiency and STC power.

Any module production is subject to **manufacturing tolerances**, which can result from a higher variation in the electrical parameters of the solar cell or from the manufacturing process, such as the quality of the cell cutting or soldering. The last in particular results into a wider spread of the relative efficiency curve within the same module batch, resulting in different low light behaviors. The knowledge of low light performance is therefore crucial to understand differences in energy yield between single modules. SUPSI is therefore measuring by default also the performance in the range of 100 to 1000 W/m<sup>2</sup>. In the project, higher variability was observed for modules with integrated bypass diodes and shingled cells, where the contact resistances are increasing significantly. The spread is expected to increase with natural ageing, with a direct impact on energy output and the benchmarking. To assess these changes, the low-light performance is measured each time the modules are disassembled for laboratory testing.

The representativeness of the technology benchmarking under optimal **mounting conditions** for Switzerland, where roof-mounted or integrated PV systems are predominant, was investigated using a test stand with the same modules but tilted at 10°. No cleaning is performed to simulate real-life conditions. In BAPV or BIPV conditions, higher temperatures, seasonal and daily variations in the angle of incidence, higher occurrence of low light conditions and frequent partial shading can in reality favor or disadvantage one or the other technology. In what extend this is the case for the test cycle 14 modules was investigated. The results showed an increase of the PR difference from  $\pm 0.9\%$  under optimal mounting conditions to  $\pm 2.1\%$  at low tilt angles. The increase is reconductable to differences in the angular



response and soiling losses. The soiling caused by the dust accumulation at the bottom of the module, increased by the presence of the frame, is impacting performance as more as closer the cells are to the border. The angular response impacts instead the winter yield where high incidence angles are more frequent also at noon. Technology benchmarking under representative test conditions are therefore crucial to demonstrate advantages or disadvantages of technology or module design choices in the field.

Furthermore, the project aimed at the detection and analysis of **early stage degradation issues**, related to the cell technology, the module design or the manufacturing quality. One of the module technologies in test cycle 14 showed a degradation rate that exceeded the warranty claims. The 3 HJT modules in question showed a loss in FF and  $P_{max}$  and, to a lesser extent, in  $I_{sc}$  and  $V_{oc}$ , resulting in the lowest PR within the benchmarking study. A non-linear trend in  $P_{max}$  was observed with a loss of -5.75%/year in the first year and -1.57%/year in the second year, while  $I_{sc}$  and  $V_{oc}$  seemed to stabilise over time suggesting an overlap of more than one degradation mode. The main part of the power loss is to be attributed to a poor bill of materials (BOM) that does not prevent moisture penetration through the backsheet. The humidity sensitivity of HJTs is known from the literature and is usually mitigated by appropriate bill of materials and module manufacturing as the use of humidity barriers in the back sheet. This degradation is generally detected through standard module qualification tests and mitigated by regular factory inspections. Considering the best temperature coefficients between the technologies the HJT modules should theoretically be within the top players, but the very high degradation cancels out this advantage.

#### Outlook: HJT technologies

In the continuation of this project SUPSI aims to further investigate HJT specific module failures, the effectiveness of different in place mitigation measures for glass/backsheet and glass/glass HJT modules, and how humidity penetration is accelerated by temperature, relevant for BIPV systems.

The study and knowledge of annual **performance loss rates (PLR)** is essential to improve the accuracy of long-term energy prediction models and warranty claims, to reduce the investment risks, and to provide guidance for standardised quantification of degradation rates [16,17]. Today manufacturers tend to declare very similar degradation rates, based on marketing strategies more than real data, with a general trend towards always lower degradation rates (1-2% first year followed by 0.2-0.6%/year  $P_{max}$  degradation). Real world degradation is technology, manufacturing and climate dependent and occurs in non-linear manner. A reliable determination of PLR requires several years of data and a good knowledge of uncertainty contributions. The PLR can be determined either through indoor or outdoor measurements, leading however to slightly different results. The methodologies behind PLR data are not always stated in literature making a direct comparison difficult. High precision indoor measurements have a direct impact on the accuracy of PLR. Within test cycle 14, SUPSI analysed the first two years degradation rates by applying two different methods, one based on indoor STC power measurements and the second on outdoor data. The two methods lead to qualitatively comparable results, but only in case of higher degradation rates, as occurring in the HJT modules, the data were also quantitatively comparable. A minimum of 4 years of data are needed to increase the accuracy of the outdoor data analysis. The around 2.2% degradation in 20 months (1.3%/year), observed in the three IBC modules is for example detectable only through indoor measurements. The monitoring of a limited number of technologies tested here does not allow for generalisation on a specific technology but generates important know-how on the evolution of degradation rates, understanding of technology benchmarking and PLR methodologies which are of strategic importance for investors, manufacturers and research community. Last but not least, the open-rack mounted modules of test cycle 14, dealt also as a reference stand for different BIPV stands, containing the same modules but exposed to higher thermal and shading stresses. BIPV specific



degradation rates and the analysis of the acceleration by different stressors within the REBI project was so possible and will be further developed. One of the future challenges will be how to determine climate or application specific degradation rates which can be used for technology benchmarking or ratings. Manufacturers producing modules with proven low degradation rates could so promote their product.

#### **Outlook: PLR data and methodologies**

The relatively short timeframe of the up to now available data (<2 years) does not allow to make accurate estimates of annual degradation rates. For this reason, the measurements will be extended to at least 5 years. This will for example allow to monitor the impact on performance and evolution over time of visual defects observed in some of the modules (e.g shingled technology) and to determine more accurately the degradation rates of the test cycle 14 modules and to contribute to international studies aiming to improve the accuracy and availability of PLR data. In 2024, the PV market continues to evolve with a clear trend towards n-type TOPCON, back-contacted cells and HJT modules. An upgrade of the SUPSI outdoor test facility to incorporate the latest technologies is therefore planned for the near future with a continuation of testing under different mounting configurations.

A further to be considered aspect are short to medium term, **reversible and non-reversible light induced degradation mechanisms** as e.g LID, LeTID, and UVID, which occurs in the field. occurrence of more at the same time with different time scales and the dependency on climatic conditions makes the detection very difficult. Very little field data are therefore available in literature. The Test cycle 14 gave the evidence of some differences between indoor and outdoor stabilisation as well as seasonal trends with differences between the modules of the same type, suggesting some meta stabilities, particularly for PERC technologies.

#### **Outlook: Light induced degradation**

The better understanding of light induced degradation phenomena in the field are crucial for energy predictions. Longer time series are needed to be able to detect this phenomena in the field, and indoor and outdoor testing has to be combined to improve the stabilization procedures used by test laboratories. SUPSI will further investigate this aspects to discern between stabilization and degradation mechanisms and to quantify its impact in different technologies.

#### Fast and high precision energy rating (ER) of high efficiency modules

Outdoor data-based technology benchmarkings, as described before relies on long-term data, are site and time dependent, are not repeatable and are correlated with higher uncertainties, but they are able to detect degradation rates and real operating conditions are reproduced. Module characterization according to the IEC 61853 Part 1 and Part 2 energy rating standard (ER) allows to determine the most important module parameters describing the outdoor performance under exclusion however of degradation or regeneration mechanisms. The ER standard provides an important mean for manufacturers to optimise their product for energy yield and test laboratories to analyse outdoor data and to discern degradation from expected energy yield. However, the execution of a full ER characterisation is very time consuming and expensive to perform in the laboratory, especially when measuring highly capacitive modules, which require time-consuming test procedures to overcome capacitive effects. The use of the multi-flash approach implemented at SUPSI PVLab guarantees a  $P_{max}$  measurement uncertainty of  $\pm 1.6\% [u\%, k=2]$ , but with an effective measurement time for a full power matrix of approximately 7 hours. Most modules on the market today are affected by capacitive effects when measured with a 10 ms pulsed solar simulator as available at SUPSI. All 7 module technologies of test cycle 14 required the use of the multi-flash approach, with PERC just at the limit of our criterium deciding on how to measure



a module (single flash versus multi-flash). The time and cost of ER measurements are a clear barrier for research and industry. One option to overcome the problem with capacitive modules is to use new generation LED steady state solar simulators, but the much higher costs compared to Xe solar simulators and other challenges related to the maintenance, the complexity and limits of spectral and thermal control compensate the advantages especially in case of an already available solar simulator. ATTRACT focused therefore on alternative procedures applicable to our pulsed solar simulator, aiming in reducing the time required for testing without affecting the measurement uncertainty. A modified dragon-back approach was introduced and validated, demonstrating a reduction in the duration of the effective measurement time for a full power matrix to around 42 minutes, which is 10 times less than with a multi-flash. The original dragon-back® method developed by SUPSI in an Innosuisse project with PASAN was therefore revised and improved. The new approach automates the setting of dragon-back® parameters for each technology and combines single sweep with multi-step dragon-back® ramps to achieve the highest accuracy in  $I_{sc}$  and  $V_{oc}$ . The methodology was validated within an international round robin with other ISO 17025 accredited test laboratories and the maintenance of measurement uncertainty confirmed.

#### **Outlook: indoor characterisation**

The project revealed some new technological challenges or limitations related to ER testing and/or the characterization of large size modules: (1) one of the bottlenecks of ER measurements remains the duration of thermal stabilisation when measuring module performance at different temperatures, (2) the size of latest modules exceeds the dimensions of the typical thermal chambers used in test laboratories to measure temperature coefficients, which is why the large size 470 Wp module of test cycle 14 could not be tested in the thermal chamber, (3) the spectral response measurement of large size modules showed some artefacts that could be due to the simulator's spectral inhomogeneity, which is still under investigation. The increasing number of requests for the testing of large size modules and energy rating in the near future requires rapid action to further improve the HW and test procedures at SUPSI.

#### Assessment of HW limitations at SUPSI for the testing of single junction perovskite modules

Last but not least, the project aimed to evaluate the testing capabilities of the SUPSI PVLab for the upcoming perovskite technology. Solaronix supplied SUPSI with a set of single-junction mini-modules, which were measured both indoors and outdoors to determine the limits of the current HW. A SW has been written to test the modules under STC conditions according to a test procedure developed by the ESTI of the Joint Research Centre (JRC), as well as outdoors under variable light conditions. The comparison with the JRC measurements showed some deviations, most likely due to dark storage and to a lesser extent to the measurement itself. The dependency from voltage sweep time was here also analysed, resulting in a 10 minute sweep to be the optimal time.

#### **Outlook: Perovskite testing**

SUPSI will continue to upgrade its test facilities for multi-junction perovskite modules and optimise maximum power point tracking algorithms for energy yield and stability measurements required for long-term studies. As the development of next-generation solar cells based on (P<sub>k</sub>/Si) perovskite-silicon tandem is gaining importance the number of outdoor tests in field to proof their stability and energy yield are expected to increase. These enhancements aim to establish the laboratory as a future candidate facility for perovskite PV research and testing, contributing to the Swiss and international industry.



## 5 Dissemination

- [SUPSI 1] G. Bardizza, et.al, 'Energy rating of PV modules - Uncertainties associated with (G T) power matrix measurements in accordance with IEC 61853-1', 40th EUPVSEC, Lisbon, 2023.
- [SUPSI 2] G. Friesen, et.al, 'Impact of technological trends in crystalline silicon PV modules on the energy yield performance: Preliminary result of the 14th SUPSI outdoor measurement campaign', 8<sup>th</sup> WCPEC, Milano, 2022.
- [SUPSI 3] G. Friesen, E. Özkay, et.al, 'Performance and degradation evaluation of crystalline silicon modules under different open-rack and residential mounting configurations', submitted to 41<sup>th</sup> EUPVSEC, Wien, 2024
- [SUPSI 4] S. Riechelmann, et.al, 'Laboratory Intercomparison on a Shading Resistance Classification of PV modules', submitted to 41<sup>th</sup> EUPVSEC, Wien, 2024.
- [SUPSI 5] J. Karas, M. Caccivio, G. Bellenda, et al., 'Results from an international interlaboratory study on light- and elevated temperature-induced degradation in solar modules', *Prog Photovolt Res Appl.* 2022; 30(11): 1255-1269. doi:10.1002/pip.3573.



## 6 References

- [1] SBA (Swiss Bankers Association) and BCG (Boston Consulting Group), “Sustainable finance Investment and financing needed for.” Accessed: Dec. 20, 2023. [Online]. Available: [https://www.swissbanking.ch/ Resources/Persistent/b/e/0/9/be0949b50b2ac8462b7459b9cd4708ffaa30da27/SBA\\_Sustainable\\_Finance\\_2021.pdf](https://www.swissbanking.ch/ Resources/Persistent/b/e/0/9/be0949b50b2ac8462b7459b9cd4708ffaa30da27/SBA_Sustainable_Finance_2021.pdf)
- [2] BFE Medienmitteilung, “Schweizer Hausdächer und -fassaden könnten jährlich 67 TWh Solarstrom produzieren.,” Apr. 2019.
- [3] T. Sample “Standards for PV - overview of IEC related PV standards and how they contribute to reduced costs of energy”, 35<sup>th</sup> EUPVSEC, Brussel, 2018
- [3] M. Pravettoni, D. Poh, J. Prakash Singh, J. Wei Ho, and K. Nakayashiki, “The effect of capacitance on high-efficiency photovoltaic modules: A review of testing methods and related uncertainties,” *Journal of Physics D: Applied Physics*, vol. 54, no. 19. IOP Publishing Ltd, May 13, 2021. doi: 10.1088/1361-6463/abe574.
- [4] E. Kobayashi et al., “Increasing the efficiency of silicon heterojunction solar cells and modules by light soaking,” *Solar Energy Materials and Solar Cells*, vol. 173, pp. 43–49, Dec. 2017, doi: 10.1016/j.solmat.2017.06.023.
- [5] J. Cattin et al., “Influence of Light Soaking on Silicon Heterojunction Solar Cells with Various Architectures.”
- [6] E. Kobayashi et al., “Light-induced performance increase of silicon heterojunction solar cells,” *Appl. Phys. Lett.*, vol. 109, no. 15, 2016.
- [7] A. Virtuani, G. Rigamonti, P. Beljean, G. Friesen, M. Pravettoni, and D. Chianese, “A fast and accurate method for the performance testing of high-efficiency C-Si photovoltaic modules using A 10 Ms single-pulse solar simulator,” in *Conference Record of the IEEE Photovoltaic Specialists Conference*, 2012, pp. 496–500. doi: 10.1109/PVSC.2012.6317664.
- [8] G. Friesen et al., *Photovoltaic Module Energy Yield Measurements: Existing Approaches and Best Practice*. 2018. Accessed: Dec. 20, 2023. [Online]. Available: [https://iea-pvps.org/wp-content/uploads/2020/01/Photovoltaic\\_Module\\_Energy\\_Yield\\_Measurements\\_Existing\\_Approaches\\_and\\_Best\\_Practice\\_by\\_Task\\_13.pdf](https://iea-pvps.org/wp-content/uploads/2020/01/Photovoltaic_Module_Energy_Yield_Measurements_Existing_Approaches_and_Best_Practice_by_Task_13.pdf)
- [9] IEC, *TECHNICAL REPORT Measurement protocols for photovoltaic devices based on organic, dye-sensitized or perovskite materials*. 2019. [Online]. Available: [www.iec.ch](http://www.iec.ch)
- [10] G. Bardizza, H. Müllejans, D. Pavanello, and E. D. Dunlop, “Metastability in performance measurements of perovskite PV devices: A systematic approach,” *JPhys Energy*, vol. 3, no. 2. IOP Publishing Ltd, Apr. 01, 2021. doi: 10.1088/2515-7655/abd678.
- [11] R.H. French et al., *Assessment of performance loss rate of PV power systems*. 2021. Accessed: Dec. 20, 2023. Available: [https://iea-pvps.org/wp-content/uploads/2021/04/IEA-PVPS-T13-22\\_2021-Assessment-of-Performance-Loss-Rate-of-PV-Power-Systems-report.pdf](https://iea-pvps.org/wp-content/uploads/2021/04/IEA-PVPS-T13-22_2021-Assessment-of-Performance-Loss-Rate-of-PV-Power-Systems-report.pdf)
- [12] Theristis M, Stein JS, Deline C, et al. Onymous early-life performance degradation analysis of recent photovoltaic module technologies. *Prog Photovolt Res Appl*. 2023; 31(2): 149-160. doi:10.1002/pip.3615



- [13] *Marc Köntges et al., Review of Failures of Photovoltaic Modules. 2014. Accessed: Dec. 20, 2023. Available: [https://iea-pvps.org/wp-content/uploads/2020/01/IEA-PVPS\\_T13-01\\_2014\\_Review\\_of\\_Failures\\_of\\_Photovoltaic\\_Modules\\_Final.pdf](https://iea-pvps.org/wp-content/uploads/2020/01/IEA-PVPS_T13-01_2014_Review_of_Failures_of_Photovoltaic_Modules_Final.pdf)*
- [14] *Hendrik Sträter et al., “An Approach for a Shading Resistance Classification of PV Modules,” WCPEC-8, 2022.*
- [15] *J. Zuboy et.al, “Getting Ahead of the Curve: Assessment of New Photovoltaic Module Reliability Risks Associated With Projected Technological Changes”, IEEE JOURNAL OF PHOTOVOLTAICS, VOL. 14, NO. 1, JANUARY 2024*
- [16] *Micheli, Leonardo, Theristis, Marios, Talavera, Diego L., Nofuentes, Gustavo, Stein, Joshua S., Almonacid, Florencia, and Fernández, Eduardo F. The economic value of photovoltaic performance loss mitigation in electricity spot markets. United States: N. p., 2022. Web. doi:10.1016/j.renene.2022.08.149.*
- [17] *Martin Libra, David Mrázek, Igor Tyukhov, Lucie Severová, Vladislav Poulek, Jiří Mach, Tomáš Šubrt, Václav Beránek, Roman Svoboda, Jan Sedláček, Reduced real lifetime of PV panels – Economic consequences, Solar Energy, Volume 259, 2023, Pages 229-234, ISSN 0038-092X, <https://doi.org/10.1016/j.solener.2023.04.063>.*



## 7 Annexes

### Ciclo 14 Dragonback Validation

< ±1%      > ±1%

Module Label	Technology	Power [W]	ΔP% (MF-Direct)
21-C14-A	PERC Halfcut	365 W	0.7%
21-C14-B	IBC	400 W	11.26%
21-C14-C	Halfcut HJT	375 W	8.94%
21-C14-D	Thirdcut PERC	385 W	1.07%
21-C14-E	Thirdcut Shingled	365 W	0.51%
21-C14-F	Integrated diode PERC	320 W	0.71%
21-C14-H	NTopcon		4.43%

Table 15: CICLO 14 Modules

21-C14-A11		Pm [W]	Isc [A]	Voc [V]	Vm [V]	Im [A]	FF [%]
1000 W/m <sup>2</sup>	MF	353.3025	10.94	40.65	34.034	10.381	79.4
	DB	353.52	10.938	40.653	34.052	10.382	79.501
	Δ%	0.061562	-0.01828	0.00738	0.052888	0.009633	0.127204
700 W/m <sup>2</sup>	MF	246.851	7.665	40.09	33.96	7.269	80.3
	DB	246.705	7.655	40.1	33.948	7.267	80.366
	Δ%	-0.05914	-0.13046	0.024944	-0.03534	-0.02751	0.082192
400 W/m <sup>2</sup>	MF	139.243	4.38	39.21	33.48	4.159	81.1
	DB	139.359	4.382	39.199	33.532	4.156	81.129
	Δ%	0.083308	0.045662	-0.02805	0.155317	-0.07213	0.035758
200 W/m <sup>2</sup>	MF	67.574	2.192	38.05	32.68	2.068	81.1
	DB	67.816	2.194	38.067	32.654	2.077	81.207
	Δ%	0.358126	0.091241	0.044678	-0.07956	0.435203	0.131936
100 W/m <sup>2</sup>	MF	32.66	1.098	36.92	31.68	1.031	80.6
	DB	32.836	1.101	36.945	31.658	1.037	80.693
	Δ%	0.538885	0.273224	0.067714	-0.06944	0.581959	0.115385

Table 16: PERC Half-cut, DB validation



21-C14-B11		Pm [W]	Isc [A]	Voc [V]	Vm [V]	Im [A]	FF [%]
1000 W/m <sup>2</sup>	MF	379.835	6.331	74.911	63.908	5.943	80.1
	DB	380.358	6.313	74.903	63.794	5.962	80.432
	Δ%	0.137691	-0.28432	-0.01068	-0.17838	0.319704	0.414482
700 W/m <sup>2</sup>	MF	265.35	4.44	73.98	63.47	4.181	80.8
	DB	265.676	4.43	73.943	63.353	4.194	81.114
	Δ%	0.122857	-0.22523	-0.05001	-0.18434	0.31093	0.388614
400 W/m <sup>2</sup>	MF	149.889	2.547	72.49	62.61	2.394	81.2
	DB	149.743	2.538	72.436	62.676	2.389	81.436
	Δ%	-0.09741	-0.35336	-0.07449	0.105414	-0.20886	0.29064
200 W/m <sup>2</sup>	MF	73.183	1.278	70.6	61.03	1.199	81.1
	DB	73.559	1.274	70.502	60.814	1.21	81.89
	Δ%	0.513781	-0.31299	-0.13881	-0.35392	0.917431	0.974106
100 W/m <sup>2</sup>	MF	35.455	0.641	68.73	59.63	0.595	80.5
	DB	35.659	0.638	68.561	59.468	0.6	81.57
	Δ%	0.575377	-0.46802	-0.24589	-0.27168	0.840336	1.329193

Table 17: IBC, DB validation

21-C14-C6		Pm [W]	Isc [A]	Voc [V]	Vm [V]	Im [A]	FF [%]
1000 W/m <sup>2</sup>	MF	337.794	10.045	43.82	36.38	9.285	76.7
	DB	337.849	10.054	43.772	36.39	9.284	76.767
	Δ%	0.016282	0.089597	-0.10954	0.027488	-0.01077	0.087353
700 W/m <sup>2</sup>	MF	238.3	7.03	43.31	36.28	6.569	78.3
	DB	237.372	7.035	43.259	36.346	6.531	78
	Δ%	-0.38943	0.071124	-0.11776	0.181918	-0.57847	-0.38314
400 W/m <sup>2</sup>	MF	136.26	4.027	42.41	35.87	3.799	79.8
	DB	136.164	4.029	42.356	36.054	3.777	79.783
	Δ%	-0.07045	0.049665	-0.12733	0.512963	-0.5791	-0.0213
200 W/m <sup>2</sup>	MF	66.595	2.014	41.21	35.02	1.902	80.2
	DB	66.684	2.017	41.054	35.221	1.893	80.518
	Δ%	0.133644	0.148957	-0.37855	0.573958	-0.47319	0.396509
100 W/m <sup>2</sup>	MF	32.18	1.009	40.49	33.86	0.95	78.7
	DB	32.558	1.014	39.656	34.452	0.945	80.998
	Δ%	1.174643	0.49554	-2.05977	1.748376	-0.52632	2.919949

Table 18: HJT, Smart-wire, DB validation



21-C14-D2		Pm [W]	Isc [A]	Voc [V]	Vm [V]	Im [A]	FF [%]
1000 W/m <sup>2</sup>	MF	375.812	11.678	40.525	33.824	11.11078	79.4
	DB	376.143	11.674	40.535	33.834	11.117	79.486
	Δ%	0.088076	-0.03425	0.024676	0.029565	0.055982	0.108312
700 W/m <sup>2</sup>	MF	263.12	8.188	39.99	33.8	7.785	80.4
	DB	263.283	8.174	39.991	33.818	7.785	80.545
	Δ%	0.061949	-0.17098	0.002501	0.053254	0	0.180348
400 W/m <sup>2</sup>	MF	149.216	4.683	39.12	33.35	4.455	81.5
	DB	149.253	4.68	39.121	33.465	4.46	81.521
	Δ%	0.024796	-0.06406	0.002556	0.344828	0.112233	0.025767
200 W/m <sup>2</sup>	MF	72.831	38.02	2.343	32.77	2.222	81.8
	DB	72.933	38.034	2.343	32.727	2.229	81.846
	Δ%	0.14005	0.036823	0	-0.13122	0.315032	0.056235
100 W/m <sup>2</sup>	MF	35.313	1.172	36.92	31.82	1.11	81.6
	DB	35.459	1.175	36.955	31.772	1.116	81.659
	Δ%	0.413445	0.255973	0.0948	-0.15085	0.540541	0.072304

Table 19: Third-cut, DB validation

21-C14-E4		Pm [W]	Isc [A]	Voc [V]	Vm [V]	Im [A]	FF [%]
1000 W/m <sup>2</sup>	MF	350.106	9.2714	47.6983	39.735	8.811	79.2
	DB	350.072	9.273	47.697	40	8.752	79.146
	Δ%	-0.00971	0.017257	-0.00273	0.666918	-0.66962	-0.06818
700 W/m <sup>2</sup>	MF	243.74	6.492	46.97	39.49	6.173	79.9
	DB	244.12	6.49	47.008	39.586	6.167	80.025
	Δ%	0.155904	-0.03081	0.080903	0.2431	-0.0972	0.156446
400 W/m <sup>2</sup>	MF	137.304	3.718	45.83	38.92	3.528	80.6
	DB	137.448	3.717	45.828	38.931	3.531	80.694
	Δ%	0.104877	-0.0269	-0.00436	0.028263	0.085034	0.116625
200 W/m <sup>2</sup>	MF	66.443	1.86	44.36	37.84	1.756	80.5
	DB	66.638	1.862	44.383	37.862	1.76	80.619
	Δ%	0.293485	0.107527	0.051849	0.05814	0.22779	0.147826
100 W/m <sup>2</sup>	MF	32.006	0.933	42.88	36.59	0.875	80
	DB	32.168	0.936	42.896	36.511	0.881	80.084
	Δ%	0.506155	0.321543	0.037313	-0.21591	0.685714	0.105

Table 20: Shingled, DB validation



21-C14-F1		Pm [W]	Isc [A]	Voc [V]	Vm [V]	Im [A]	FF [%]
1000 W/m <sup>2</sup>	MF	304.9156	9.834	40.71	32.955	9.252	76.2
	DB	305.075	9.815	40.697	32.973	9.252	76.378
700 W/m <sup>2</sup>	Δ%	0.052277	-0.19321	-0.03193	0.05462	0	0.233596
	MF	215.413	6.9	40.13	33.16	6.496	77.8
400 W/m <sup>2</sup>	DB	215.591	6.873	40.118	33.141	6.505	78.193
	Δ%	0.082632	-0.3913	-0.0299	-0.0573	0.138547	0.505141
200 W/m <sup>2</sup>	MF	123.458	3.945	39.21	33.09	3.73	79.8
	DB	123.42	3.938	39.215	33.123	3.726	79.915
100 W/m <sup>2</sup>	Δ%	-0.03078	-0.17744	0.012752	0.099728	-0.10724	0.14411
	MF	60.518	1.976	38.04	32.54	1.86	80.5
	DB	60.759	1.973	38.074	32.474	1.871	80.867
	Δ%	0.398229	-0.15182	0.08938	-0.20283	0.591398	0.455901
	MF	29.463	0.988	36.92	31.74	0.928	80.7
	DB	29.752	0.991	36.971	31.712	0.938	81.233
	Δ%	0.980891	0.303644	0.138137	-0.08822	1.077586	0.660471

Table 21: PERC diode per cell, DB validation



## Pm Matrix Dragonback Validation

< ±1%

> ±1%

Module Label	Technology	Power [W]	ΔP% (MF-Direct)
METRO-PV-F	PERC	360 W	0.95%
METRO-PV-G	Halfcut HJT Smart Wire	380 W	9.35%

Table 22: Power matrix, modules for DB validation

15 °C		Pm [W]	Isc [A]	Voc [V]	Vm [V]	Im [A]	FF [%]	25 °C		Pm [W]	Isc [A]	Voc [V]	Vm [V]	Im [A]	FF [%]
1100 W/m <sup>2</sup>	MF	386.85	10.67	45.93	37.978	10.186	78.9	1100 W/m <sup>2</sup>	MF	375.26	10.722	44.83	36.735	10.215	78.1
	DB	386.751	10.656	45.914	37.985	10.182	79.051		DB	375.016	10.715	44.817	36.709	10.216	78.094
	Δ%	-0.02559	-0.13121	-0.03484	0.018432	-0.03927	0.191381		Δ%	-0.06502	-0.06529	-0.029	-0.07078	0.00979	-0.00768
1000 W/m <sup>2</sup>	MF	352.66	9.688	45.79	38.045	9.269	79.5	1000 W/m <sup>2</sup>	MF	341.68	9.747	44.67	36.772	9.292	78.5
	DB	353.353	9.68	45.785	38.076	9.254	79.506		DB	341.843	9.735	44.671	36.804	9.288	78.608
	Δ%	0.196507	-0.08258	-0.01092	0.018482	-0.16183	0.007547		Δ%	0.047705	-0.12311	0.002239	0.087023	-0.04305	0.13758
800 W/m <sup>2</sup>	MF	283.2	45.42	7.756	38.172	7.419	80.4	800 W/m <sup>2</sup>	MF	274.69	7.798	44.29	36.905	7.443	79.5
	DB	282.928	45.412	7.745	38.146	7.417	80.445		DB	274.31	7.79	44.285	36.904	7.433	79.514
	Δ%	-0.09605	-0.01761	-0.14183	-0.06811	-0.02696	0.05597		Δ%	-0.13834	-0.10259	-0.01129	-0.00271	-0.13435	0.01761
600 W/m <sup>2</sup>	MF	211.88	5.804	44.93	38.118	5.559	81.3	600 W/m <sup>2</sup>	MF	205.52	5.84	43.78	36.903	5.569	80.4
	DB	212.063	5.797	44.927	38.16	5.557	81.417		DB	205.535	5.832	43.78	36.899	5.57	80.499
	Δ%	0.08637	-0.12061	-0.00668	0.110184	-0.03598	0.143911		Δ%	0.007299	-0.13699	0	-0.01084	0.017957	0.123134
400 W/m <sup>2</sup>	MF	140.26	3.863	44.27	37.955	3.696	82	400 W/m <sup>2</sup>	MF	136.05	3.887	43.08	36.685	3.709	81.3
	DB	140.36	3.856	44.243	37.943	3.699	82.273		DB	136.072	3.882	43.078	36.684	3.709	81.375
	Δ%	0.071296	-0.18121	-0.06099	-0.03162	0.081169	0.332927		Δ%	0.016171	-0.12863	-0.00464	-0.00273	0	0.092251
200 W/m <sup>2</sup>	MF	68.86	1.939	43.07	37.268	1.848	82.5	200 W/m <sup>2</sup>	MF	66.79	1.951	41.89	35.99	1.856	81.7
	DB	69.217	1.934	43.135	37.333	1.854	82.973		DB	66.854	1.948	41.899	35.953	1.859	81.922
	Δ%	0.518443	-0.25786	0.150917	0.174412	0.324675	0.573333		Δ%	0.095823	-0.15377	0.021485	-0.10281	0.161638	0.271726
100 W/m <sup>2</sup>	MF	33.4	0.968	41.9	36.412	0.917	82.4	100 W/m <sup>2</sup>	MF	32.35	0.974	40.69	35.059	0.923	81.7
	DB	33.721	0.965	41.955	36.333	0.928	83.31		DB	32.467	0.972	40.699	34.957	0.929	82.099
	Δ%	0.961078	-0.30992	0.131265	-0.21696	1.199564	1.104369		Δ%	0.361669	-0.20534	0.022118	-0.29094	0.650054	0.488372
50 °C		Pm [W]	Isc [A]	Voc [V]	Vm [V]	Im [A]	FF [%]	75 °C		Pm [W]	Isc [A]	Voc [V]	Vm [V]	Im [A]	FF [%]
1100 W/m <sup>2</sup>	MF	341.8	10.87	41.81	33.339	10.252	75.2	1100 W/m <sup>2</sup>	MF	306.13	11.001	38.78	29.947	10.222	71.8
	DB	341.08	10.865	41.753	33.308	10.24	75.186		DB	306.536	10.995	38.676	30	10.218	72.082
	Δ%	-0.21065	-0.046	-0.13633	-0.09298	-0.11705	-0.01862		Δ%	0.132623	-0.05454	-0.26818	0.176979	-0.03913	0.392758
1000 W/m <sup>2</sup>	MF	312.1	9.877	41.61	33.486	9.32	75.9	1000 W/m <sup>2</sup>	MF	279.72	9.995	38.53	30.065	9.304	72.6
	DB	310.772	9.874	41.543	33.363	9.315	75.758		DB	279.922	9.988	38.517	30.08	9.306	72.763
	Δ%	-0.4255	-0.03037	-0.16102	-0.36732	-0.05365	-0.18709		Δ%	0.072215	-0.07004	-0.03374	0.049892	0.021496	0.224518
800 W/m <sup>2</sup>	MF	250.89	7.902	41.23	33.633	7.46	77	800 W/m <sup>2</sup>	MF	225.36	7.996	38.16	30.246	7.451	73.8
	DB	250.738	7.898	41.228	33.569	7.469	77.003		DB	224.782	7.988	38.017	30.1	7.468	74.018
	Δ%	-0.06058	-0.05062	-0.00485	-0.19029	0.120643	0.003896		Δ%	-0.25648	-0.10005	-0.37474	-0.48271	0.228157	0.295393
600 W/m <sup>2</sup>	MF	187.85	5.919	40.67	33.556	5.598	78	600 W/m <sup>2</sup>	MF	169.2	5.993	37.61	30.244	5.594	75.1
	DB	187.989	5.912	40.706	33.549	5.603	78.113		DB	168.772	5.989	37.482	30.128	5.602	75.181
	Δ%	0.073995	-0.11826	0.088517	-0.02086	0.089318	0.144872		Δ%	-0.25296	-0.06674	-0.34034	-0.38355	0.143001	0.107856
400 W/m <sup>2</sup>	MF	124.13	3.937	39.94	33.324	3.725	78.9	400 W/m <sup>2</sup>	MF	111.75	3.987	36.71	29.948	3.731	76.3
	DB	124.346	3.937	39.965	33.323	3.732	79.04		DB	111.331	3.987	36.66	30	3.711	76.159
	Δ%	0.174011	0	0.062594	-0.003	0.187919	0.17744		Δ%	-0.37494	0	-0.1362	0.173634	-0.53605	-0.1848
200 W/m <sup>2</sup>	MF	60.76	1.979	38.65	32.563	1.866	79.5	200 W/m <sup>2</sup>	MF	54.54	2.003	35.39	29.237	1.865	76.9
	DB	61.088	1.974	38.712	32.693	1.869	79.947		DB	54.554	1.998	35.354	29.129	1.873	77.213
	Δ%	0.539829	-0.25265	0.160414	0.399226	0.160772	0.56264		Δ%	0.025669	-0.24963	-0.10172	-0.36939	0.428954	0.407022
100 W/m <sup>2</sup>	MF	29.29	0.986	37.32	31.572	0.928	79.6	100 W/m <sup>2</sup>	MF	26.19	0.995	33.98	28.24	0.927	77.4
	DB	29.551	0.985	37.385	31.578	0.936	80.218		DB	26.172	0.999	33.899	27.958	0.936	77.262
	Δ%	0.891089	-0.10142	0.174169	0.019004	0.862069	0.776382		Δ%	-0.06873	0.40201	-0.23838	-0.99858	0.970874	-0.17829

Table 23: PERC, DB validation

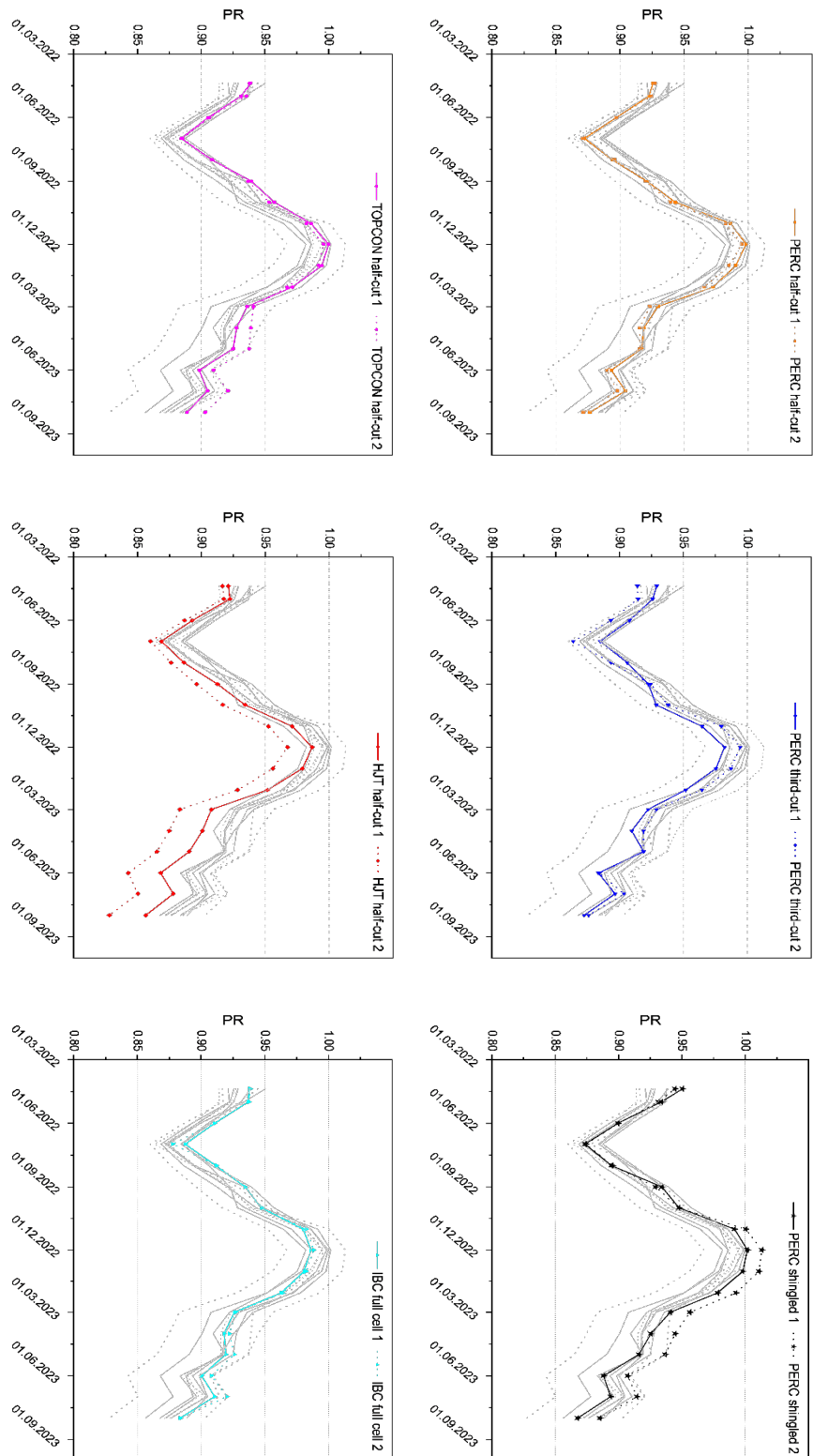


15 °C		Pm [W]	Isc [A]	Voc [V]	Vm [V]	Im [A]	FF [%]	75 °C		Pm [W]	Isc [A]	Voc [V]	Vm [V]	Im [A]	FF [%]
1100 W/m <sup>2</sup>	MF	413.76	11.42	45.33	38.246	10.818	79.9	1100 W/m <sup>2</sup>	MF	348.19	11.737	38.92	32.041	10.867	76.2
	DB	412.903	11.426	45.299	37.998	10.866	79.778		DB	347.437	11.752	38.806	31.737	10.947	76.187
	Δ%	-0.20712	0.052539	-0.06839	-0.64843	0.443705	-0.15269		Δ%	-0.21626	0.127801	-0.29291	-0.94878	0.736174	-0.01706
1000 W/m <sup>2</sup>	MF	375.88	10.385	45.19	38.195	9.841	80.1	1000 W/m <sup>2</sup>	MF	316.03	10.673	38.76	31.885	9.911	76.4
	DB	375.758	10.384	45.166	38.042	9.877	80.116		DB	316.231	10.682	38.776	31.777	9.952	76.343
	Δ%	-0.03246	-0.00963	-0.05311	-0.40058	0.365816	0.019975		Δ%	0.063602	0.084325	0.04128	-0.33872	0.413682	-0.07461
800 W/m <sup>2</sup>	MF	300.23	8.301	44.9	38.215	7.856	80.5	800 W/m <sup>2</sup>	MF	251.07	8.536	38.35	31.697	7.921	76.7
	DB	300.26	8.305	44.871	38.094	7.882	80.577		DB	251.277	8.537	38.399	31.627	7.945	76.65
	Δ%	0.009992	0.048187	-0.06459	-0.31663	0.330957	0.095652		Δ%	0.082447	0.011715	0.127771	-0.22084	0.302992	-0.06519
600 W/m <sup>2</sup>	MF	223.75	6.227	44.49	37.928	5.899	80.8	600 W/m <sup>2</sup>	MF	186.07	6.405	37.95	31.354	5.934	76.5
	DB	224.074	6.231	44.445	37.794	5.929	80.907		DB	186.339	6.412	37.805	31.066	5.998	76.869
	Δ%	0.144804	0.064236	-0.10115	-0.3533	0.508561	0.132426		Δ%	0.144569	0.10929	-0.38208	-0.91854	1.078531	0.482353
400 W/m <sup>2</sup>	MF	147.06	4.144	43.87	37.655	3.905	80.9	400 W/m <sup>2</sup>	MF	121.12	4.271	37.17	30.87	3.924	76.3
	DB	147.839	4.15	43.807	37.461	3.946	81.321		DB	121.457	4.276	37.073	30.566	3.974	76.62
	Δ%	0.529716	0.144788	-0.14361	-0.5152	1.049936	0.520396		Δ%	0.278236	0.117069	-0.26096	-0.98477	1.27421	0.419397
200 W/m <sup>2</sup>	MF	71.28	2.076	42.73	36.705	1.942	80.3	200 W/m <sup>2</sup>	MF	57.83	2.174		29.698	1.947	
	DB	71.689	2.075	42.587	36.587	1.959	81.136		DB	58.079	2.14	35.655	29.534	1.967	76.128
	Δ%	0.573793	-0.04817	-0.33466	-0.32148	0.875386	1.041096		Δ%	0.430572	-1.56394	-	-0.55223	1.02721	-
100 W/m <sup>2</sup>	MF	34.13	1.038	41.45	35.459	0.962	79.3	100 W/m <sup>2</sup>	MF	27.07	1.07		28.012	0.966	
	DB	34.31	1.038	41.17	35.586	0.964	80.3		DB	27.272	1.071	33.887	27.915	0.977	75.174
	Δ%	0.527395	0	-0.67551	0.35816	0.2079	1.261034		Δ%	0.746214	0.093458	-	-0.34628	1.138716	-

Table 24: HJT power matrix, DB validation



## Monthly Performance inter-comparison of test cycle 14





## Indoor STC measurements test cycle 14

	P <sub>max1</sub>	P <sub>max1</sub>	P <sub>max2</sub>	V <sub>oc0</sub>	V <sub>oc1</sub>	V <sub>oc2</sub>	I <sub>sc0</sub>	I <sub>sc1</sub>	I <sub>sc2</sub>	P <sub>max stab.</sub>	V <sub>oc stab.</sub>	I <sub>sc stab</sub>	P <sub>max degr.</sub>	V <sub>oc degr.</sub>	I <sub>sc degr.</sub>
	out of the box	out of after stabil. months	out of the box	(X1-X0)/X0	(X1-X0)/X0	(X1-X0)/X0	(X2-X1)/X1	(X2-X1)/X1	(X2-X1)/X1						
PERC half-cut															
30° 1 *	356.22	354.27	354.36	40.84	40.84	40.68	10.95	10.88	10.91	-0.55%	0.00%	-0.60%	0.02%	-0.39%	0.28%
30° 2	355.75	356.09	353.17	40.86	40.87	40.63	10.95	10.97	10.94	0.10%	0.02%	0.15%	-0.82%	-0.59%	-0.25%
10° *	356.85	351.44	353.30	40.91	40.85	40.65	10.98	10.83	10.94	-1.52%	-0.15%	-1.38%	0.53%	-0.49%	1.08%
PERC third-cut															
30° 1	382.92	382.15	376.36	41.07	41.06	40.56	11.74	11.73	11.66	-0.20%	0.00%	-0.09%	-1.51%	-1.23%	-0.54%
30° 2	383.20	382.09	375.81	41.08	41.05	40.53	11.74	11.73	11.68	-0.29%	-0.07%	-0.09%	-1.64%	-1.28%	-0.45%
PERC shingled															
10°	382.88	382.07	374.92	41.03	41.02	40.51	11.73	11.72	11.63	-0.21%	-0.03%	-0.13%	-1.87%	-1.24%	-0.72%
PERC shingled															
30° 1 *	357.41	349.14	350.11	48.35	48.18	47.70	9.38	9.21	9.27	-2.31%	-0.35%	-1.80%	0.28%	-1.00%	0.68%
30° 2 *	357.94	353.07	349.13	48.43	48.25	47.78	9.39	9.31	9.27	-1.36%	-0.38%	-0.86%	-1.12%	-0.98%	-0.47%
PERC shingled															
10° *	357.31	352.69	351.83	48.32	48.20	47.91	9.39	9.31	9.30	-1.29%	-0.26%	-0.88%	-0.24%	-0.60%	0.00%
PERC shingled															
30° 1 *	469.01	470.23	469.21	54.73	54.78	54.64	10.67	10.68	10.67	0.26%	0.10%	0.10%	-0.22%	-0.24%	-0.09%
TOPCon half-cut															
30° 2	466.34	468.78	468.55	54.61	54.72	54.55	10.67	10.66	10.68	0.52%	0.21%	-0.08%	-0.05%	-0.30%	0.12%
10° *	467.67	467.84	465.03	54.64	54.69	54.54	10.67	10.65	10.59	0.04%	0.09%	-0.19%	-0.60%	-0.28%	-0.61%
HJT half-cut															
30° 1	357.43	356.70	337.79	44.32	44.28	43.82	10.19	10.14	10.05	-0.20%	-0.09%	-0.53%	-5.30%	-1.03%	-0.91%
30° 2	358.08	356.54	333.25	44.36	44.22	43.62	10.22	10.18	10.08	-0.43%	-0.31%	-0.38%	-6.53%	-1.35%	-0.92%
10°	356.94	339.56	44.40	44.36	43.80	10.19	10.22	10.03	1.02%	-0.08%	0.27%	-7.06%	-1.27%	-1.80%	
HJT half-cut															
30° 1	391.41	389.17	379.91	76.21	76.00	74.95	6.36	6.35	6.34	-0.57%	-0.28%	-0.09%	-2.38%	-1.38%	-0.14%
IBC full cell															
30° 2	390.56	388.29	379.84	76.08	75.89	74.91	6.35	6.34	6.33	-0.58%	-0.25%	-0.06%	-2.18%	-1.29%	-0.15%
10°	389.91	387.69	379.59	76.03	75.86	74.92	6.36	6.35	6.32	-0.57%	-0.22%	-0.05%	-2.09%	-1.24%	-0.54%
PERC integer. diodes															
10°	301.98	301.27	304.92	40.67	40.71	9.85	9.82	9.83	-0.24%	0.00%	-0.38%	1.21%	0.10%	0.18%	

\*outdoor light soaking



## Indoor STC measured $P_{max}$ respect to nominal power test cycle 14

